Investigation into the role of small nucleolar RNA U44 in leukaemia

By Chloe Gawlik

MPhil Cancer Studies

March 2019

Supervised by Dr Mirna Mourtada-Maarabouni

School of Life Sciences

Faculty of Natural Sciences

Contents

i List of Abbreviations 4
ii Abstract 5
iii Acknowledgments 6
1 Introduction 7
1.1 Cancer and its hallmarks 7
1.2 Role of non-coding RNAs in cancer 12
1.2.1 Non-coding RNAs 12
1.2.2 Role of long non-coding RNAs 13
1.2.3 Role of Small non-coding RNAs in cancer 18
1.3 Small nucleolar RNAs (snoRNAs) 22
1.3.1 Role of snoRNAs in cancer 23
1.4 Growth arrest specific transcript 5 (*GAS5*) and its snoRNAs 28
1.4.1 *GAS5* and its role in cancer 28
1.4.2 *GAS5* snoRNAs 33
1.5 Aims of the study 35
2 Materials and Methods 36
2.1 Materials 36
2.1.1 Cell culture 36
2.1.2 Transient transfections 36
2.1.3 Short term functional assays 36
2.1.4 RNA isolation and Reverse transcription 37
2.1.5 RT-PCR 37
2.2 Methods 37
2.2.1 Cell culture 37
2.2.2 Maxi prep of *SNORD44* and *SNORD44* mutant 38
2.2.3 Nucleofection 39
2.2.4 Electroporation 40
2.2.5 Determination of cell survival and apoptosis following transfection 40
2.2.6 Cell cycle analysis 42
2.2.7 RNA isolation 44
2.2.8 Real time PCR using miRCURY LNA miRNA PCR System. 44
2.2.9 Z-VAD-FMK treatment 48
2.2.10 MTS assay 48

2.2.11 Statistical analysis.....49
3 Results.....50
3.1 Optimisation of transfection.....50
3.2 Optimisation of nucleofection programme.....52
3.2 Effects of *SNORD44* transient expression on the survival of Jurkat T cells.....54
3.3 Effects of *SNORD44* transient expression on the survival of CEM-C7 T leukemic cells.....61
3.4 Effects of Overexpression of mutant SNORD44 on the viability of leukemic T cells.....67
3.5 Effects of pan-caspase Inhibitor Z-VAD-FMK on the pro-apoptotic effects of *SNORD44*.....77
4 Discussion.....82
5 References.....93
6 Appendices.....101
Appendix A.....101
Appendix B.....103
Appendix C.....107

i List of Abbreviations

Small Nucleolar RNAs : snoRNAs

Platelet-derived growth factor : PDGF

Vascular endothelial growth factor-A : VEGF-A

Non-coding RNAs : ncRNAs

Transfer ribonucleic acid : tRNA

Ribosomal ribonucleic acid : rRNA

Long non-coding RNAs : lncRNAs

Small non-coding RNAs : sncRNAs

X-inactive specific transcript : Xist

RNA-induced silencing complex : RISC

Metastasis associated lung adenocarcinoma transcript-1 : MALAT-1

MicroRNAs : miRNAs

Small nuclear RNAs : snRNAs

Extracellular RNAs : exRNAs

Small cajal body-specific RNAs : scaRNAs

Multidrug resistance protein 1 : MDR1

C/D box snoRNAs : SNORDs

H/ACA box snoRNAs : SNORAs

Ribonucleoproteins : RNP

5’-terminal oligopyrimidine : 5’-TOP

Growth arrest specific transcript 5 : GAS5

pcDNA3.1-SNORD44 wild type : pcDNA3.1-U44

pcDNA3.1-mutant SNORD44 : pcDNA3.1-U44$^{(-)}$

SNORD44 : snoRNA U44

SNORD44$^{(-)}$: snoRNA U44 mutant

ii Abstract

Small nucleolar RNAs (snoRNAs) are a class of small non-coding RNAs that act as guide RNAs for post-transcriptional chemical modifications of ribosomal and spliceosome RNAs. Recent independent reports have indicated that these small non-coding RNAs are involved in the control of cell fate and their dysfunction or dysregulation of their expression might be associated with oncogenesis. *SNORD44* is a C/D box small nucleolar RNA that has been reported to show decreased expression levels in breast cancer and head and neck squamous cell carcinoma tissues. The *SNORD44* host gene is the long non-coding RNA growth arrest specific transcript 5 (*GAS5*), which has been strongly implicated in various types of cancers. Expression of *SNORD44* has been reported to be decreased in breast cancer cells along with leukemic T-cells. However, the function of *SNORD44* in the regulation of leukemic cell fate is still unknown. In this study, the effects of *SNORD44* overexpression have been investigated in two leukemic T-cell lines, Jurkat and CEM-C7. Overexpression of *SNORD44* caused a reduction in the number of viable and total cell count and an increase in basal apoptosis. Mutations in *SNORD44* abolished the growth inhibitory and proapoptotic effects of *SNORD44*, suggesting that the structure of *SNORD44* is important to perform its effects. Treating the cells with the pan-caspase inhibitor Z-VAD-FMK also inhibited *SNORD44* growth inhibitory effects, implicating caspases in *SNORD44* mechanisms of action. Overall the data showed that *SNORD44* has tumour suppressing effects on leukemic T-cells. From these findings we postulate that control of survival and apoptosis by *SNORD44* has significant consequences for leukaemia pathogenesis.

iii Acknowledgments

I would like to thank my supervisor Dr Mirna Mourtada-Maarabouni for the endless support I have received throughout my studies. I would also like to thank Professor Gwyn Williams, Nadieh Kavousi and Katerina Bountali for being a pleasure to work with during my studies. Thank you to Dr Mark Pickard and Professor Gwyn Williams for providing the *SNORD44* sequences used in this study.

1 Introduction

1.1 Cancer and its hallmarks

Cancer is a disease in which abnormal cells of the body divide uncontrollably. Cancerous cells acquire biological capabilities to be able to evade the body's defences and survive in a tissue micro-environment. There are ten principle mechanisms in which cancer cells employ to be able to survive. Hanahan and Weinberg (2000) first described six of these hallmarks, the first of these being the ability of cancerous cells to sustain proliferative signalling. Normal tissues control the release of mitogenic growth signals that progress the cells through the cell cycle, but cancerous cells deregulate these signals which enable them to continuously progress through the cell cycle and growth cycle from a dormant phase. Mitogenic growth signals are usually produced by one cell type but cancer cells acquire the ability to produce these mitogenic growth factors themselves to have a continuous supply. This method of producing growth factors signals themselves will result in autocrine proliferative stimulation. Platelet-derived growth factor (PDGF) is a growth factor that is important in blood vessel formation. Glioblastomas are excellent at producing this growth factor to allow for an increased blood supply to the tissue (Farooqi and Siddik, 2015).

A second hallmark of cancer is the ability of cells to evade growth suppressors. Tumour suppressor genes are already present in cells and have the capability to negatively regulate cell proliferation. In tumour cells, these suppressor genes are typically downregulated which consequently results in an evasion of senescence and apoptosis. The *TP53* gene receives information from the cells on stress and abnormalities within the genome. When there is damage present in the genome or the levels of nutrients required for cell growth are too low, the *TP53* gene can inhibit

cell cycle progression until the damage or levels of nutrients are fixed by releasing the gene product p53. In extreme conditions, p53 can trigger apoptosis to kill cells that are irreparable (Hanahan and Weinberg, 2011). Over half of all tumours are found to have a mutation or deletion in the *TP53* transcription factor gene which means that the proteins produced by this gene cannot be produced and therefore cannot stop cell cycle progression if cell damage is detected (Gutschner and Diederichs, 2012).

Another hallmark is replicative immortality, the ability to divide indefinitely. Normal cells can only replicate a set number of times due to chromosome shortening, resulting in cell death. On the other hand, cancerous cells express an enzyme called telomerase which has a primary function of adding telomeric repeats to the end of telomeres, allowing the cells to carry on replicating. Telomerase is almost non-existent in mature cells but is found in high quantities in cancerous cells. This enables cancerous cells to evade the inevitable senescence seen when normal cells reach the end of their replicative potential (Hanahan and Weinberg, 2011).

The fourth hallmark of cancer cells is the ability to invade other parts of the body and metastasize. Cancer cells must undergo biological changes to be able to invade other tissues and eventually into the blood system. These biological changes include how they attach to the extracellular matrix and other cells. The process of cancerous cells being able to move around the body is called the invasion-metastasis cascade. Local invasion of normal cells is the first process, followed by invasion into the blood stream. From the blood stream these cells can travel around the body and invade any tissue, forming a secondary tumour (Talmadge and Fidler, 2010). Integrins are an example of important player in the invasion-metastasis cascade when cancerous cells are formed from epithelial cells. Integrins mediate

cell adhesion to important components of the extracellular matrix which allows the cancer cells to invade other tissues (Talmadge and Fidler, 2010). During this process cancerous cells must not be detected by the body's own defence system.

Inducing angiogenesis is the fifth hallmark of cancer cells. As the tumour grows, the requirement for oxygen and nutrients is increased therefore the cells must find a delivery system for these increased requirements. Cancerous cells can form new blood vessels to deliver these nutrients straight to the tumour. New blood vessels can be formed by inducing pro-angiogenic factors or blocking antiangiogenic signals. One of the most well-known angiogenic factors is vascular endothelial growth factor-A (*VEGF-A*) gene. This gene encodes ligands that are used during embryonic development as they have an important role in producing new blood vessels. Cancer cells can trigger *VEGF-A* expression which will in turn allows for blood vessel production (Ferrara, 2010). This hallmark is one of the first to be triggered when a tumour is growing.

The sixth hallmark is the ability of cancer cells to evade cell death, therefore rendering them immortal. *TP53* loss or mutation can make cells more resistant to apoptosis as it can arrest the cell cycle or induce apoptosis when damage is detected within the genome. This mutation/loss is present in 50% of cancers. An increased expression of factors that help cell survival can also help cells evade apoptosis. An example of one of these apoptotic inhibitors is Bcl-2. Bcl-2 binds to Bax and Bak, pro-apoptotic trigger proteins, to inhibit them. When these proteins are inhibited, cytochrome C cannot be released and therefore the caspase cascade cannot be initiated (Hanahan and Weinberg, 2011).

In 2011, Hanahan introduced four new hallmarks of cancer, bringing the total up to ten. Figure 1 below shows the most up to date number of hallmarks.

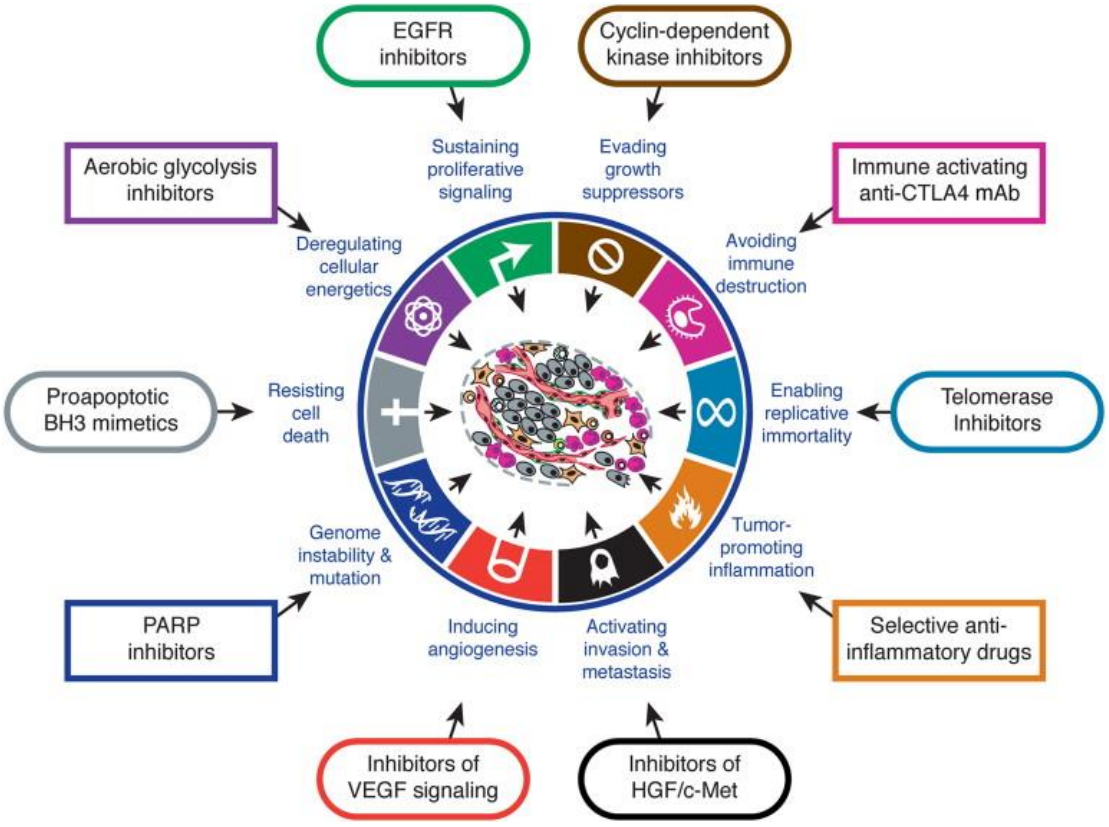

Figure 1: The ten proposed hallmarks of cancer, including the therapeutic targets for each (Hanahan and Weinberg, 2011) The text in coloured outlines shows the possible methods to target each hallmark. Genome instability and mutation, tumour-promoting inflammation, deregulating cellular energetics and avoiding immune destruction are the 4 new proposed hallmarks bringing the total up to 10.

The seventh hallmark proposed is genome instability and mutation. This hallmark relies on the basis that some genotypes have a survival advantage over others and allow the original six hallmarks to be more successful. Cancer cells can increase the rates of mutation within the genome. This ability is performed by increasing the cells sensitivity to mutagenic agents, e.g., carcinogens, or by compromising the detection systems of damaged cells (Hanahan and Weinberg, 2011).

The eighth hallmark is inflammation inducing tumour formation. Tumours often have many cells from the innate and adaptive immune systems within them. Inflammation

provides growth factors, proangiogenic factors and extra-cellular matrix modifying enzymes such as matrix metalloproteinases to the tumour microenvironment. Similarly, to the seventh hallmark, providing these biological molecules to the microenvironment allows the six original hallmarks to be more successful (Hanahan and Weinberg, 2011). Inflammatory cells release reactive oxygen species which are mutagenic (Grivennikov et al., 2010). This means that any healthy cells nearby may become cancerous and help to grow the tumour.

The ninth hallmark is the ability of cancerous cells to evade immune destruction. The immune system is constantly detecting abnormal cells but sometimes these cells can evade detection and are able to grow out of control. Tumours can evade the immune system in several ways, one of them being damaging cytotoxic T cells functionality via the creation and secretion of immune suppressive cytokines. Any cell, healthy or not, can produce these cytokines if they are present in the tumour microenvironment (Landskron et al., 2014). Cytotoxic T cells are crucial in killing cancerous cells along with any cell that has been infected or damaged.

The final hallmark is the deregulation of normal metabolism pathways. Warburg (1930) first described the way in which cancer cells can re-programme the metabolism of glucose to purely perform glycolysis, a state which is called ‘aerobic glycolysis’. The normal glucose metabolism of oxidation of pyruvate, the citric acid cycle and the electron transport chain are halted. Glucose transporters, such as GLUT-1, are upregulated in cancer cells to compensate for the lower efficiency of ATP production caused by a change to glycolysis as a method of producing glucose. An upregulation of glucose transporters leads to more glucose being transported to the cytoplasm (Hanahan and Weinberg, 2011).

1.2 Role of non-coding RNAs in cancer

1.2.1 Non-coding RNAs

The ENCODE project used high-throughput sequencing of transcripts within the genome of eukaryotes to reveal that while approximately 90% of genomic DNA is transcribed, only 1-2% of the transcribed genomic DNA encodes for proteins (the ENCODE Project Consortium et al., 2007). Non-coding RNAs (ncRNAs) are RNA molecules that do not translate into a protein and surprisingly compose 88-89% of all transcribed genomic DNA. The genome of mammalian cells is transcribed to produce sense, antisense, intergenic, intronic and bidirectional ncRNAs (Carninci, et al, 2005) which are categorised depending on their distance from protein coding genes. An example of this categorisation is ncRNAs located between two genes being named intergenic ncRNAs.

Historically, proteins were considered as the only molecules that could perform biological functions; however, this is now known to be false. Jacob and Monod (1961) were the first to conclude that ncRNAs regulate genes, however, at the time it was still widely believed that ncRNAs only performed basic cell functions that were already confirmed, such as transfer ribonucleic acid (tRNA) and ribosomal ribonucleic acid (rRNA) being involved in mRNA translation (Mattick and Makunin, 2006). Brannan et al. (1990) set out to discover new protein coding genes by screening a cDNA library of foetal liver but in fact discovered novel ncRNAs which were clearly different to the already established classic ncRNAs such as rRNAs and tRNAs.

There have been various controversies surrounding the function of ncRNAs, Rajendra et al. (2001) proved that ncRNAs have a role in the developmental process not only in mammalian cells but in other organisms such as *Drosophila*

melanogaster. Interestingly, Liu et al. (2013) confirmed that there is a strong correlation between the complexity of an organism and the proportion of non-coding RNA genes present in the genome. This finding firmly supports the idea that ncRNAs must have functional roles within the genome. The hypothesis that these ncRNA loci are 'junk' is therefore severely outdated and these transcripts should be investigated further. The technology to analyse and identify these transcripts has improved dramatically in the past decade and consequently new ncRNAs have been discovered. Many studies have already been performed and provided substantial links between ncRNAs and human diseases. For example, BACE1 is an enzyme that has an important role in the formation of Aβ plaques in nerve cells. Inhibition of BACE1 may prevent Aβ plaque formation. Faghihi et al. (2008) reported that the antisense BACE1 (BACE1-AS) transcript is upregulated 6-fold in patients with Alzheimer's disease compared to healthy patients and the elevated levels of BACE1-AS contributes to the disease progression. BACE1 protein production is tightly regulated by BACE1-AS, therefore any alterations in levels of BACE1-AS could influence the production of BACE1. In this case, the alteration in BACE1-AS influences the production of amyloid-beta (Aβ) which can cause the assembly of Aβ plaques, a key indicator of Alzheimer's disease.

ncRNAs are split into two groups, long non-coding RNA (lncRNAs) and small non-coding RNAs (sncRNAs). These two groups are differentiated by the length of nucleotides, 200 nucleotides or less being sncRNA and any transcripts with more than 200 nucleotides is classed as lncRNA (Peschansky and Wahlestedt, 2014).

1.2.2 Role of long non-coding RNAs

lncRNAs are classified into six subtypes, antisense, intergenic, overlapping, intronic, bidirectional and processed. RNA is classified into these groups depending on the

direction and position of transcription when compared against other genes (Peschansky and Wahlestedt, 2014). Many of these RNA molecules have important functions in regulating gene expression including gene activation and inhibition. An insight into the variety of functions lncRNAs perform can be seen in Figure 2.

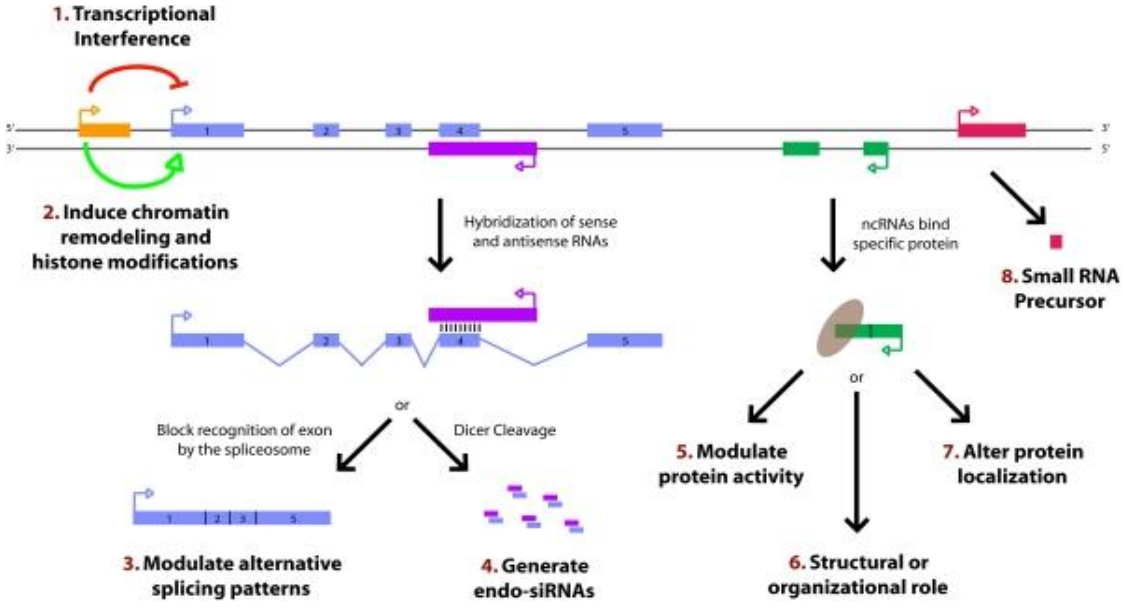

Figure 2: An overview of the functions of lncRNA. The blue boxes show the introns and exons and the yellow box shows the initial lncRNA gene. (1) Transcription of lncRNA can either positively (green arrow) or negatively (red arrow) (2) effect the expression of a nearby gene. (3) Antisense of sense RNA can block the recognition of exons to result in alternative splicing or (4) Dicer cleavage to produce siRNA. Dicer is an enzyme that cleaves double-stranded RNA and pre-microRNA into smaller fragments. Binding of ncRNA to specific proteins can result in protein activity being modulated (5). It can also play a structural/organisational role that forms a complex (6) or it can change where the protein is in the cell (7). LncRNA can be further processed to produce sncRNA (8) (Wilusz et al., 2009).

lncRNAs can either positively or negatively affect the expression of genes. Transcription of ncRNAs can negatively affect the ability of genes nearby to be expressed. If transcription of a ncRNA along the promoter region of another RNA would inhibit transcription factor binding, there would be no expression of the RNA. Another function of lncRNAs is to act as a precursor to other smaller non-coding RNAs. miRNAs can be produced by the cleavage of lncRNAs by drosha and dicer. lncRNAs can also affect the location and function of the proteins they bind to. NRON (noncoding repressor of NFAT) is a lncRNA that is a key regulator in the

movement of NFAT around the cell. NRON binds to cytoplasmic machinery to inhibit the accumulation of NFAT (Wilusz et al., 2009).

Long intergenic non-coding RNAs (lincRNA) are a subset of lncRNAs that are classified based on their location between protein coding genes. There is an estimated 3,000 lincRNA genes present in the human genome but only 1% of these have been fully investigated (Khalil et al., 2009). Identifying lincRNA molecules that are present in cancer cells in either significantly lower or higher levels than normal cells could determine whether they function in oncogenesis. Ching et al., (2016) performed this analysis identifying lincRNAs relating to tumour diagnosis, subtyping cancers and prognosis of the disease, and identified thousands of differentially expressed lincRNA genes in only 12 cancer types. From this study, they were able to identify a group of six lincRNAs that could be potentially used as pan-cancer diagnostic biomarkers. These lincRNAs are PCAN-1, PCAN-2, PCAN-3, PCAN-4, PCAN-5 and PCAN-6. More recently, a link between knockdown of lincRNA-p21 and the increased radio sensitivity of hypoxic tumour cells was identified which could enhance radiotherapy treatment of cancer (Shen et al., 2017).

One of the earliest lincRNAs discovered is X-inactive specific transcript (Xist) that is 15-17kb long and the gene is located on the X chromosome. This RNA is transcribed from the *XIST* gene (Brown et al., 1991) and is important in X inactivation. X inactivation ensures that the transcript levels are equal between males and females. Xist has already been shown to be upregulated in several types of cancer which suggests a potential for its use in biomarker diagnostics (Hu et al., 2017). Due to Xist possessing a huge role in development and growth, it is natural to investigate its potential as a target to inhibit cancer cell growth. Yildirim et al. (2013) have proved that Xist deletion in the stem cells of glioblastoma patients decreased cell

proliferation and promoted apoptosis (Yildirim et al., 2013). The study also confirmed that Xist and miR-152 have a reciprocal suppressive effect which indicates there is some relationship between the two ncRNAs. Expanding on this point, the binding active site of Xist is functional for miR-152 therefore some silencing effects by the miR-152 could be occurring via the RNA-induced silencing complex (RISC). The RISC is a ribonucleoprotein complex with a single strand RNA incorporated. This single stand acts as a template for the complex to eventually cleave target mRNA via argonaute (Pratt and MacRae, 2009). The RISC acts in a post-transcriptional fashion. Metastasis associated lung adenocarcinoma transcript 1 (MALAT-1) is an extensively studied lincRNA regarding its involvement in cancer. Ji et al. (2003) first discovered MALAT-1 at high levels in non-small cell lung cancer. MALAT-1 is 8000 nt long and expressed from chromosome 11q13. MALAT-1 is conserved in a variety of species which suggests its importance for cell function (Ma et al., 2015). In breast cancer, this lincRNA is upregulated significantly (Guffanti et al., 2009) and has the potential to be used as a diagnostic biomarker. The levels of MALAT-1 varies from cancer to cancer therefore a specific threshold of what is considered an upregulation must be established before any research is performed. Following on from this point, the potential for MALAT-1 to be a diagnostic biomarker has been researched. Wang et al. (2016) used the GEO database to determine if MALAT-1 can be used as a biomarker. A total of 19 datasets were identified from the GEO database with a total of 2142 samples. The data collected showed that MALAT-1 can be used as a biomarker in a variety of cancers as an indicator of good/bad prognosis. Li et al. (2017) concur with the previous conclusion and concludes that MALAT-1 can be used a biomarker for bladder cancer. To determine the functions of MALAT-1, the relationship between MALAT-1 levels and overall

survival of patients was established. This is shown in the Kaplan-Meier plot in Figure 3.

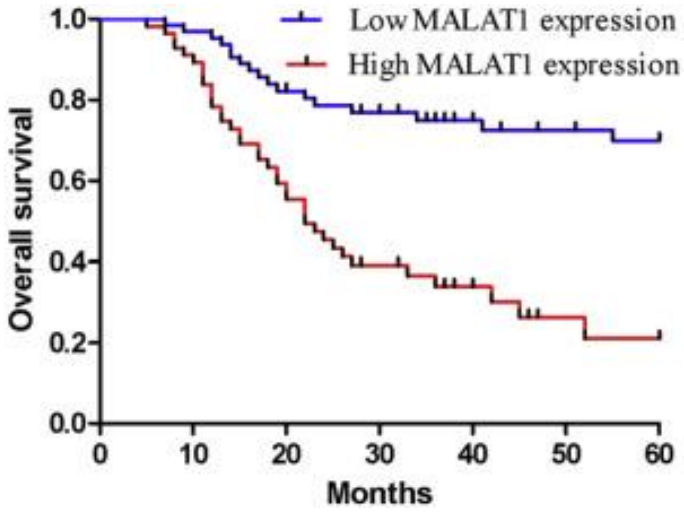

Figure 3: Relationship between MALAT-1 levels and the overall survival of patients with bladder cancer. Kaplan-Meier plot to show the relationship between expression of MALAT-1 and the overall survival of patients in months (Li et al., 2017)

Figure 3 shows that the levels of MALAT-1 correlate to cancer progression, including the migration of cancer to the lymph nodes. Han et al. (2013) agreed with these results finding that levels of MALAT-1 are elevated in invasive bladder cancer compared to non-invasive. Detecting the levels of MALAT-1 in patients could determine the intensity of treatment needed based on the overall survival rate and in turn can determine prognosis.

Luan et al. (2016) analysed that MALAT-1 acts as a competing RNA to sponge miR-22 to promote malignant melanoma growth and metastasis. This research was crucial in understanding how lncRNAs interact with other RNA molecules such as miRNAs. Subsequent studies have been executed exploring possible interactions between MALAT-1 and miRNAs with the intention to understand how MALAT-1 is involved in cancer. Zuo et al. (2017) determined that MALAT-1 induces proliferation

and invasion of cancer cells by targeting miR-129-5p in triple-negative breast cancer. Both studies hint at using MALAT-1 as a target for a novel cancer therapy.

1.2.3 Role of Small non-coding RNAs in cancer

Since the discovery of sncRNAs (Lee et al, 1993; Hamilton and Baulcombe, 1999), the understanding of how gene expression is controlled has been altered considerably. High throughput RNA/DNA sequencing has been a reliable method to identify a variety of these small non-coding RNAs (Ryvkin et al., 2014). This group of ncRNAs can be differentiated further into subgroups depending on their properties and functions including how they are produced. These subgroups are microRNAs (miRNAs), small interfering RNA (siRNAs), piwi-interacting RNAs (piRNAs), small nucleolar RNAs (snoRNAs), small nuclear RNA (snRNAs), extracellular RNA (exRNAs), and small cajal body-specific RNA (scaRNAs). snoRNAs are a class of small non-coding RNA that has a primary function of inducing chemical modifications of other RNAs, including transfer and ribosomal RNA. Modification can include methylation and pseudouridylation.

Small non-coding RNAs have important roles in cancer development and progression. miRNAs have already been discovered to have tumour suppression and oncogenic properties (Zhou et al., 2017). They are also involved in drug resistance of cancer and can be used as biomarkers to detect the presence of cancer (Ogata-Kawata et al., 2014).

miRNAs originate from pri-miRNA that is cleaved by Drosha to form pre-miRNA in the nucleus. The pre-miRNA is then cleaved by DICER to form smaller fragments of RNA called miRNA. miRNA genes are transcribed by RNA polymerase II. They are involved in RNA silencing along with post-transcriptional regulation of gene

expression. miRNAs use complementary base sequencing to silence target mRNAs (Wahid et al., 2010). The first link between miRNAs and cancer was established by Calin et al. (2004) whilst examining chronic lymphocytic leukaemia (CLL). It was found that an area on chromosome 13q14 that is deleted when a patient has CLL, in fact is made up of two genes that code for miRNAs. This finding lead to the same research group mapping 186 miRNAs and comparing their location to the regions involved in genetic mutations. It was concluded that 52.5% of the miRNAs mapped were in cancer-associated regions. This discovery sparked a revolution of research into the roles of miRNAs in cancer progression and diagnostics.

miRNAs have shown great promise in being possible diagnostic tools for cancer. Ogata-Kawata et al. (2014) identified that seven miRNAs, miR-1229, miR-1246, miR-150, miR-21, let-7a, miR-223 and miR-23a, had higher levels in the serum samples of colon cancer patients at every stage of the disease. To add to this, the same study identified that colon cancer cell lines expressed these miRNAs at higher levels than normal colon cell lines. Mishra et al. (2015) investigated further into the possibilities of miRNAs as biomarkers by expression profiling peripheral blood mononuclear cells (PBMCs) of breast cancer patients. From the expression profile created, 40 miRNAs were validated and analysed in PBMCs, blood plasma and breast tissue samples. Alongside these factors, the expression of miRNAs was also analysed in PBMCs from patients in early and advanced stage breast cancer and patients that had triple negative and positive diagnosis. It was concluded that in early stage breast cancer miR-195-5p and miR-495 levels are downregulated therefore a combination of these miRNAs could potentially be used as biomarkers for early stage breast cancer. Todeschini et al. (2017) concur with Ogata-Kawata et al. (2014) and Mishra et al. (2015) on the view that miRNA can be used as future biomarkers.

Todeschini et al. (2017) reported that miR-1246 can be used as a diagnostic marker in high-grade ovarian carcinoma. miR-1246, miR-595 and miR-2278 were found to be at elevated levels in the sera of HGSOC patients compared to healthy controls. Using Receiver Operating Characteristic curves, it was found that miR-1246 was the most suitable to use as a diagnostic marker for this type of cancer due to its accuracy of 84%.

Several lines of evidence have also implicated miRNAs in drug resistance. For example, Chen et al. (2016) confirmed a relationship between many miRNAs and drug resistance in breast cancer tissues in vivo. This study indicates that 9 miRNAs can be used to optimise chemotherapy drug dispensing so analyse which drugs will be most effective in specific patients. The breast cancer Formalin-Fixed Paraffin-Embedded (FFPE) tissue from a patient can be extracted and be used in vivo to profile the expression of miRNAs that play a role in chemoresistance. Kovalchuk et al. (2008) has established that miR-451 regulates the expression of multidrug resistance protein 1 (*MDR1*) gene. *MDR1* is found in the cell membrane and pumps foreign substances out of the cell. Additionally, transfection of miR-451 into MCF-7 cells resulted in an increased sensitivity to the chemotherapy drug doxorubicin. Normalising levels of miR-451 could therefore lead to drug resistance being reduced.

siRNAs are double stranded small RNAs of 20-25 nt in length, that take part in regulating gene expression. They regulate gene expression by degrading target mRNAs after transcription so that they cannot be translated. These ncRNAs are produced by the dicer enzyme from double stranded RNA and small hairpin RNAs. Following on from miRNA being involved in chemotherapy drug resistance, there have been a plethora of studies performed with siRNAs to overcome the same

problem due to its role in interfering with gene expression. Azimi et al. (2017) explored the use of siRNAs to overcome drug resistance to doxorubicin with the aim of supressing the expression of p53R2. Saad et al. (2008) concluded that siRNA targeted to BCL2, MRP1 and MDR1 mRNA induces apoptosis in HepG2 cells. Using doxorubicin in combination with these targeted siRNA requires a smaller dosage to kill cancer cells. Polo-like kinase-1 (PLK1) has already been identified as a target for tumour suppression as it is essential for spindle formation in mitosis (Spänkuch-Schmitt et al., 2002). This study also suggested an opportunity to investigate the anti-proliferative effects of siRNA in relation to PLK1.

Li et al. (2016) generated a multi-target siRNA pool as a possible therapeutic technique in hepatocellular carcinoma (HCC) targeting Neuroepithelial cell transforming 1 (NET-1), cortactin gene (*EMS1*) and vascular endothelial growth factor (VEGF). NET-1 is a gene involved in cancer cell proliferation, *EMS1* is involved in cancer cell motility and VEGF promotes angiogenesis. Inhibiting the expression of these genes would potentially inhibit the cancer cell survival. Indeed, the study showed that the proliferation and migration of cancer cells were inhibited when the mutli-target siRNAs pool was transfected into HCC cells. Apoptosis was also induced in the cells transfected with the siRNA pool. The study provided evidence that there is a therapeutic potential for such approach.

snoRNAs are another subclass of small non-coding RNAs in which the current study will be focused on. The function of many of these RNAs in cancer are yet to be fully understood. The rest of this section will be focused on snoRNAs.

1.3 Small nucleolar RNAs (snoRNAs)

snoRNAs are a subtype of sncRNAs that are known to have an important role in the post-transcriptional modification of ribosomal RNAs and small nuclear RNAs (snRNAs). Such modifications are essential for the biogenesis of ribosomes. In addition to their role in ribosomal RNA biogenesis, emerging evidence is implicating snoRNAs in several cellular functions including alternative RNA splicing, regulation of chromatin structure, metabolism, and oncogenesis (Warner et al., 2018). Typically, snoRNAs are 60-300 nt long, single stranded and can be mainly classified into two types based on the presence of highly conserved sequences. These include C/D box snoRNAs (SNORDs) and H/ACA box snoRNAs (SNORAs) (Balakin et al., 1996). C/D box snoRNAs are associated with 2'-*O*-methylation whilst H/ACA box snoRNAs are associated with pseudouridylation. Figure 6 below depicts the differences between these two types of snoRNAs.

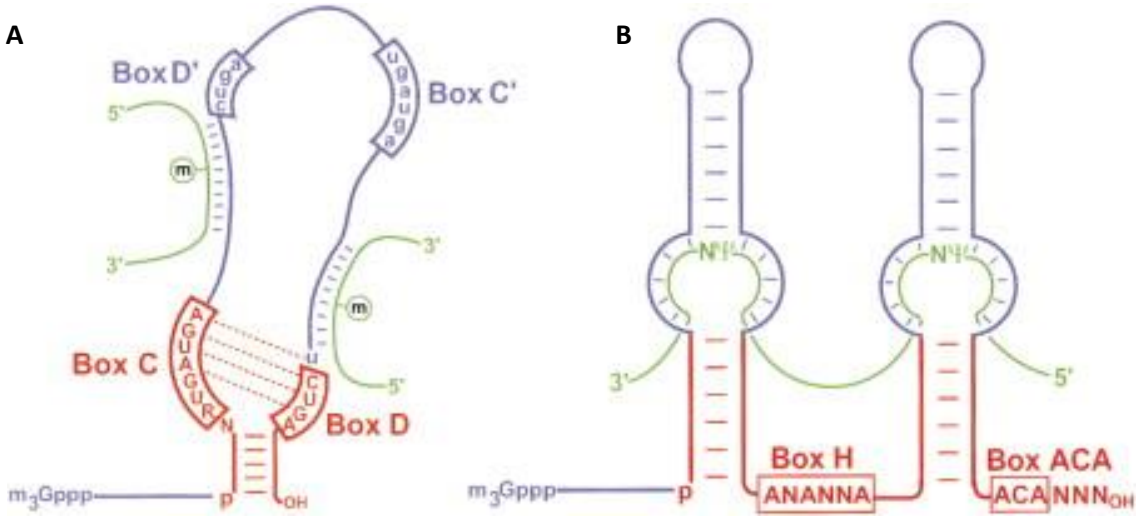

Figure 6: Diagram to show the two types of snoRNAs. (A) a C/D box snoRNA. (B) a H/ACA box snoRNA. The C/D box snoRNAs contain the motifs of C (RUGAUGA) and D (CUGA) whilst the H/ACA box snoRNA contain the motifs H (ANANNA) and ACA (Tamas, 2002).

Most snoRNAs are found already encoded within the transcript of other genes, also known as 'host genes' but also can be transcribed from RNA polymerase II or III

units. snoRNA can associate themselves with ribonucleoproteins (RNP) to form a new molecule called snoRNPs which in turn have their own individual function to regulate rRNA. The C/D box snoRNPs regulate specific 2′-*O*-methylation of ribose (Kiss-laszlo et al., 1996) while the H/ACA snoRNPs catalyse isomerization of uridine (Ganot et al., 1997). A third category of snoRNAs have been discovered, named small Cajal body-specific RNAs (scaRNAs). These scaRNAs are found in Cajal bodies and have an important role in post-transcriptional modification including methylation and pseudouridylation, of spliceosomal small nuclear RNAs U1, U2, U4, U5, and U12 (Scott and Ono, 2011).

1.3.1 Role of snoRNAs in cancer

snoRNAs are of interest due to their proven involvement in oncogenic diseases such as cancer. The first link between snoRNAs and carcinogenesis was made by Chang et al., (2002) where h5sn2 was found to be highly expressed in a normal brain while its expression level in patients with meningioma was greatly decreased. This correlation discovery sparked a burst of research on snoRNAs in recent years.

An example of snoRNAs involvement in cancer is the effects that altered *SNORA42* levels have on non-small cell lung cancer (NSCLC) progression and tumour growth. Mei et al. (2012) reported that the knockdown of *SNORA42* inhibited H460 and H1944 NSCLC cell colony formation and, when using nude mice animal models, the same inhibition of tumour colony formation was observed. Opposing this, the overexpression of *SNORA42* activates the growth of NSCLC cancer cells according to the same study. A strong correlation was shown between expression of *SNORA42* and survival of patients with non-small cell lung carcinoma (Mei et al., 2012).

Dong et al. (2008; 2009) identified a novel C/D box snoRNA, *SNORD50A* that is clinically significant to breast and prostate cancers. *SNORD50A* (U50) is located within chromosome 6q4.31, a locus known to harbour a tumour suppressor gene. U50 snoRNA levels were found to be down-regulated in breast and prostate cancers. Overexpression of *SNORD50A* in prostate cancer cells inhibits colony formation. Interestingly, a homozygous deletion of 2 base pair in *SNORD50A* was found to be significantly associated with prostate cancer. Overexpression of the *SNORD50A* mutant form abolished the inhibitory effects on colony formation observed with overexpression with *SNORD50A* wild type (Dong et al., 2009). U50 could therefore be acting as tumour suppressor and a target for a possible therapy as it is proven by these studies to play a role in breast and prostate cancer development. Yi (2018) performed a study on *SNORA42* in relation to its role as an oncogene in prostate cancer. This study also looked at the effect of overexpressing and knocking down *SNORA42* on the cell cycle. Overall, overexpressing *SNORA42* promotes the cell cycle progression. It was also shown that *SNORA42* overexpression decreases basal apoptosis whilst siRNA induced silencing of *SNORA42* increases basal apoptosis, providing evidence that *SNORA42* could act as an oncogene.

The number of snoRNAs investigated thoroughly is low and therefore a gap in scientific knowledge is present. Analysing the role of these snoRNAs in cancer may lead to novel targets for cancer therapy being established. Gong et al., (2017) profiled approximately 10,000 samples of cancer patients covering 31 cancer types for the snoRNAs that are involved to further understand the relationship between snoRNA and tumorigenesis. 46 snoRNAs were found to be clinically relevant. Figure

7 below shows the number of snoRNAs found to be involved in specific cancer types.

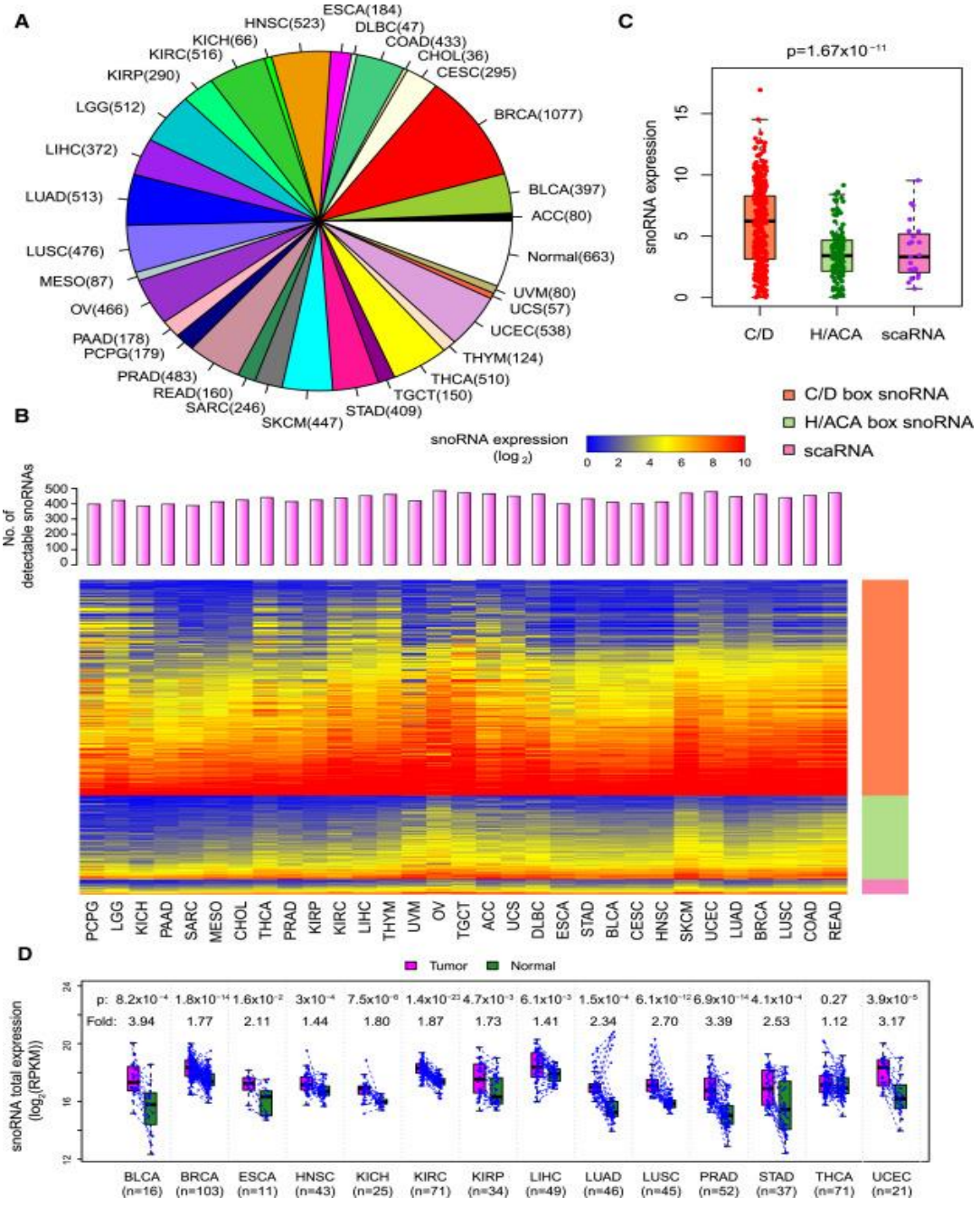

Figure 7: Graphs to show the spread of snoRNAs found in 31 different cancer types and from 10,000 samples. (a) A pie chart of the number of samples taken from each cancer type. (b) The types of snoRNAs against the number of detectable snoRNAs. (c) The expression of snoRNAs against the two types of snoRNAs and scaRNAs. (d) The snoRNAs total expression of 14 types of cancer against normal samples (Gong et al., 2017).

Figure 7b shows that more than 300 snoRNAs are involved in all 31 cancer types. This suggests that snoRNAs may have role in tumorigenesis and could be a possible target for therapy. The altered levels of snoRNAs between normal cells and cancer cells shown in Figure 7d is a second indication of snoRNAs involvement in cancer. An example of one clinically relevant snoRNA identified by this paper was C/D box *SNORD*78, a snoRNA localised in the intronic region of growth arrest specific 5 gene (*GAS5*). *SNORD78* has already been identified to be overexpressed in NSCLC and prostate cancer, and in this study has proven to have clinical significance in 14 cancer types in total, including Cholangiocarcinoma.

SnoRNAs are small molecules that are relatively stable in serum which stimulated research into their potential as disease biomarkers. It is of extreme importance that non-small-cell lung cancer (NSCLC) is diagnosed early as it is one of the leading causes of cancer related deaths. Liao et al., (2010) performed analysis on patient samples that have been diagnosed with NSCLC and found that six snoRNAs are significantly associated with NSCLC. These include *SNORD33*, *SNORD66*, *SNORD73B*, *SNORD76*, *SNORD78* and *SNORA42*. The levels of three of these snoRNAs, *SNORD33*, *SNORD66* and *SNORD76*, were found to be significantly increased when compared to patients with chronic obstructive pulmonary disease (COPD), a disease that shows similar symptoms to NSCLC. This data therefore suggests that these three snoRNAs can be used as biomarkers of NSCLC. Yoshida et al. (2017) investigated the potential of *SNORA21* as a biomarker in human colorectal cancer, the second leading cause of death in cancer patients. The study used a wide variety of bioinformatics analysis and datasets from 489 colorectal cancer tissue samples. Results showed that *SNORA21* is significantly upregulated in colorectal cancer and its increased levels correlated with metastasis and poor

prognosis, highlighting its potential as biomarker for the disease. Xenograft models are important as *in vitro* and *in vivo* models can react differently when the same experiment is performed. In this study, colorectal adenocarcinoma SW48 cells that had been treated with CRISPR-*SNORA21*/Control constructs were injected into mice to monitor tumour growth. After 42 days, the tumour growth of the cells with the control construct was significantly larger than the CRISPR-*SNORA21* construct cells. This data indicates that knockdown of *SNORA21* reduces tumour growth *in vivo* and confirmed that *SNORA21* must be important for tumour growth and could be used a biomarker for the disease (Yoshida et al., 2017).

Many snoRNA are found transcribed from the intronic regions of their 'host genes' which can be protein coding or non-protein coding. The first host gene discovered was the ribosomal protein S1 gene from *Xenopus laevis* in which several forms of U15 snoRNAs are encoded (Pellizzoni et al., 1994). UHG is another host gene that encodes the snoRNA U22. This host gene is a lncRNA and does not encode a protein product. UHG also encodes seven C/D box antisense snoRNAs, named U25 to U31 (Frey et al., 1997). Another lncRNA which acts as snoRNA host gene is *GAS5*. *GAS5* plays an important role in controlling the survival of many cancer cell types and have been shown to act as tumour suppressor in various cancers.

1.4 Growth arrest specific transcript 5 (*GAS5*) and its snoRNAs

1.4.1 *GAS5* and its role in cancer

GAS5 is a long intergenic RNA that was initially identified by cDNA cloning of genes that are expressed in growth arrested cells (Schneider et al., 1988). It acts as a repressor of the glucocorticoid receptor by acting as a glucocorticoid response element (GRE) which competitively competes with the actual DNA GRE substrate (Kino et al., 2010). *GAS5* is located on chromosome 1q25 which is associated with many cancers including prostate cancer (Pickard et al., 2013). The *GAS5* gene consists of 12 exons with a very short open reading frame and many stop codons within its sequence. Exon 1 contains a 5'-terminal oligopyrimidine (5'-TOP) tract, a common motif found in genes that encode proteins and involved in the biogenesis of ribosomes and translation. The *GAS5* transcript hosts ten snoRNAs within its introns and is therefore classified as a snoRNA host gene (Smith and Steitz, 1998). These snoRNAs are called U74, U75, U76, U77, U44, U78, U79, U80, U47 and U81. While U44 is involved in the 2'-O-methylation of 18S rRNA; the rest of these snoRNAs serve as a guide to modify 28S ribosomal RNA (Smith and Steitz, 1998). The location of these snoRNAs within the transcript is shown in Figure 8.

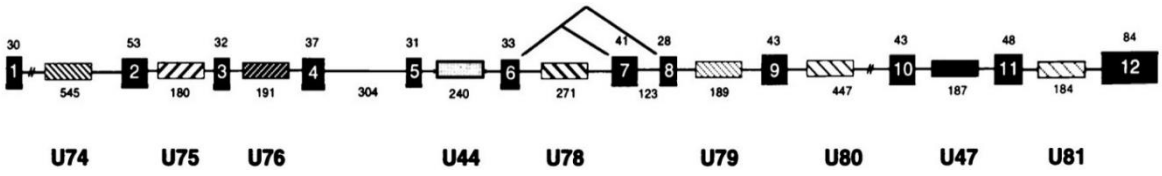

Figure 8: *GAS5* is a multi-snoRNA host gene. The black boxes represent the 12 exons in the *GAS5* transcript. The hatched boxes represent the snoRNAs present in the transcript. The lines above exon 6/7/8 represent the alternative splicing that occurs to include exon 7 (Smith and Steitz, 1998)

Smith and Steitz (1998) confirmed that *GAS5* transcripts are elevated in growth arrested cells which agrees with Schneider et al., (1988). The reason behind *GAS5* accumulation is the interplay of the mammalian target of rapamycin (mTOR) pathway (important in regulation of the cell cycle) and nonsense-mediated decay

(NMD) pathway (reduces errors in gene expression by removing stop codons in mRNA sequences). Due to the presence of the 5'-TOP sequence, *GAS5* translation would be promoted in actively growing cells due to the increased activity of mTOR pathway. However, the presence of short open reading frame and multiple stop codons in the *GAS5* transcript lead to the degradation of the *GAS5* transcripts via the NMD pathway resulting in a decrease in *GAS5* transcript levels in the actively growing cells. However, the decrease in the activity of the mTOR pathway in growth arrested cells implies that *GAS5* will not be translated, resulting in a reduced degradation of its transcripts by the NMD pathway and the accumulation of its transcripts (Pickard and Williams, 2014).

Early studies have shown that the *GAS5* transcript displays many patterns of alternative splicing and in fact has a very small open reading frame that is poorly conserved (Muller et al., 1998). The human *GAS5* gene, along with hosting snoRNAs, has two full length isoforms and 5 expressed sequence tags (ESTs) formed from alternative splicing of the transcript (Figure 9). The two isoforms differ due to changes in exon 7 which alter the length of the transcript.

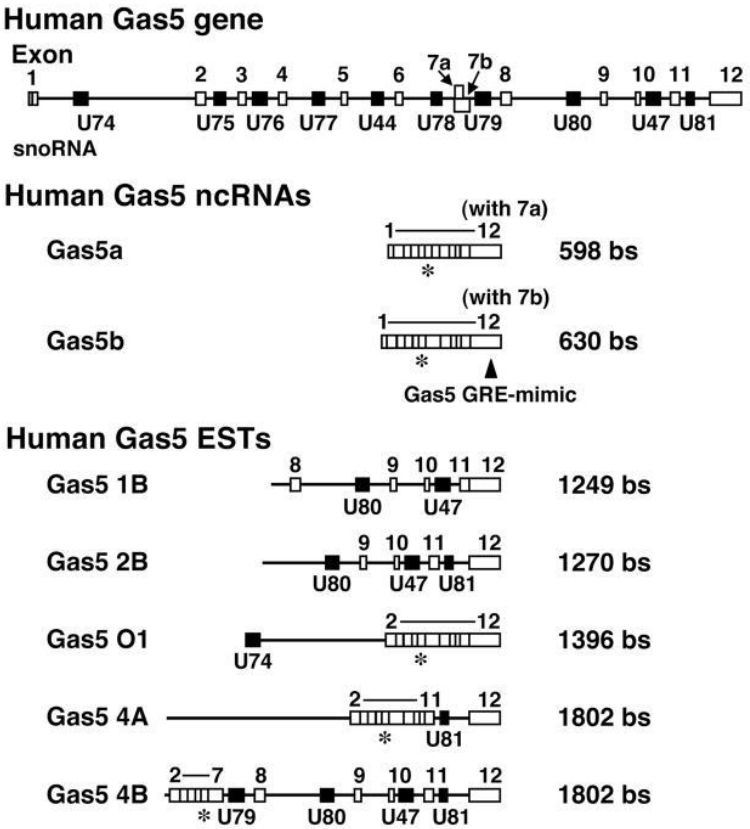

Figure 9: The organization of the *GAS5* gene and its ncRNA products. The human *GAS5* ncRNAs are produced due to alternative splicing which includes or removes exon 7. There are also 5 expressed sequence tags of the human *GAS5* transcript in which can be seen above all ranging in size. The * depicts where the siRNA was placed in the transcript to form the shorter transcripts seen in the two ncRNAs and *GAS5O1, GAS54A* and *GAS54B* (Kino et al., 2010).

Mourtada-Maarabouni et al. (2008) established that *GAS5* has a crucial role in apoptosis and in regulating normal growth arrest in both T-leukemic cell lines and non-transformed human lymphocytes. Their work showed that overexpression of *GAS5* in the T-leukemic cell lines causes both an increase in basal apoptosis and in cell cycle arrest in G0/G1. They also confirmed that *GAS5* downregulation inhibits apoptosis and results in an increased rate in cell cycle progression, highlighting the fact that *GAS5* expression is important for normal growth arrest in leukemic T-cell lines as well as human peripheral blood T-cells. Transfecting the different ESTs into leukemic T-cell lines had different effects on the cells. Transfecting *GAS54A* into leukemic cells resulted in a reduced in cell number by 77%. Transfecting *GAS5O1* also resulted in a lower cell density and viable cell density compared to the control with a percentage decrease of 56%.

Further studies examined the effects of modulation of *GAS5* expression levels on breast and prostate cancer cell fate. Mourtada-Maarabouni et al. (2009) showed that overexpression of *GAS5* in the human breast cancer cell line MCF-7, the non-tumorigenic breast epithelial cell line MCF-10A and additionally the human embryonic kidney HEK293T cell line resulted in increased levels of basal apoptosis and increased sensitivity of the cells to many apoptotic stimuli. In addition, Mourtada-Maarabouni et al., (2009) showed a decrease in *GAS5* transcript levels in samples from breast cancer patients compared to control samples. Pickard et al. (2013) also reported a decreased *GAS5* expression level in cDNA samples from patients with prostate cancer compared to cDNA from normal tissue. The study also investigated whether *GAS5* overexpression influences apoptosis and cell survival in prostate cancer cell lines. Plasmid containing various *GAS5* transcripts, including mature *GAS5* and a cloned *GAS5* sequence containing exons 1-12, were transfected into 22Rv1 and PC-3 prostate cancer cells. The results showed an increase in apoptosis drastically as the expression of *GAS5* increased. The use of *GAS5* transcript with exons 1-12 present confirms that the exons alone are enough to cause the apoptotic effects in prostate cancer cell lines.

Subsequent studies have confirmed that *GAS5* is involved in different types of cancers where it can act as tumour suppressor. The levels of *GAS5* transcripts have been found to be lower in Renal Cell Carcinoma (RCC) patient tissues than normal tissue samples (Qiao et al., 2013). *GAS5* was transfected into the human RCC A498 cell line to determine whether it influences the survival of these cells. From functional assays on the *GAS5* transfected RCC cells, it was concluded that overexpressing *GAS5* in A498 RCC cells induces apoptosis, interrupts the cell cycle and inhibits cell proliferation. Sun et al. (2014) found that the levels of *GAS5* transcripts are

downregulated in gastric cancer and a lower level of *GAS5* transcripts in gastric cancer correlated with a poor survival rate of patients. Overexpressing *GAS5* in gastric cancer cells resulted in a reduced cell growth rate compared to cells with *GAS5* silenced. Performing a colony forming assay with the cells that have overexpression of *GAS5* resulted in poor colony formation. *GAS5* overexpression also induced apoptosis in gastric cancer cells. Interestingly, the overexpression of *GAS5* was also performed *in vivo*, using nude mice. From this experiment, it was observed that overexpressing *GAS5* in these mouse models inhibited tumour growth. Wang et al. (2018) confirmed that *GAS5* has pro-apoptotic effects using bladder cancer cells. *GAS5* has a low expression in bladder cancer cell lines and its overexpression resulted in an increase in apoptosis. From a previous study by this research group, it was shown that Enhancer of zeste homolog 2 (*EZH2*) is essential for regulation of cell activity of bladder cancer cells. *EZH2* participates in histone modification and is found on the Polycomb Repressive Complex 2 (*PRC2*), which is responsible for healthy embryonic development. This study has shown that *GAS5* negatively regulated *EZH2* transcription in these cells and therefore a lower expression of *EZH2* was observed.

Identifying novel biomarkers is of great value to identify different stages and progression of diseases. Han et al., (2016) evaluated the *GAS5* transcript as a biomarker for assessing the progress a patient is making after breast surgery. This research concluded that the *GAS5* transcript could be used a biomarker post breast surgery. Liang et al., (2016) agreed with the use of the *GAS5* transcript as a biomarker alternatively for non-small cell lung cancer. PCR was conducted to analyse the expression levels of the *GAS5* transcript in all samples. As expected, the levels of the *GAS5* transcript in NSCLC patients were significantly lower than in

healthy samples. To further enhance the reliability of this study, the levels of the *GAS5* transcript were measured after surgery to remove the tumour. 7 days post-surgery, the expression of the *GAS5* transcript increased. Using the data collected it was concluded that the *GAS5* transcript can be used as a biomarker to detect NSCLC.

1.4.2 *GAS5* snoRNAs

As mentioned earlier, *GAS5* is a host gene to ten C/D box snoRNA genes, 9 of which including U74, U75, U76, U44, U78, U79, U80, U47, and U81 are encoded within introns. The fourth intron does not produce a stable detectable RNA molecule but has been named as *SNORD*77 (Smith and Steitz, 1998). Studies have reported that *GAS5* derived snoRNAs have an increased expression in various diseases, suggesting that they may play a role in the pathogenesis of this diseases.

Krell et al., (2014) performed a paramount analysis on the expression levels of RNA molecules in patients with colorectal cancer compared to healthy patients and showed that two snoRNA molecules derived from the *GAS5* transcript, *SNORD*47 (U47) and *SNORD44* (U44), have an increased level in patients with colorectal cancer. *SNORD47* found between exons 10 and 11 of the *GAS5* transcript, has been indicated to be a tumour suppressor in glioblastoma. Xu et al. (2017) overexpressed *SNORD*47 in glioblastoma cells and noted that it inhibited the proliferation, colony formation, migration and the invasion abilities of these cells. Cell cycle analysis also showed a G2-phase arrest. This suggests a tumour suppression capability of *SNORD47* in glioblastoma. The effects of *SNORD47 in vivo* was also studied in conjunction with the chemotherapeutic drug temozolomide. The brain tissues of the subjects were stained to reveal that treating with *SNORD*47 and temozolomide, both separately and in conjunction, reduced the tumour volume.

Combining both therapies improved the efficiency of the chemotherapeutic drug (Xu et al., 2017). In hepatocellular carcinoma (HCC), U47 has been shown to have an opposite effect to those reported in glioblastoma by Xu et al. (2017). *SNORD47* is highly expressed in HCC cells compared to adjacent healthy tissue samples. This study also identified that patients with high levels of *SNORD47* had a poor survival rate compared to patients with tumours with low amounts of *SNORD47*. Further functional analysis showed that a knockdown of *SNORD47* in HCC cells induces apoptosis and suppressed cell invasion (Li et al., 2017). The conclusion from this study was that *SNORD47* promotes tumorigenesis in HCC.

Two *GAS5* snoRNAs, U74 and U80, have also been shown to be significantly downregulated in NSCLC (Gao et al., 2014). Wu et al. (2018) studied the clinical significance of *SNORD76* (U76) as an oncogene and a potential diagnostic biomarker in hepatocellular carcinoma. *SNORD76* is found in the *GAS5* transcript in between exons 3 and 4. *SNORD76* knockdown inhibited the proliferation of hepatocellular carcinoma cells by inducing apoptosis and causing the cells to arrest at G0/G1 in the cell cycle. On the other hand, overexpressing *SNORD76* caused an increase in cell proliferation. This study suggests that *SNORD76* may have a role in tumorigenicity and therefore could be used as a potential biomarker as its expression is increased during the production of tumours.

SNORD44 is a C/D box snoRNA found between exon 5 and 6 of the *GAS5* transcript. Krell et al. (2014) found that there was a strong correlation between p53 expression, a tumour suppressor, and *SNORD44*. Levels of p53 was found to be increased in colorectal cancer tissues compared to normal colorectal tissues. Levels of p53 was then correlated with *SNORD44* levels to determine whether a relationship existed. Using Pearson's correlation coefficient, it was found that a

positive correlation exists between the levels of p53 and *SNORD44*. This suggests a possible link between p53 and *SNORD44*. P53 regulates cellular response to DNA damage so this could mean *SNORD44* may have an important role in this response. Such results suggest that *SNORD44* may have an important function in tumour suppression and highlight the importance to study the function of this snoRNA in the control of cell fate.

1.5 Aims of the study

The aims of this study are to investigate the hypothesis that *SNORD44* may play a role in the regulation of leukemic cell survival. The study will determine the effects of SNORD44 overexpression on leukemic T cell survival.

2 Materials and Methods

2.1 Materials

2.1.1 Cell culture

RPMI-1640 medium (# R0883), L-Glutamine (# G7513) and Gentamicin (# G1272) were all purchased from Sigma-Aldrich. Fetal bovine serum (FBS) (# FB-1001S) was purchased from Biosera.

2.1.2 Transient transfections

Iscoves Modified Dulbecco's medium (# I3390) was from Sigma-Aldrich. Ingenio solution (# MIR50111) and nucleofection cuvettes (# MIR50115) were purchased from Mirus Bio LLC. The Nucleofector™ 2b device (# AAB-1001) was from Lonza Biosciences. 0.4 mm electroporation cuvettes (# FBR-204) were from Scientific laboratory supplies Ltd. Bio-Rad Gene Pulser II (# 1652660) was purchased from Bio-Rad. Opti-mem® medium (# 31985062) was from Gibco. Endofree plasmid maxi kit (# 12362) was obtained from Qiagen (Crawley, UK). Z-VAD-FMK (# G7231) was purchased from Promega.

2.1.3 Short term functional assays

Trypan Blue (# T8154) and acridine orange (# A6014) were from Sigma-Aldrich. Muse Cell Analyser (# 0500-3115), Muse® Count and Viability assay kit (# MCH100102) and Muse Cell Cycle assay kit (# MCH100106) were purchased from Merck Millipore (Darmstadt, Germany). MTS (3-(4,5-dimethylthiazol-2-yl)-5-(3-carboxymethoxyphenyl)-2-(4-sulfophenyl)-2H-tetrazolium) (# G5421) was purchased from Promega.

2.1.4 RNA isolation and Reverse transcription

TriSure™ (# BIO-38032) was purchased from Bioline (London, UK). Direct-zol RNA Miniprep kit (# R2050) was purchased from Zymo Research. miRCURY LNA miRNA RT Kit (# 339340) was from QIAGEN. Thermo-Cycler (# WZ-93945-09) was from Cole-Palmer. Nanodrop 1000 spectrometer was obtained from Thermo-Fisher Scientific.

2.1.5 RT-PCR

miRCURY® LNA miRNA PCR Assay Kit (# 339345), *SNORD44* (# YP00203902) and U6 primers (# YP00203907) were purchased from QIAGEN. AriaMx Real Time PCR System (# G8830A) was purchased from Agilent Technologies.

2.2 Methods

2.2.1 Cell culture

Two cell lines, Jurkat and CEM-C7 cell lines, were used in the present study. Both Jurkat and CEM-C7 cells are T-lymphocytic leukemia cell lines. Both cell lines were cultured in RPMI-1640 medium with added 10% Fetal Bovine Serum (FBS), 2 mM L-Glutamine and 200 μg/ml gentamicin. RPMI-1640 medium supplemented with the above is complete. The cell lines were grown in a humidified incubator at 37^{o}C with 5% CO_2. All cells were passaged every 3-4 days to replenish the medium. To passage the cells, a sterile 25 ml flask was used in which 9 ml of RPMI-1640 medium at 37^{o}C was added. 1 ml of cells was added to the medium in the flask and were then incubated at 37^{o}C with 5% CO_2. Cell stocks were replaced every two months with fresh stocks. All experiments were performed using cells in the log phase.

2.2.2 Maxi prep of *SNORD44* and *SNORD44* mutant

The U44 sequences TOPO cloned into pcDNA3.1 V5-His-TOPO vector were obtained from Dr. Mark Pickard and Prof. Gwyn Williams (Keele University). The mutant U44 sequence was PCR-amplified from Jeko-1, the mantle cell lymphoma cell line whereas the wild type U44 was PCR-amplified from CEM-C7 cells. PCR amplified sequences were TOPO cloned into pcDNA3.1 V5-His-TOPO vector Life Technologies Ltd. (Paisley, UK).

Glycerol stocks of pcDNA3.1-SNORD44 wild type (pcDNA3.1-U44), pcDNA3.1-mutant SNORD44 (pcDNA3.1-U44$^{(-)}$) and empty vector pcDNA3.1 in *Escherichia coli* (*E. coli*) were cultured for 24 hours to increase the amount of plasmid available in the *E. coli*. To culture the bacteria from the glycerol stocks, 5 ml of LB broth media was supplemented with 5 µl of 100 mg/ml Ampicillin in a universal tube. A pipette tip with a small amount of glycerol stock was added to this LB media. This was then incubated in a shaker for 6 hours at 37ºC. After 6 hours, 100 ml LB media was added to a conical flask along with 100 µl Ampicillin. 1-2 ml of culture was added to this conical flask and was incubated overnight on a shaker at 37ºC. After 24 hours, the culture was centrifuged at 6000xg for 15 minutes at 4ºC, and all supernatant was removed. The QIAGEN Endofree plasmid maxi kit was used to purify the plasmid DNA following the kit protocol. The cells were resuspended in buffer P1 and an identical quantity of the lysis buffer P2 was then introduced and incubated for 10 minutes. The neutralisation buffer P3 was added and the solution was transferred into the QIAfilter cartridge and a further incubation period of 10 minutes was completed before inserting a plunger into the cartridge to filter the cell lysate. Buffer ER was then added to the lysate and an incubation of ice for 30 minutes occurred. Buffer ER removes endotoxins from the lysate. A QIAGEN-tip 500 was then

equilibrated with buffer QBT (equilibration buffer). Once the incubation period is over, the filtered lysate was added to the QIAGEN-tip 500 to allow it to filter by the gravity flow. The QIAGEN-tip 500 was then washed twice with buffer QC (wash buffer). The first wash was to remove all contaminants. The second wash was necessary as a large quantity of culture was being used; this ensured that all contaminants were removed completely. Buffer QN (elution buffer) was then used to elute the DNA that was extracted. The DNA was then precipitated by adding room temperature isopropanol and centrifuging at 15,000 x g for 15 minutes at 4^{o}C. The isopropanol also washes away all the remaining salt residues. The pellet gained from this centrifugation was then washed using endotoxin free room temperature 70% ethanol and centrifuged for a further 10 minutes at 15,000 x g and 4^{o}C. This step facilitates the replacement of isopropanol with ethanol as it is more volatile and allows the DNA to be re-dissolved easier. The collected DNA pellet was then resuspended in buffer TE. Buffer TE protects the DNA from degradation. To check the concentration of the DNA product produced, the NanoDrop 1000 spectrophotometer was used. DNA with a 260/280 ratio of ~1.8 was considered good quality DNA. The identity of the plasmid DNA and insert were verified by sequencing (MWG, Eurofins). See Appendix A for the blast results from the sequences received.

2.2.3 Nucleofection

1x10^{6} Jurkat cells were collected from a 25 ml flask. Cells were centrifuged and resuspended in 100 μl Ingenio solution and added to nucleofection cuvettes along with 2 μg DNA. The Nucleofector^{TM} 2b device (Lonza) was used to introduce the DNA into the cells using the programme A-017. Cells were recovered in Iscoves Modified Dulbecco's medium with added 200 mM L-Glutamine and 20% FBS.

2.2.4 Electroporation

$1x10^7$ CEM-C7 cells were collected from a 25 ml flask. Cells were centrifuged and resuspended in 1X Opti-mem® medium. 400 µl of 1X Opti-mem® medium was used for each sample. 0.4 cm gap cuvettes were used to perform the electroporation. plasmid DNA was added to the cuvettes along with the cells. Empty pcDNA3.1 vector, *SNORD44* and *SNORD44*$^{(-)}$ were transfected into the cells with the parameters 238V (actual 250V) and a capacitance 1050F using the Bio-Rad Gene Pulser II. Cells were recovered in Iscoves Modified Dulbecco's medium with added 200 mM L-Glutamine and 20% FBS.

2.2.5 Determination of cell survival and apoptosis following transfection

At 24 hours, 48 hours and 72 hours post transfection, cell counting was performed by staining the cells with 0.1% w/v trypan blue and counting using a haemocytometer. This method is called vital dye staining and is important to determine the number of total and viable cells in a sample. 0.1% w/v trypan blue was used as a stain in this method as it would not kill living cells and would only be taken up by dead cells. Cells that have not stained (are white) were viable whilst cells that have stained blue are non-viable. To calculate the number of cells per ml, the following equation was used:

Average Number of Cells in Four Large Squares X Dilution Factor X 10^4

Each sample was counted 3 times and an average was taken.

Additionally, viable and total cell count was analysed using flow cytometry and the Muse Cell Analyser (Merck). The Muse® Count and Viability assay kit was used for this cell count. A secondary method of counting cells is important to gain a reliable

set of data for total and viable cell count. This assay is based on differential permeability of two DNA-binding dyes. The nuclear dye stains only live cells, while the viability dye stains dying and dead cells. Cell debris is not counted and therefore excluded. To perform this assay, 20 µl of cells were suspended in 380 µl of Muse™ Cell Count and Viability reagent (1:20 dilution). Each sample was vortexed before reading on the Muse Cell Analyser. An expected plot of results is shown below in Figure 10.

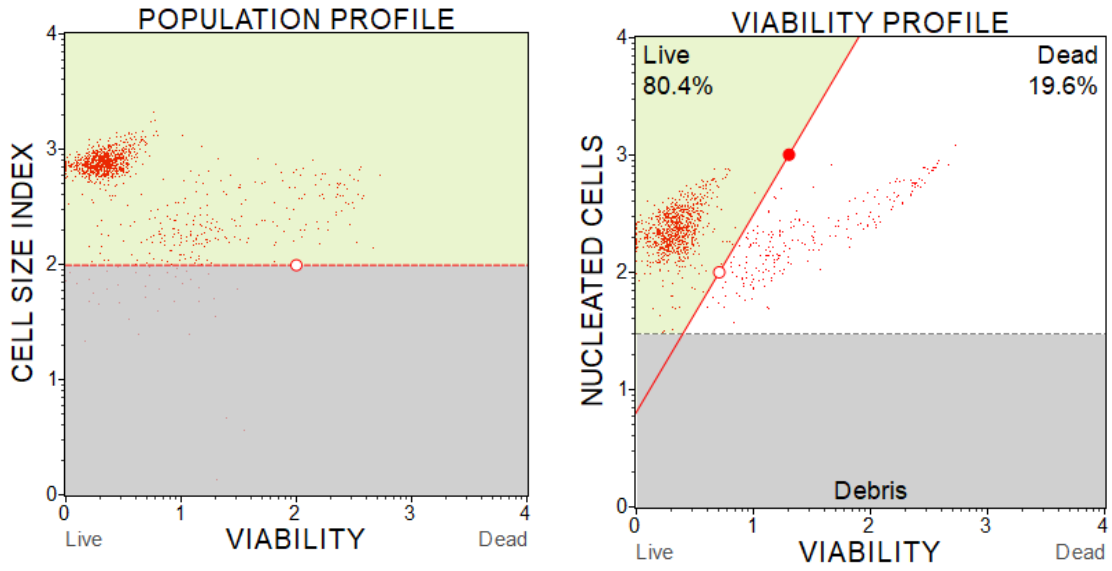

Figure 10: Representative plots following data acquisition on Muse™ Cell Analyzer. This image shows an expected set of results for a count and viability assay. The first graph shows the viability vs the cell size. The gate set on this graph eliminates all debris from the analysis. The second graph shows the viability vs nucleated cells. All live cells are shown on the left of the plot whilst dead cells are shown on the right side of the gate.

The percentage of apoptotic cells was determined at 24 hours, 48 hours and 72 hours using acridine orange (25µg/ml) to stain the cells. 0.5ml of cells were centrifuged at 1500xg for 5 minutes. The supernatant was removed, leaving 20 µl of supernatant at the bottom. 20 µl of acridine orange was added to the cells and the cells were resuspended. 20 µl of the resuspension was plated onto a microscope slide and a cover slip applied on top. This slide was then analysed under a

fluorescent microscope. The changes in nuclear morphology of apoptotic cells allowed for the apoptotic cells to be identified. The percentage of apoptotic cells was calculated using the following equation:

(Number of Apoptotic cells/Total Number of cells) x100 = percentage of apoptotic cells

Each sample was counted 3 times and an average was taken.

2.2.6 Cell cycle analysis

Cell cycle analysis was performed to determine the percentage of cells in the sample that are in each stage of the cell cycle. Such analysis is important to determine whether transfected cells are progressing through the cell cycle in the way it would be expected. This assay works by staining fixed cells with propidium iodide (PI) and quantifying the DNA content of the cells using and flow cytometry. The cells were fixed to allow the dye to enter the cells as living cells would pump the dye out. Cells in different stages of the cell cycle stain differently by PI dye which is stoichiometric and will bind in proportion to the amount of DNA present in the cell. Cells in the G0/G1 phase will have the dimmest staining with PI, whereas cells in S phase which are in the process of synthesizing the DNA, will fluoresce more brightly and will appear between the two major peaks on the graph produced and cells in G2/M phase which will have double their DNA content and will stain twice as brightly as the G0/G1 peak.

Cell cycle analysis was performed using the Muse Cell Analyser (Merck) and the muse cell cycle assay kit. $1x10^6$ cells were transferred to a microcentrifuge tube, 24 hours post re-plating. Cells were then centrifuged at 300 x g for 5 minutes. The

supernatant was then removed and 1X PBS was added to wash the cells. Cells with added 1X PBS were then centrifuged at 300xg for 5 minutes. The supernatant was then removed, leaving a small quantity of supernatant left in the bottom of the tube. Whilst vortexing the tube, cells were fixed by adding 1 ml of ice-cold 70% ethanol was added to the tube. This was then left overnight at -20ºC. After the overnight incubation period, the cells were washed with 1X PBS and centrifuged at 300xg for 5 minutes. The supernatant was removed, and the pellet was resuspended in 200 µl of Muse™ Cell Cycle Reagent. The resuspension was then incubated for 30 minutes in the dark before being run on the Muse Cell Analyser. An expected set of

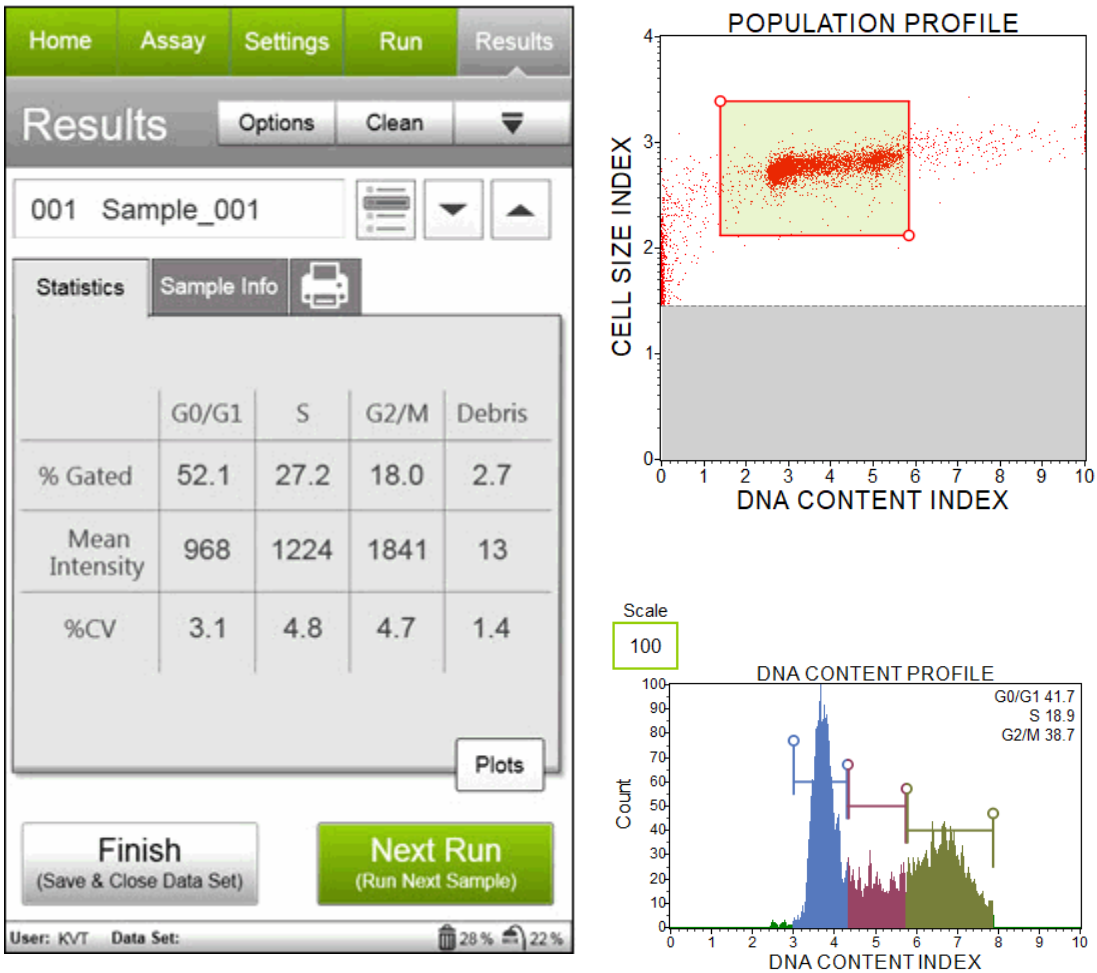

Figure 11: **Cell cycle profile after data acquisition on the Muse Cell analyser.** An image shows an example of an expected set of results when performing the cell cycle assay. The percentage of cells in each stage of the cell cycle is shown in a table along with the mean intensity of the cells when stained with PI. Two graphs are produced in which the cell size vs DNA content and count vs DNA content is plotted. A higher number of cells in the G0/G1 phase is expected. The cells were gated to show % cells each phase of the cell cycle.

2.2.7 RNA isolation

$1x10^6$ cells were centrifuged and resuspended in TriSure™ to lyse the cells. The cellular RNA was isolated using the Direct-zol RNA Miniprep kit. The protocol for this kit was followed. It is important that all centrifugation steps in this protocol were run at 13,000 x g for 30 seconds at 4°C unless the protocol stated specific time periods. An equal volume of 100% ethanol was added to the lysed cell suspension and then transferred to a Zymo-Spin™ IIC column. The mixture was then centrifuged at the parameters stated above. A DNase I treatment is important to perform as it removed possible DNA contaminants. 5 µl DNase I and 75 µl DNA digestion buffer were added to each column to perform the DNase treatment. This was then incubated for 15 minutes at room temperature. The column was then treated with RNA Prewash Buffer and RNA Wash Buffer. Finally, the RNA was eluted using RNase free water and stored at -20°C. To check if RNA was isolated, a gel was run in which 2 bands at 18S and 28S would be seen when a successful isolation has been performed. The RNA was quantified using nanodrop spectrometer 1000. Good quality RNA had a 260/280 nm of ~2.0.

2.2.8 Real time PCR using miRCURY LNA miRNA PCR System.

To check if transfection of *SNORD44* has resulted in overexpression of the snoRNA, RT-PCR must be performed. The miRCURY LNA PCR System (Qiagen) was used as it is highly specific for the detection and quantification of small RNAs including miRNAs. The principle of this approach combines universal reverse transcription with LNA PCR amplification of the small RNA. LNA or 'locked nucleic acids' are a class of RNA analogs in which the ribose ring is described to be locked in the ideal conformation for Watson-Crick binding. The miRCURY LNA miRNA RT Kit was used to carry out reverse transcription. The approach involves addition of poly(A)

tail to the mature miRNA/small RNA template followed by the synthesis of cDNA using a Poly(T) primer with a 3' degenerate anchor and a 5' universal tag. The cDNA template is then used to amplify miRNAs or other small RNAs using two small RNA -specific and LNA-enhanced forward and reverse primers. The LNA enhanced primers ensures high sensitivity with a low background. SYBR Green is used for product detection. Figure 12 below depicts the principles of this method.

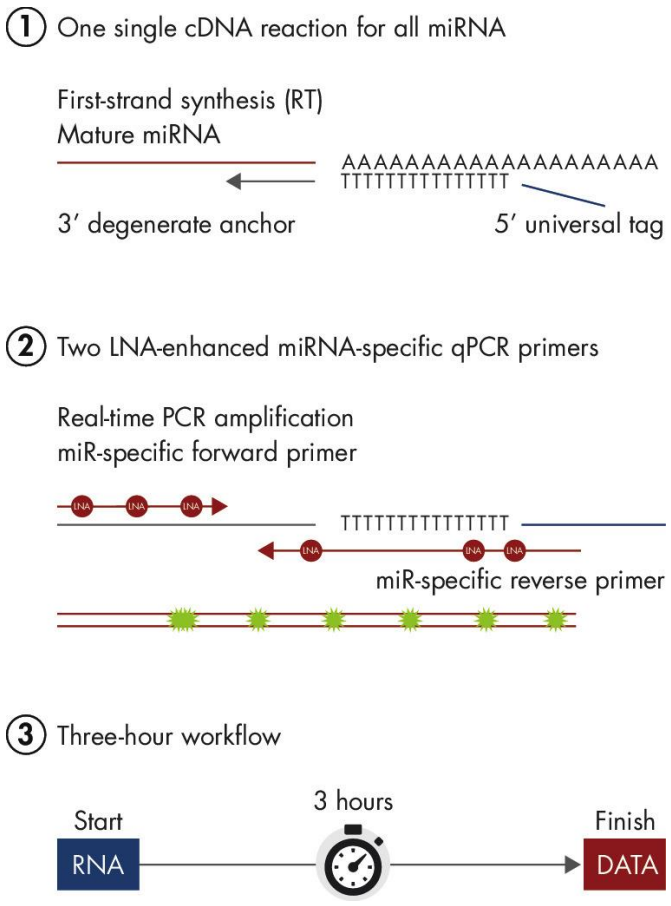

Figure 12: miRCURY LNA miRNA PCR System at a glance (Qiagen, 2018). During step one, a poly(A) tail is added to the template and the cDNA is then produced using the poly(T) primer. The poly(T) primer has a 3' degenerate anchor and a 5' universal tag. The cDNA template is then amplified in step 2 using the LNA-enhanced primers. SYBR green is then used for detection.

cDNA synthesis was performed on the isolated RNA using the miRCURY LNA miRNA RT Kit. The protocol contained in this kit was followed. To begin, the RNA had to be diluted to 5 ng/µl with RNase free water. The reaction mix was set up in a microcentrifuge tube according to the protocol with a total volume of 10 µl. The volumes used of each reagent from the kit are shown in Table 1.

Table 1: Volumes of each reagent used in miRCURY LNA RT kit. The total volume reaction was 10µl.

Reagent	**Volume**
5X miRCURY RT Reaction Buffer	2 µl
RNase-free water	4.5 µl
10X miRCURY RT enzyme mix including Mg^{2+}, RT primers and dNTPs	1 µl
Synthetic RNA Spike in	0.5 µl
Template RNA (5ng/µl)	2 µl
Total Volume	10µl

UniSp6 spike-in was used to determine the quality control of the RT-PCR. The diluted RNA was then added to the reaction mixture and put into a thermocycler (cole-parmer). The cycle consisted of 60 minutes at 42^{o}C and 5 minutes at 95^{o}C to inactivate the reverse transcriptase. The mixture must then be immediately cooled to 4^{o}C and can be stored in a freezer at -20^{o}C.

Following reverse transcription, the cDNA template was used to amplify SNORD44. The protocol received with the kit was followed. To begin the cDNA had to be diluted x60. *SNORD44* and U6 primers were used in this RT-PCR, to detect not only the

amplification of *SNORD44*, but also the amplification of U6. U6 was used as the normaliser as it has a stable gene expression across various tissues and cells (Yi et al., 2018). The reaction mix was set up according to the protocol as shown in Table 2.

Table 2: Table showing the volumes of reagents used for the miRCURY SYBR green PCR assay.

Components	**Volume**
2X miRCURY SYBR Green Master Mix	5µl
PCR Primer Mix	1µl
cDNA Template	3µl
RNase-free water	1.5µl
Total Volume	10µl

The total reaction volume for each sample was 10µl which was placed in a singular well of a 96-well plate. cDNA synthesised from parental cells RNA were used as a control. The plate was then span in a centrifuge to remove all possible bubbles formed when pipetting. The AriaMx Real Time PCR System (Agilent Technologies) was used to perform the PCR which was set up using the following parameters shown in Table 3.

Table 3: Table detailing the parameters in which the SYBR green PCR assay have been set up on the AriaMx RT-PCR system.

Step	**Time**	**Temperature (ºC)**
PCR Initial heat activation	2 minutes	95
2-Step cycle- 40 cycles		
Denaturation	10 seconds	95
Combined annealing/extension	60 seconds	56

The melting curve analysis was performed at 60-95^{o}C. Melting curve analysis is important as it allows for detection of contamination. If two peaks are visible on the melting curve for the same sample, it suggests there is a presence of contamination.

Expression comparisons were made relative to the calibrator using the $2^{-\Delta\Delta Ct}$ comparative method. The equation for the ΔΔCt method is below in which the calibrator is the control and the normaliser is U6:

$$\textbf{Ct (gene of interest)}^{\textbf{sample}} \textbf{ – Ct (Normaliser)}^{\textbf{sample}} \textbf{ = ΔCt Sample}$$

$$\textbf{Ct (gene of interest)}^{\textbf{calibrator}} \textbf{ – Ct (Normaliser)}^{\textbf{calibrator}} \textbf{ = ΔCt Calibrator}$$

$$\textbf{ΔCt Sample – ΔCt Calibrator = ΔΔCt}$$

To find the overall gene expression, $2^{-\Delta\Delta Ct}$ is calculated from the ΔΔCt.

2.2.9 Z-VAD-FMK treatment

Z-VAD-FMK is a pan caspase inhibitor. To determine whether the apoptotic property of *SNORD44* was dependent on caspases, the pan-caspase inhibitor Z-VAD-FMK was utilised. Jurkat cells were grown in RPMI-1640 medium supplemented 10% Fetal Bovine Serum (FBS), 2 mM L-Glutamine, 200 μg/ml gentamicin and one flask with 1 mM Z-VAD-FMK for 24 hours pre-transfection. After 24 hours, the Jurkat cells were transfected with pcDNA3.1-U44 or empty vector using nucleofection as described previously in 2.2.3. Following transfection, the total and viable cells were measured at 24, 48 and 72 hours post transfection. An MTS assay was also performed at 48 and 72 hours post transfection.

2.2.10 MTS assay

The MTS assay analyses the metabolic activity of cells. In the presence of phenazine methosulfate (PMS), MTS produces a formazan product that has an

absorbance maximum at 490 nm. The production of formazan is measured by a plate reader. An MTS assay was performed on Z-VAD treated cells transfected with *SNORD44* and pcDNA3.1. 100 µl of cells were plated onto a 96-well plate at 48 and 72-hours post-transfection. 3 aliquots of 100 µl per sample were taken at the two different time points. 20 µl of MTS reagent was added to the cells and the plate was incubated at 37^{o}C for 2 hours. After this time, the plate was read using a plate reader and the results were plotted onto graphs.

2.2.11 Statistical analysis

All graphs are shown as the mean of results with the standard error of this mean. N stands for the number of experimental repeats performed. To determine the presence of statistical significance, a one-way ANOVA or unpaired t-test was performed. The one-way ANOVA was used to compare 3 sets of data whilst the unpaired t-test was used to compare 2 sets. A p value of below 0.05 was statistically significant. All statistical analysis was performed in GraphPad Prism 7.

3 Results

3.1 Optimisation of transfection

Every cell type has different requirements to provide the optimum insertion of foreign DNA, therefore, it is important to optimise transfection conditions before starting a series of experiments. It is essential to obtain the highest transfection efficiency and the lowest loss of viability when performing transfections. The concentration of DNA required to achieve the highest transfection efficiency and lowest loss of viability when using electroporation was determined using the plasmid pmax-GFP (Lonza) which encodes green fluorescent protein (GFP). A transfection using different concentrations of pmax-GFP plasmid (Appendix C) was performed to identify the concentration that will give good transfection efficiency. Four different amounts of pmax-GFP were used in four separate experiments, 2 µg, 5 µg, 10 µg and 20 µg. 20 µg of pmax-GFP inhibited the cells recovery, producing a transfection efficiency of less than 5%. It was decided that 20 µg was too high concentration to use during these transfections. At 48 hours post transfection, 5 µg and 10 µg showed a transfection efficiency of ~50% with no significant difference between the two. 5 µg was used in the subsequent transfections due to the transfection efficiency being the highest with respect to all other amounts of pmax-GFP. The transfection efficiency of 10 µg pmax-GFP was very similar to using 5 µg therefore using the latter amount was more beneficial to save wastage of product (Figure 13A). The viability of cells transfected with 5 µg and 10 µg pmax-GFP showed the highest viability of ~75% at 48 hours but showed no significant differences to each other at all the three-time points. 20 µg of pmax-GFP showed a cell viability of below 20% for all the three-time points (Figure 13B).

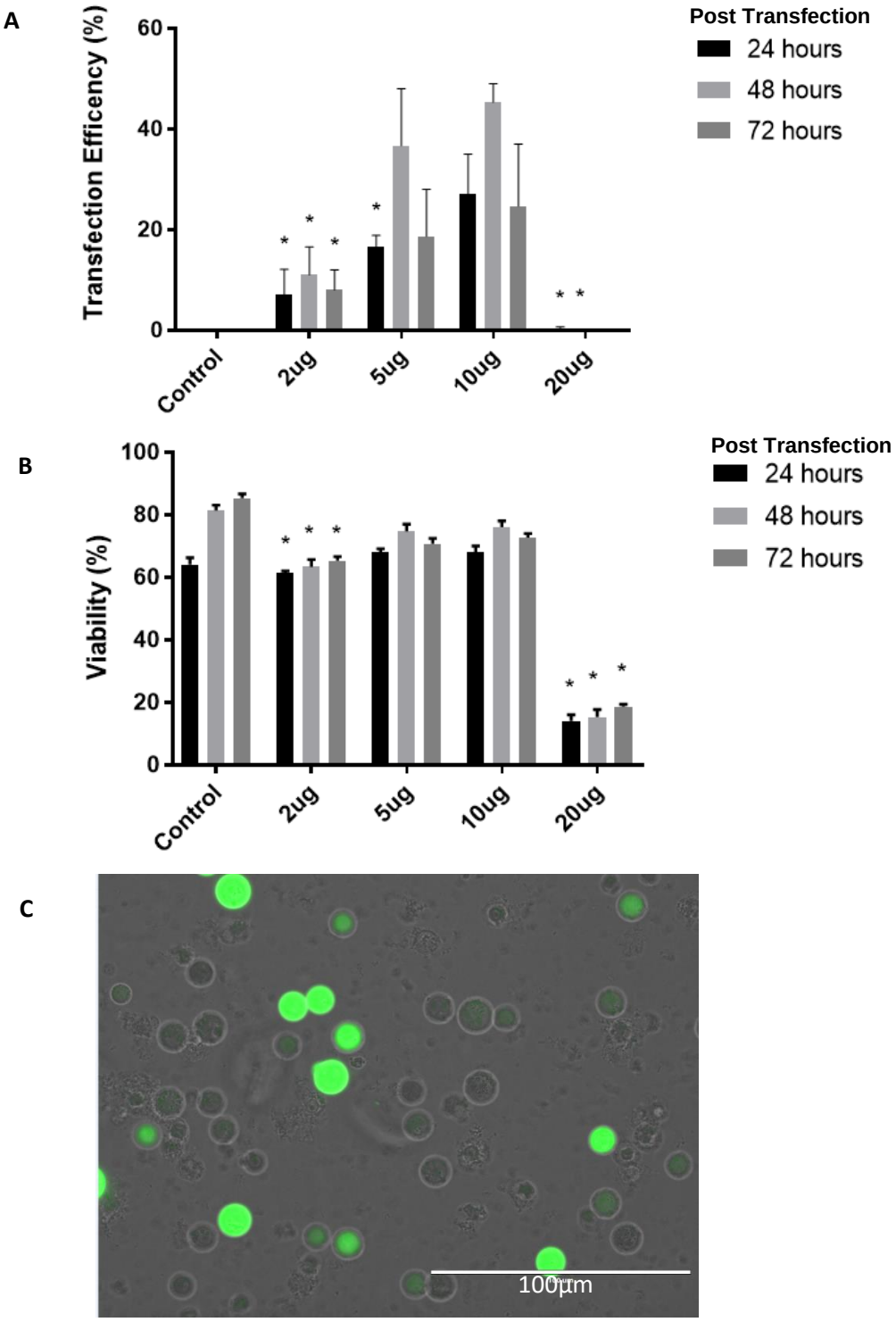

Figure 13: Optimisation of plasmid DNA transfection. Electroporation of Jurkat cells were performed using four different amounts pmax-GFP (n=4 cultures). Transfection efficiency was determined using fluorescent microscopy (A). Cell viability was measured by using a haemocytometer and trypan blue (B). (C) shows an example of the fluorescence produced when pmax-GFP was transfected into cells. A one-way ANOVA and tukey test was utilised to analyse the significance of results, comparing the transfection efficiencies against each other. *P<0.001 comparing programmes at the same time points.

3.2 Optimisation of nucleofection programme

The Nuclofector™ 2b device provides 3 programmes for transfection into leukemic cells such as Jurkat cells, these are A-017, C-016 and G-010. This optimisation is important as it allows a programme that provides an optimum transfection efficiency to be identified. The percentage viability determines the potential of the cells to recover after nucleofection. Nucleofection of the cells using G-010 resulted in viability below 70% in both the control and pmax-GFP cultures. This was significantly lower compared to A-017 and C-016. The viability of both A-017 and C-016 was around 80% for the control transfection and around 70% for the pmax-GFP transfections. There was no significant difference between these two programmes in viability of transfected cells (Figure 14A). The transfection efficiency of these cells was also recorded after 48 hours. All transfections showed a statistical significance with A-017 having the highest transfection efficiency of pmax-GFP at 76% (Figure 14B). It was determined that A-017 was the best programme to use to achieve the highest transfection efficiency along with having a high viability of cells.

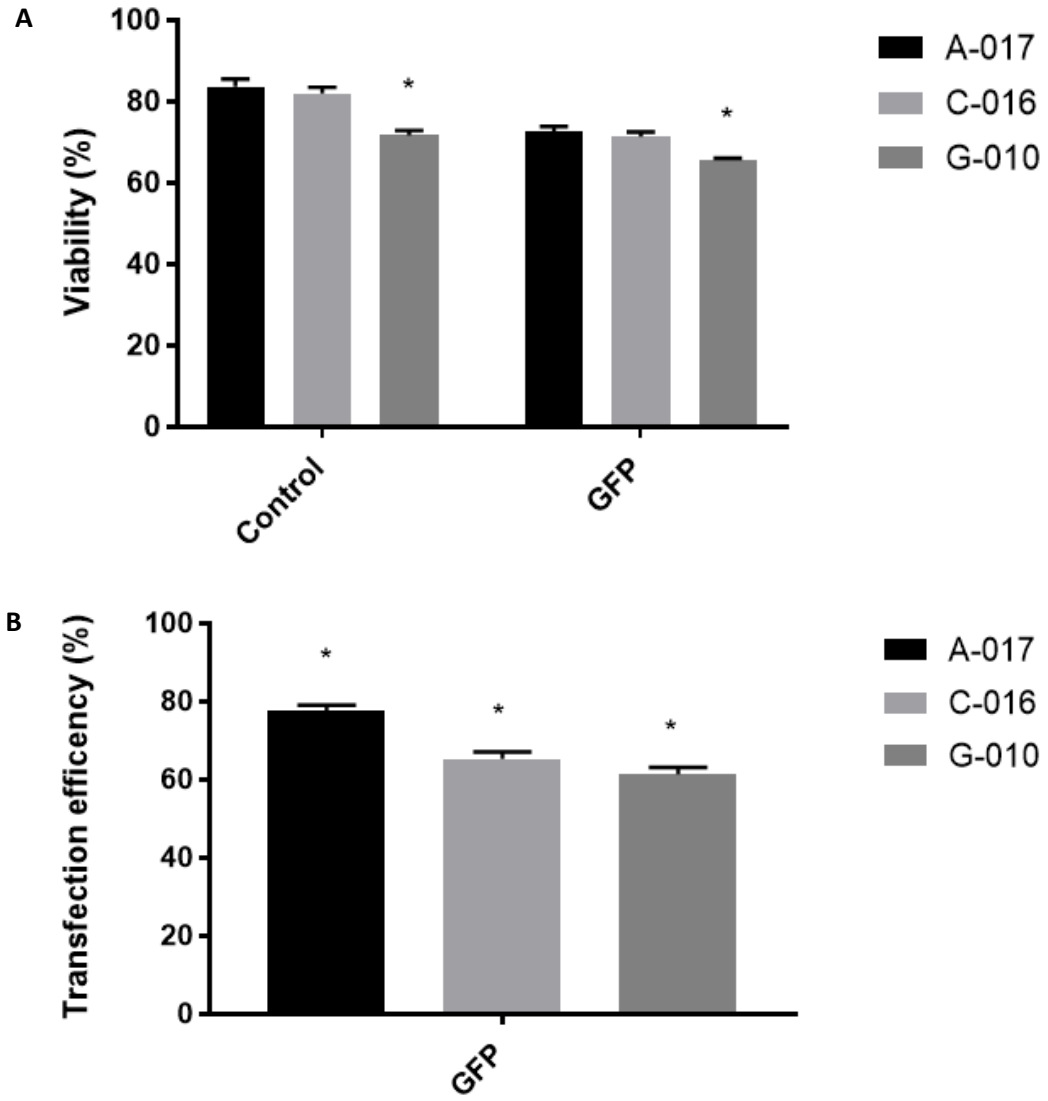

Figure 14: Ability of cells to recover after nucleofection with three different programmes. Three programmes were used in three separate nucleofections, A-017, C-016 and G-010 (n-=3). Pmax-GFP was transfected into Jurkat cells along with a blank control. Percentage viability of Jurkat cells at 48 hours (A). The transfection efficiency was measured using fluorescent microscopy. (B) A one-way ANOVA and tukey test was performed to analyse the significance of results. * P<0.001 on comparing the same transfections using different programmes (A). *P<0.01 on comparing GFP transfections to each other with different programmes (B).

3.2 Effects of *SNORD44* transient expression on the survival of Jurkat T cells

SNORD44 has a predicted secondary structure as shown below in Figure 15.

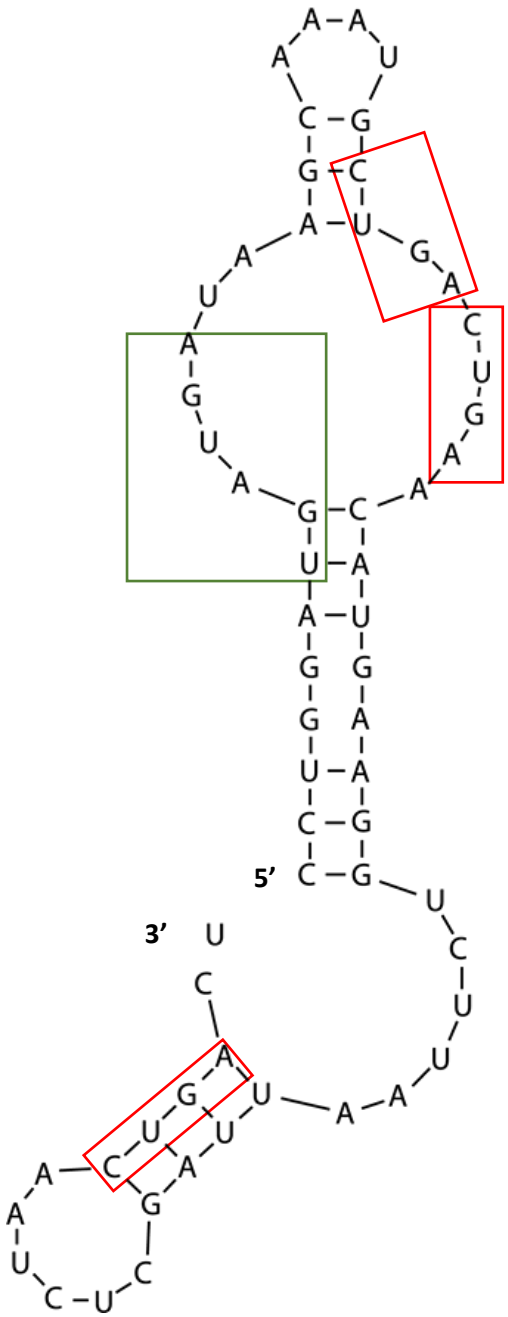

Figure 15: The predicted secondary structure of *SNORD44*. The nucleotide backbone is shown with all 61 bases. The 18S rRNA binding site is located at the bottom ring with the nucleotide sequence GCUCUAAC. The red boxes depict the D boxes within the structure whilst the green box shows the C box (Bai et al., 2014).

Nucleofection was used as the method of transfection to overexpress SNORD44 in Jurkat cells, Jurkat cells were nucleofected with either pcDNA3.1-U44 or pcDNA3.1. A control was also used in which no DNA was added. Transfection of pcDNA3.1-U44 resulted in a~16-fold increase in SNORD44 expression compared to cells transfected with pcDNA3.1 and mock transfected cells (Figure 16). This indicates that overexpression of SNORD44 has occurred in Jurkat cells following the transfection with pcDNA3.1-U44.

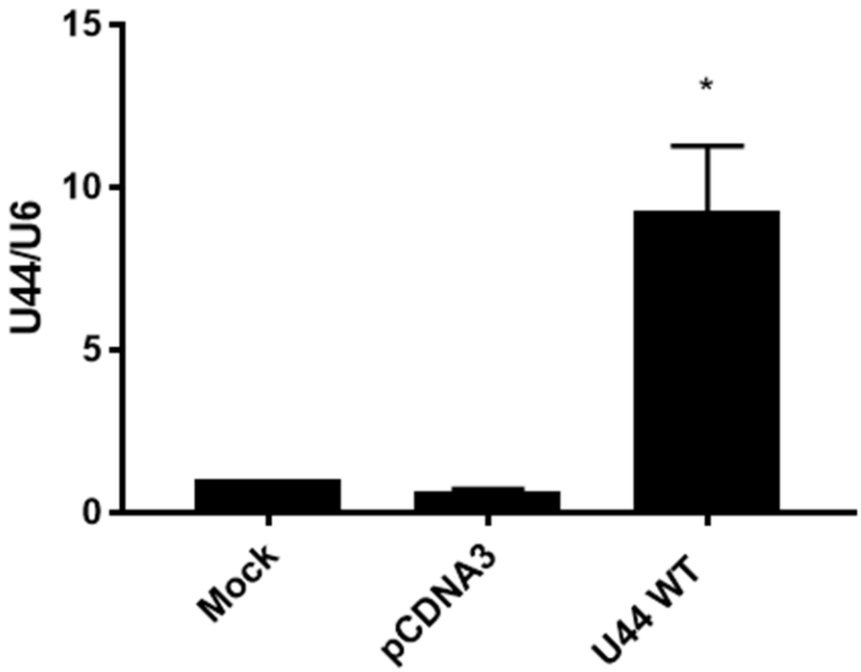

Figure 16: **qRT-PCR analysis to determine SNORD44 overexpression in transfected Jurkat cells.** Jurkat T cells were transfected with either pcDNA3.1 or pcDNA3.1-U44. A control was also used in which cells were nucleofected with no DNA. RNA was collected which was used to produce cDNA. SYBR green RT-PCR experiments were run using the cDNA produced and analysed using the $2^{-\Delta\Delta Ct}$ method to calculate the U6:U44 ratio (n=3). An unpaired T-test was used to analyse the statistical significance of the results. *P<0.0001 for pcDNA3.1-U44 transfection compared to pcDNA3.1 transfections into Jurkat cells. U44 WT = *SNORD44*

The effects of SNORD44 overexpression on the total and viable cell number were determined at 24, 48 and 72 hours post-transfection, using vital dye staining. The viable cell count of pcDNA3.1-U44 transfected cells showed a 55% decrease after 72 hours compared to cells transfected with empty vector (Figure 17A). The total cell count of pcDNA3.1-U44 transfected cells showed a 70% decrease after 72 hours when compared to the empty vector transfected cells (Figure 17B).

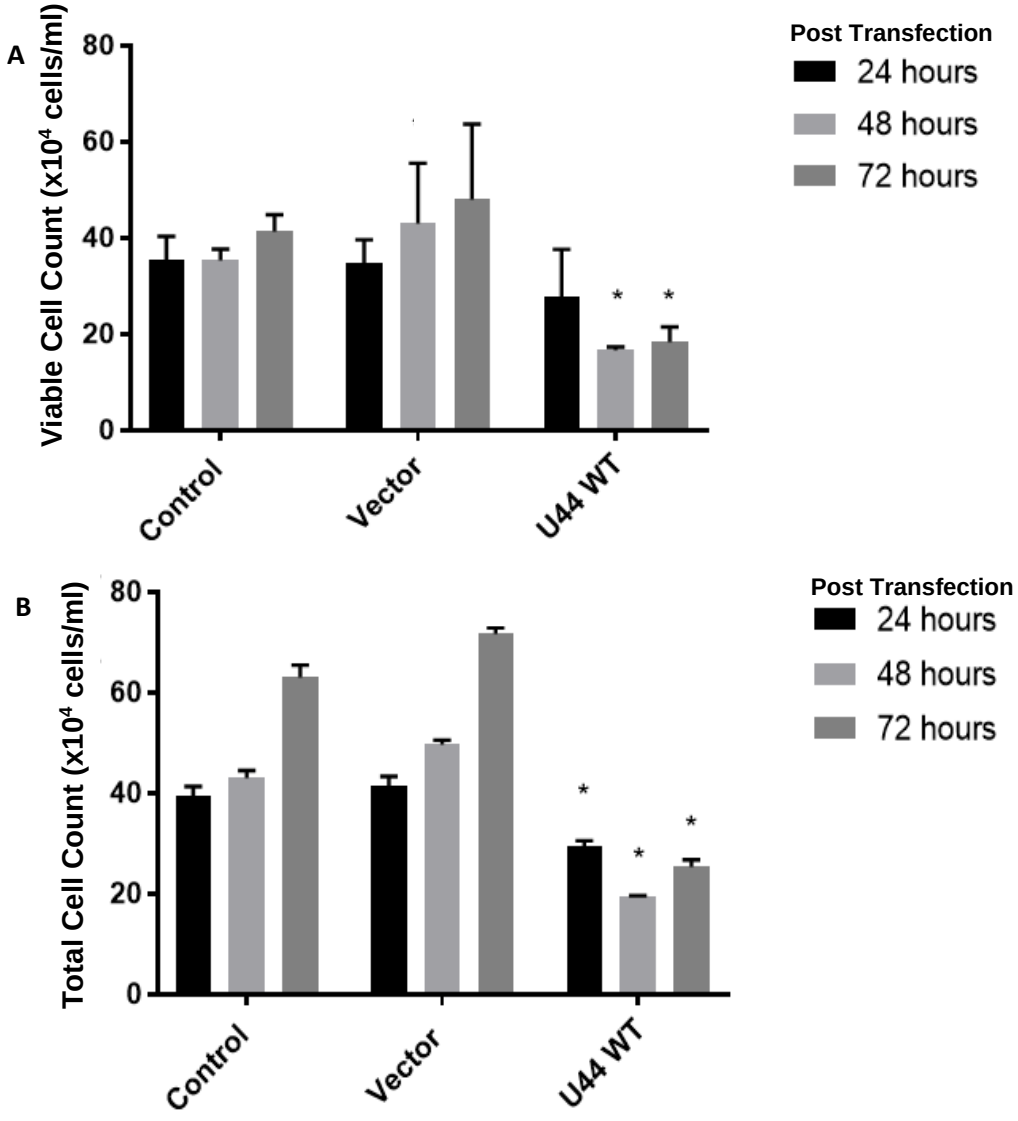

Figure 17: **Effects of SNORD44 overexpression on the number of total and viable cell number of Jurkat cells.** Graph of the total (B) and viable (A) cell count (cells/ml) of transfected Jurkat cells at 24, 48 and 72 hours post transfection of N=3 experiments as determined using vital dye staining after 24, 48 and 72 hours. A one-way ANOVA with tukey test was performed to analyse the statistical significance of the results. The asterisk above the bars symbolises a statistical significance between pcDNA3.1-U44 and the vector transfections. *P<0.01 comparing to mock and vector transfected cells. U44 WT = *SNORD44*

To confirm the validity of the cell counting performed using a haemocytometer, flow cytometry was utilised to further determine the effects of SNORD44 overexpression on the total and viable cell count. The total cell count of pcDNA3.1-U44 transfected cells showed a 67% decrease after 48 hours and a 40% decrease after 72 hours when compared to the empty vector transfected cells (Figure 18A). The viable cell count of pcDNA3.1-U44 transfected cells showed a 56% decrease after 48 hours and a 64% decrease after 72 hours compared to cells transfected with empty vector (Figure 18B). The viable and total cell count was much lower in pcDNA3.1-U44 transfections than the pcDNA3.1 transfections.

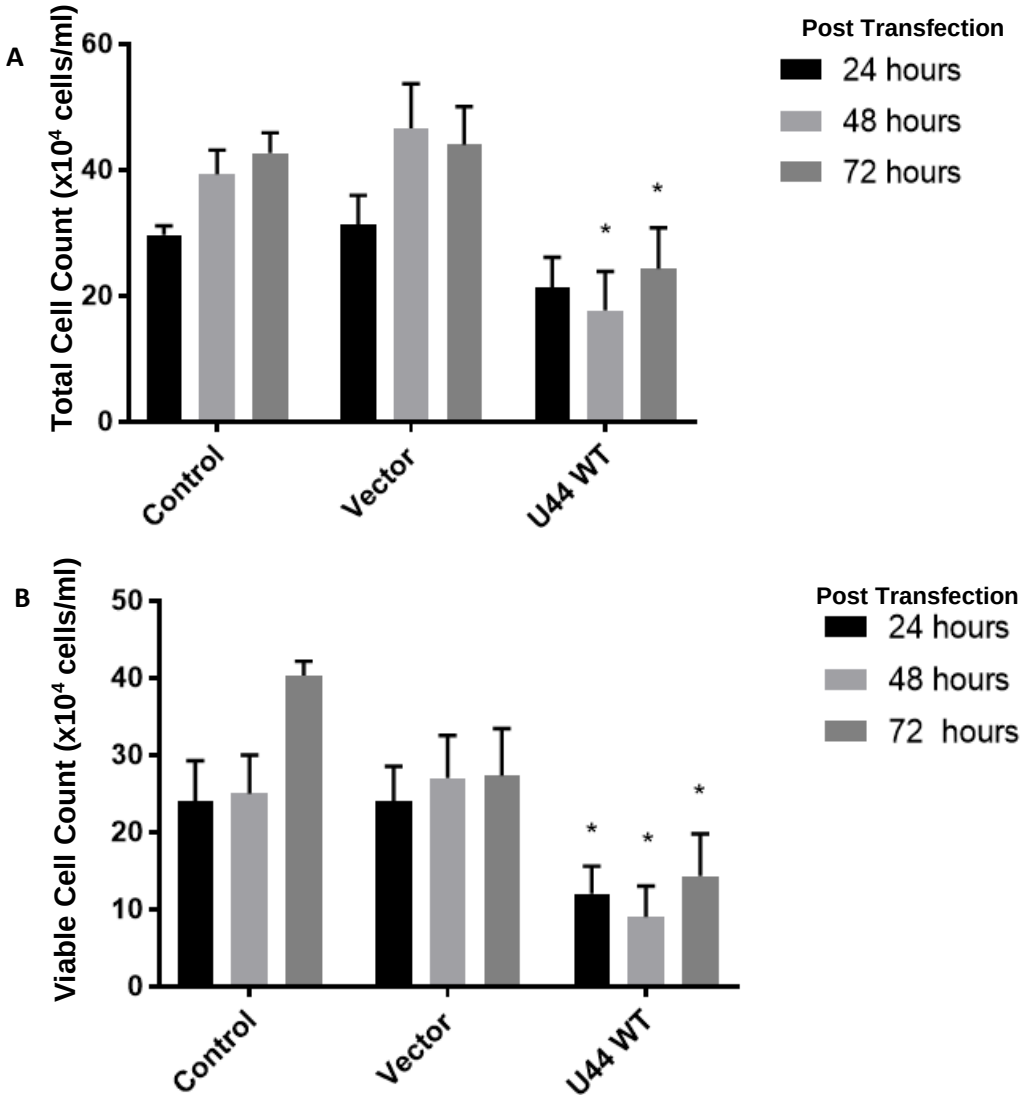

Figure 18: **Effects of SNORD44 overexpression on the number of total and viable cell number of Jurkat Cells.** Graph of the total (A) and viable (B) cell count (cells/ml) of transfected Jurkat cells at 24, 48 and 72 hours post transfection of N=3 experiments. $1x10^6$ Jurkat cells were used during this nucleofection. pcDNA3.1 and pcDNA3.1-U44 were transfected into Jurkat cells. A control was also used in which no RNA/DNA was transfected into the cells. Using flow cytometry, the cell count was analysed. A one-way ANOVA with tukey test was performed to analyse the statistical significance of the results. The asterisk above the bars symbolises a statistical significance between pcDNA3.1-U44 and the vector transfections. *P<0.001 comparing vector and pcDNA3.1-U44 transfections at equal time points. U44 WT = *SNORD44*

Further experiments were carried out to analyse the effects of SNORD44 over-expression on the basal apoptosis levels. To analyse the number of apoptotic cells, acridine orange was utilised to stain the cells. The percentage of apoptotic cells to total cells was then calculated and plotted onto a graph. The data shows that SNORD44 overexpression resulted in more than a 2-fold increase in basal apoptosis compared to cells transfected with pcDNA3.1 and mock transfected cells (Figure 19).

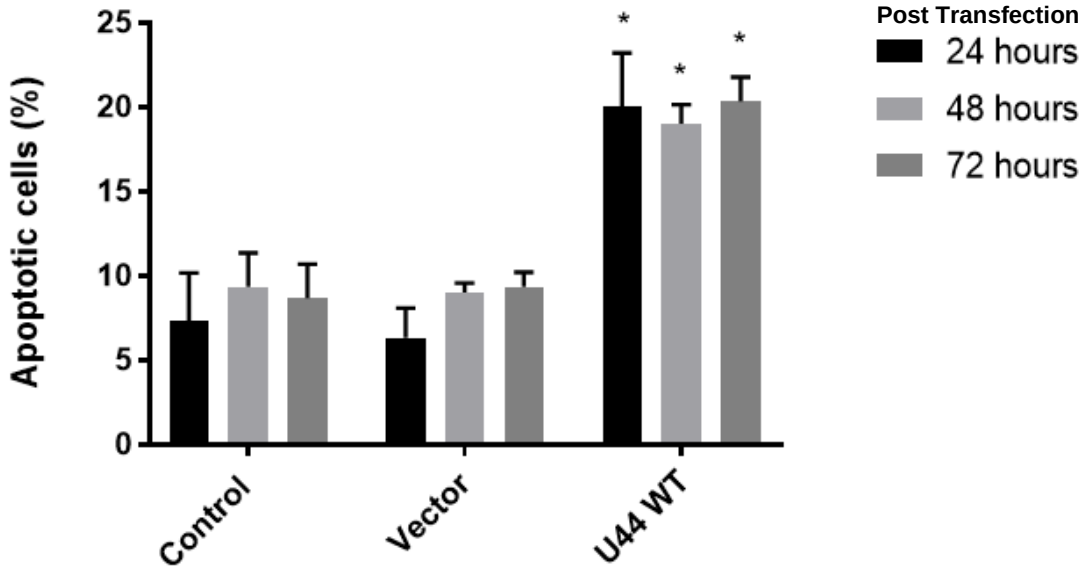

Figure 19: **The effect of overexpressing SNORD44 on basal apoptosis levels of Jurkat cells**. 1x10^6 Jurkat cells were used during this nucleofection (n=3). pcDNA3.1 and pcDNA3.1-U44 were transfected into Jurkat cells. A control was also used in which DNA was not included in the transfection. The apoptotic cells were determined using acridine orange to stain the cell nuclei. A one-way ANOVA with a tukey test was performed to analyse the statistical significance of the results. The asterisk above the bars symbolises a statistical significance between pcDNA3.1-U44 and the vector transfections. * P<0.0001 comparing pcDNA3.1-U44 transfections with vector transfections at all time points. U44 WT = *SNORD44*

Cell cycle analysis was performed was also performed to assess if increased *SNORD44* levels can affect cell cycle progression. All transfections show a very similar percentage of cells in each of the cell cycle stages. Cells in the G0/G1 phase were around 60%, S phase was ~20% and G2/M phase were around 23% (Figure

20). These results showed that SNORD44 overexpression did not have any effect on cell cycle progression.

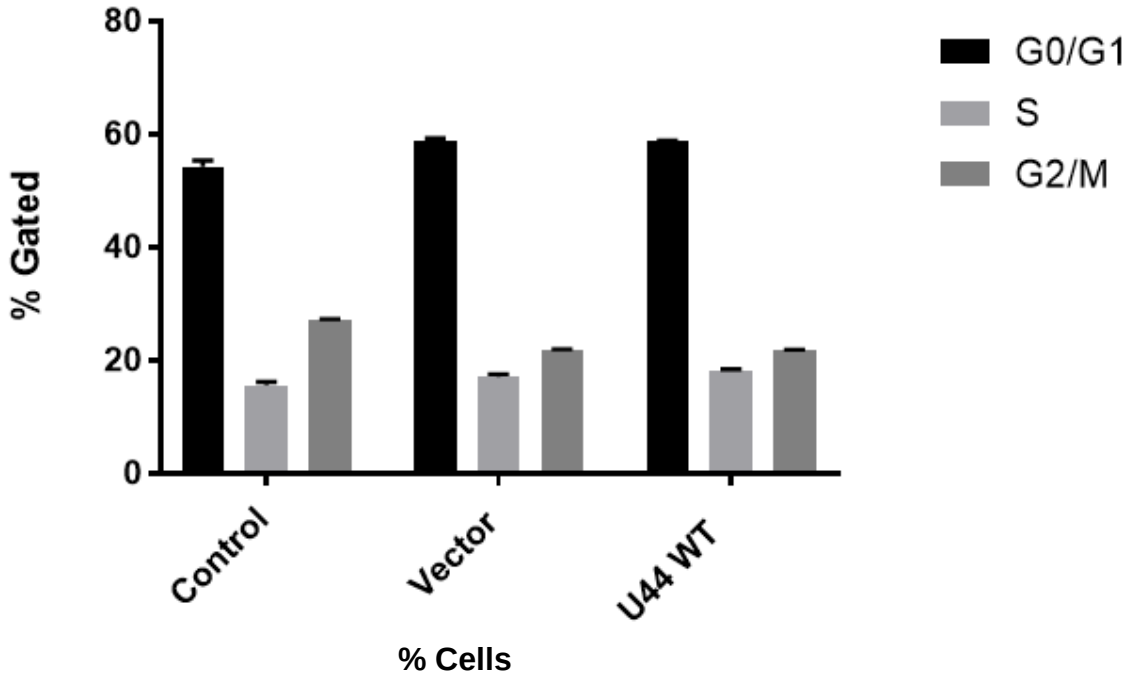

Figure 20: The effect of overexpressing SNORD44 on cell cycle progression. Cell cycle analysis was performed on transfected cells. Flow cytometry was used along with the Muse cell cycle assay kit (n=3). The cells were gated to include everything G0/G1, S and G2/M phases. U44 WT = *SNORD44*

3.3 Effects of *SNORD44* transient expression on the survival of CEM-C7 T leukemic cells

A second leukemic T cell line, CEM-C7 was utilised to determine whether the effects observed due to SNORD44 overexpression is unique to Jurkat T cells or expands along more leukemic T cell lines. To begin, both nucleofection and electroporation were performed to determine which method would be the most suitable for this cell line. On performing nucleofection, the cells did not recover and therefore it was determined that nucleofection would not be suitable for this set of experiments. Electroporation was the method chosen for CEM-C7 cells.

Expression analysis using real time PCR showed a significant increase in the expression levels of SNORD44 in cells transfected with pcDNA3.1-U44 compared to cells transfected with pcDNA3.1. A ~10-fold increase in SNORD44 expression was seen in CEM-C7 cells transfected with SNORD44 compared to those transfected with pcDNA3.1 (Figure 21).

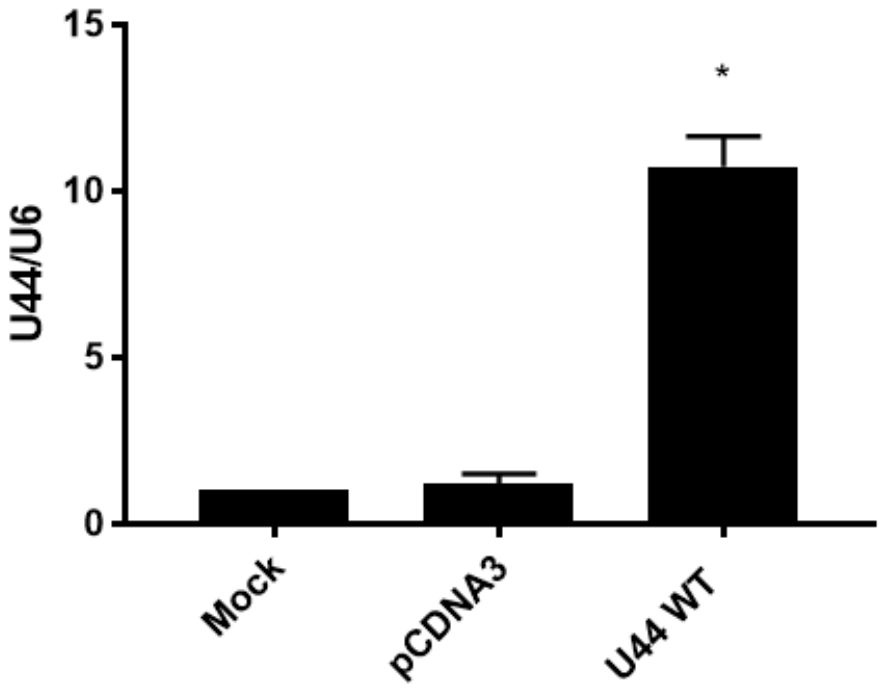

Figure 21: **PCR analysis to determine the presence of SNORD44 overexpression in transfected CEM-C7 cells**. 1x10^7 CEM-C7 cells were used during this nucleofection. pcDNA3.1 and pcDNA3.1-U44 were transfected into the cells. A control was also used in which no DNA added to the transfected CEM-C7 cells. RNA was collected from the transfected cells and used to produce cDNA (n=3). SYBR green qPCR experiments were run using the cDNA produced and analysed using the $2^{-\Delta\Delta Ct}$ method to calculate the U44:U6 ratio. An unpaired T-test was used to analyse the statistical significance of the results. *P<0.0001 for pcDNA3.1-U44 transfection comparing to pcDNA3.1 transfections into CEM-C7 cells. U44 WT = *SNORD44*

The number of viable and total cells were determined at 24, 48 and 72 hours post transfection using vital dye staining. The total cell count decreased by 46% in the culture of pcDNA3.1-U44 transfected cells compared to the culture transfected with empty pcDNA3.1 vector at 72 hours. At 48 hours, there was a decrease of 50% in the total cell number comparing pcDNA3.1-U44 transfections to pcDNA3.1 transfections (Figure 22A). The viable cell count decreased by a percentage of 49% from pcDNA3.1-U44 wild type transfections compared to the vector transfections at 72 hours. Comparing these two transfections at 48 hours showed a decrease of 44% (Figure 22B). pcDNA3.1-U44 transfections had a much lower total and viable cell count at 48 and 72 hours post transfection than pcDNA3.1 transfections.

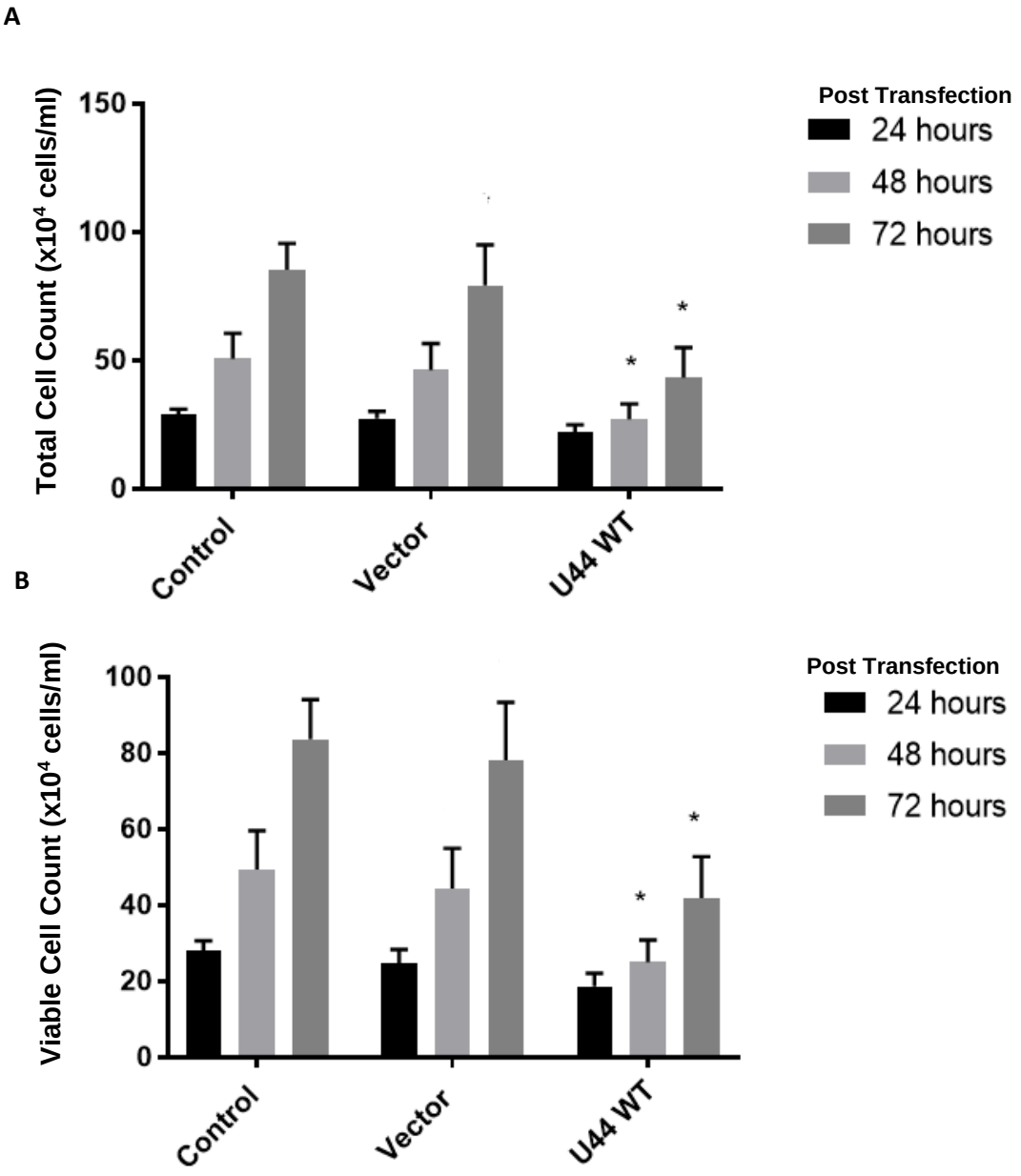

Figure 22: **Effects of SNORD44 overexpression on the number of total and viable cell number of CEM-C7 cells.** Graph of the total (A) and viable (B) cell count (cells/ml). $1x10^7$ CEM-C7 cells were nucleofected with pcDNA3.1 and pcDNA3.1-U44. Mock transfected cells were also used. Cells were counted using vital dye staining at 24, 48 and 72 hours. A one-way ANOVA with a tukey test was performed to analyse the statistical significance of the results. The asterisk above the bars symbolises a statistical significance between pcDNA3.1-U44 and the vector transfections. * $P<0.01$ comparing the transfections of vector against pcDNA3.1-U44 at equal time points. U44 WT = *SNORD44*

The effects of SNORD44 overexpression on the total and viable cell count (cells/ml) was also assessed using flow cytometry. After 72 hours, a 33% decrease in total cell count (cells/ml) comparing the pcDNA3.1-U44 transfections with the vector transfections was observed. At 48 hours, the percentage decrease was at 40% comparing the total cell count (cells/ml) of pcDNA3.1-U44 transfections to empty pcDNA3.1 transfections (Figure 23A). The viable cell count at 72 hours showed a 47% decrease comparing the pcDNA3.1-U44 transfections to the empty pcDNA3.1 transfections. At 48 hours, the viable cell count of pcDNA3.1-U44 transfections compared to pcDNA3.1 transfections had a decrease of 44% (Figure 23B).

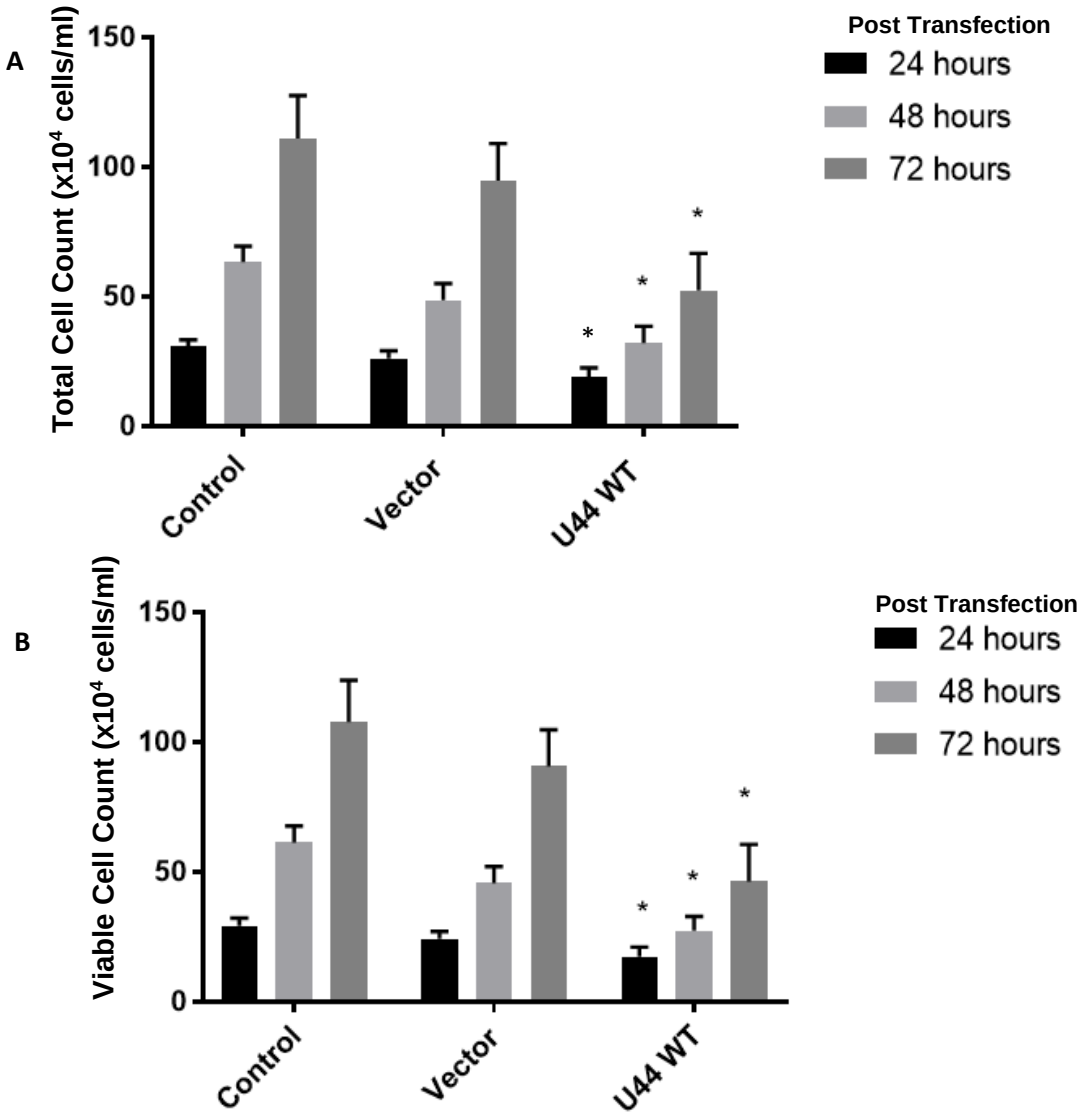

Figure 23: **Effects of SNORD44 overexpression on the number of total and viable cell number of CEM-C7 cells.** Graph of the total (A) and viable (B) cell count (cells/ml). $1x10^7$ CEM-C7 cells were transfected with pcDNA3.1 and pcDNA3.1-U44. A control was also used in which no RNA/DNA was inserted. Using flow cytometry, the cell count was analysed at 24, 48 and 72 hours post transfection (n=3). A one-way ANOVA with a tukey test was performed to analyse the statistical significance of the results. The asterisk above the bars symbolises a statistical significance between pcDNA3.1-U44 and the vector transfections. *P<0.01 comparing transfections of pcDNA3.1-U44 to vector at equal time points. U44 WT = *SNORD44*

The effects of SNORD44 overexpression on the basal apoptosis level of CEM-C7 was determined using acridine orange staining. At all-time points analysed, the percentage of apoptotic cells was significantly higher in transfections with pcDNA3.1-U44 than transfections with empty pcDNA3.1 vector. There was more than a 2-fold increase in the percentage of apoptotic cells in the cells transfected with pcDNA3.1-U44 compared to empty pcDNA3.1 vector at 72 hours (Figure 24).

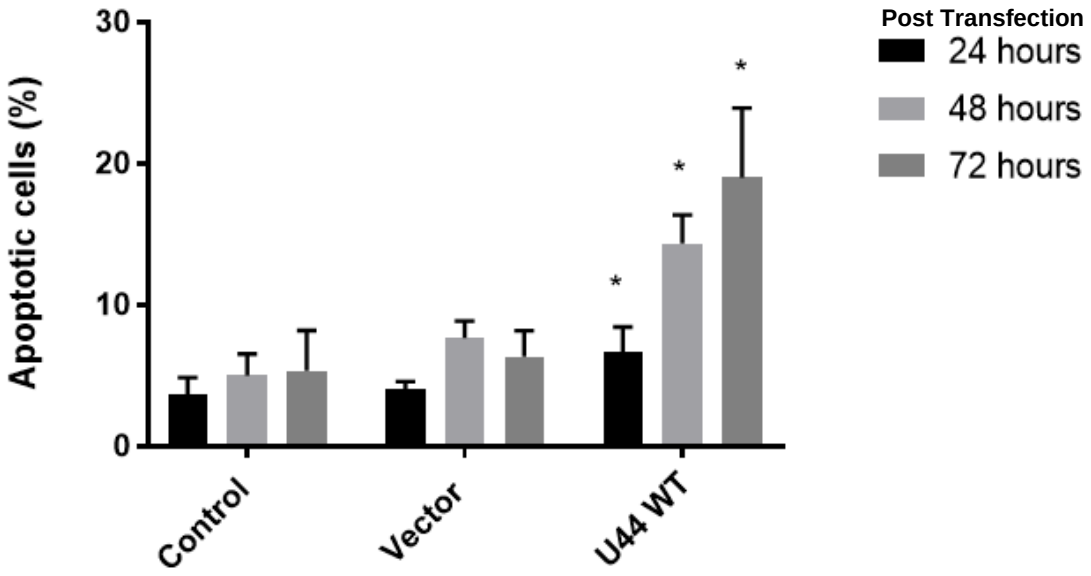

Figure 24: **Effects of SNORD44 overexpression on basal apoptosis of CEM-C7 cells.** $1x10^7$ CEM-C7 cells were used during this electroporation. pcDNA3.1 and pcDNA3.1-U44 were transfected into CEM-C7 cells. The % apoptotic cells was determined using acridine orange after 24, 48 and 72 hours. A one-way ANOVA with a tukey test was performed to analyse the statistical significance of the results. The asterisk above the bars symbolises a statistical significance between pcDNA3.1-U44 and the vector transfections. *P<0.01 comparing transfections of pcDNA3.1-U44 and vector transfections at equal time points. U44 WT = *SNORD44*

A cell cycle assay was also performed and similar to the results obtained with Jurkat T cells, the results showed that pcDNA3.1-U44 transfection did not affect the cell cycle profile of CEM-C7 cells. All transfected cells showed a very similar percentage of cells in each stage of the cell cycle. The percentage of cells in G0/G1 was ~45%, S phase was ~20% and G2/M phase was ~29%. This suggests there is no effect on cell cycle progression when pcDNA3.1-U44 is overexpressed in CEM-C7 cells (Figure 25).

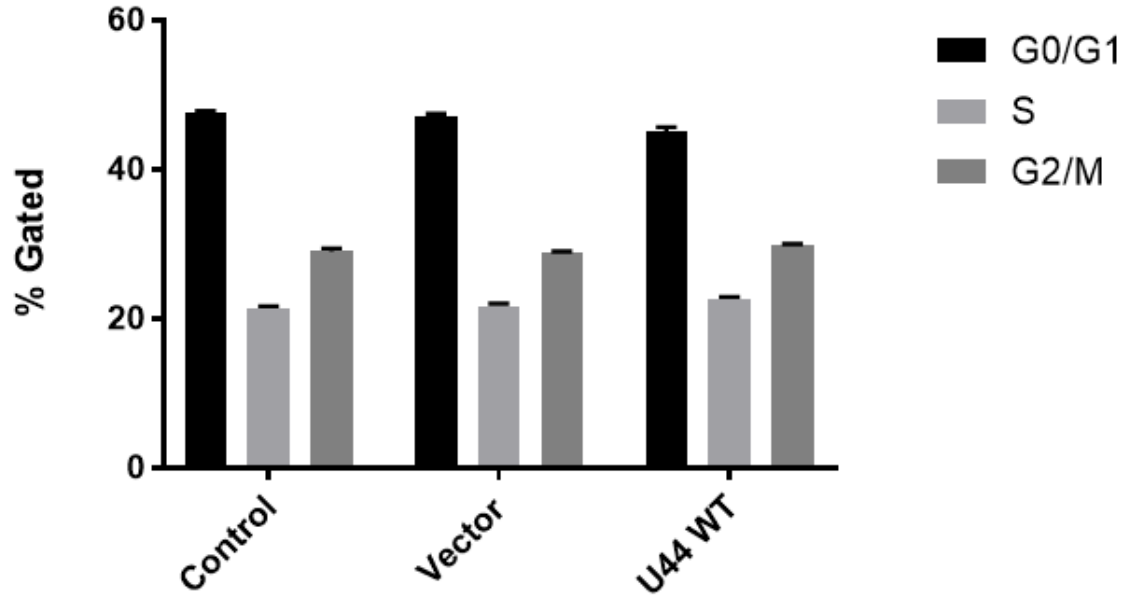

Figure 25: The effect of overexpressing SNORD44 on cell cycle progression. Flow cytometry was used along with the Muse cell cycle assay kit to analyse the cell cycle of transfected cells. The CEM-C7 cells were stained and the assay was used in flow cytometry the day after staining. N=3 experiments were combined to produce this graph. The cells were gated to include G0/G1, S and G2/M phases and to exclude dead cells. Statistical analysis was not performed on this data. U44 WT = *SNORD44*

3.4 Effects of Overexpression of mutant SNORD44 on the viability of leukemic T cells

SNORD44 amplified from the B lymphoma cells Jeko1 and cloned into pcDNA3.1 (by Dr. Pickard and Prof. Williams, personal communication) showed to have two mutations. The mutations are located at bases 16 and 25 within the sequence. This heterozygous mutation changes the G bases to A. Figure 26 shows the nucleotide sequence of the mutated *SNORD44* (*SNORD44*$^{(-)}$) including the location of the mutations.

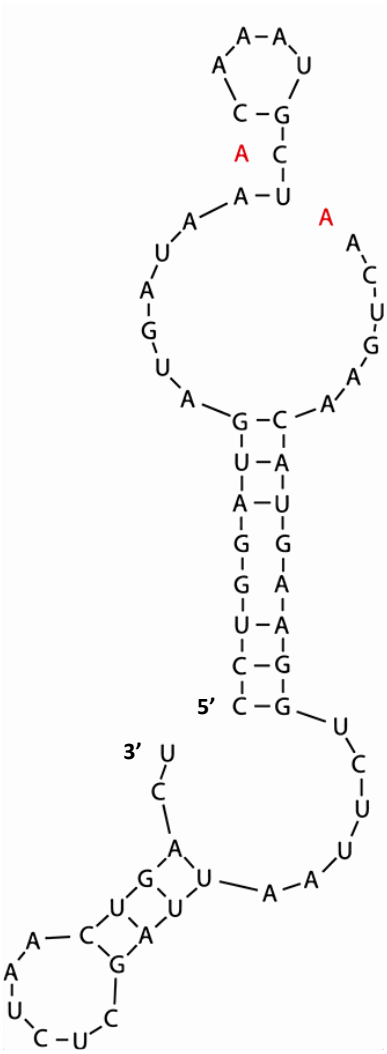

Figure 26: **Mutant U44 snoRNA isolated from Jeko1 cell line.** Diagram showing the nucleotide sequence of snoRNA U44 mutant including the mutations (in red) located at position 16 and 25, changing the bases from a G to an A.

To overexpress SNORD44$^{(-)}$ in Jurkat cells, nucleofection was used. Jurkat cells were transfected with pcDNA3.1- and *SNORD44*$^{(-)}$ whilst control cells received no RNA. Expression levels of SNORD44 in transfected cells were measured using qRT-PCR. Results showed that transfection with the mutant snoRNA resulted in a 12-fold increase in the endogenous levels of SNORD44 compared to pcDNA3.1 transfected cells (Figure 27).

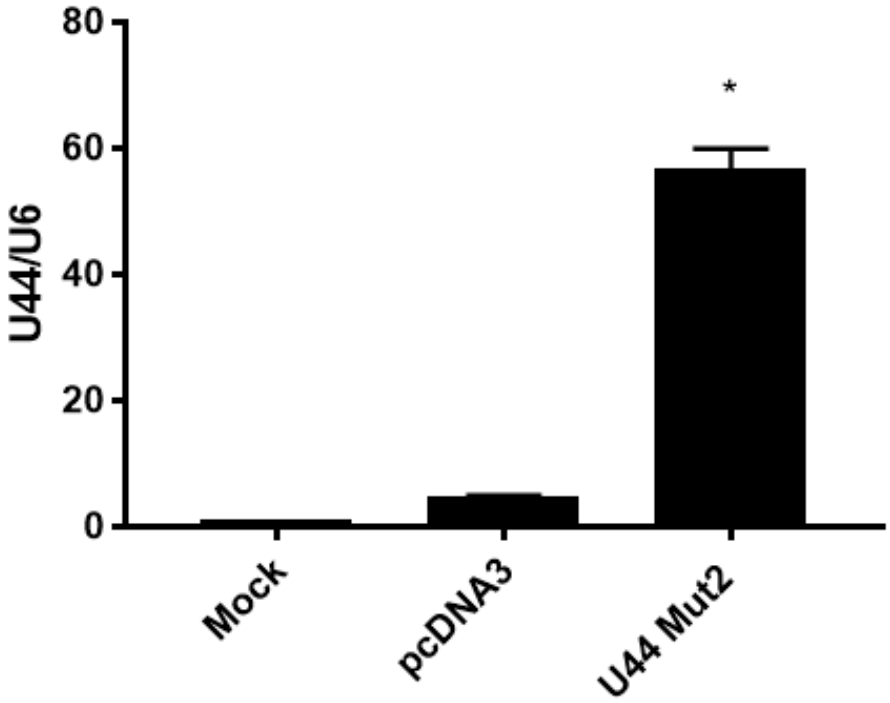

Figure 27: **PCR analysis to determine the expression levels of SNORD44 in Jurkat cells**. Graph to show the ratio of U44:U6 (n=3). $1x10^6$ Jurkat cells were nucleofected with pcDNA3.1 or pcDNA3.1-U44$^{(-)}$. Mock cells were nucleofected with no DNA. RNA was collected from the transfected cells and used to produce cDNA. SYBR green RT-PCR experiments were run using the cDNA produced and analysed using the $2^{-\Delta\Delta Ct}$ method to calculate the U44:U6 ratio. An unpaired T-test was used to analyse the statistical significance of the results. *P<0.0001 for pcDNA3.1-U44$^{(-)}$ transfections compared to vector pcDNA3.1 transfections into Jurkat cells. U44 Mut2 = *SNORD44$^{(-)}$*

Cells were counted at 24, 48 and 72 hours post transfection to assess the effects of pcDNA3.1-U44$^{(-)}$ overexpression on the total and viable cell count of Jurkat cells. The statistical analysis performed on the results shows that there was no significant difference between the total and viable cell count (cells/ml) of pcDNA3.1-U44$^{(-)}$ transfections and vector transfections at any time point (Figure 28 A and B).

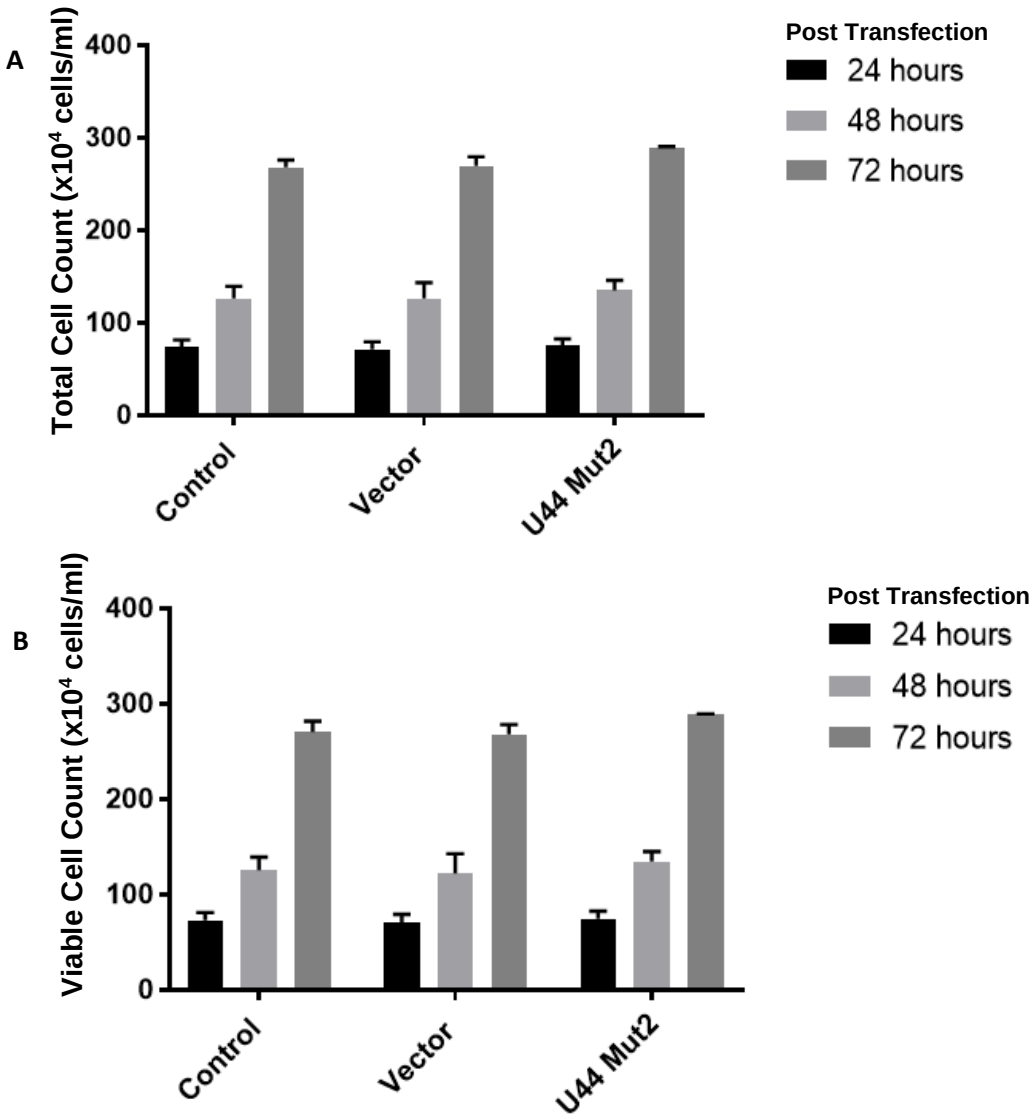

Figure 28: **Effects of the overexpression of SNORD44$^{(-)}$ on the total and viable cell count of Jurkat cells**. Graph of the total (A) and viable (B) cell count (cells/ml) of transfected Jurkat cells at 24, 48 and 72 hours post transfection of N=3 experiments. 1x10^6 Jurkat cells were used during this nucleofection. pcDNA3.1 and pCDNA3.1-U44$^{(-)}$ were transfected into Jurkat cells. A control was also used in which no RNA/DNA was transfected into Jurkat cells. Using a haemocytometer, cells were stained with trypan blue and counted under a microscope at 24, 48 and 72 hours. A one-way ANOVA with a tukey test was performed to analyse the statistical significance of the results. U44 Mut2 = *SNORD44$^{(-)}$*

To confirm the validity of the cell counting performed using vital dye staining, flow cytometry was utilised to further assess the effects of overexpression of SNORD44$^{(-)}$ on the cell number. While no effects on viable and total cell count after 24 and 48 were observed, a 10% increase in the number of total and viable cells in the culture of cells transfected with pcDNA3.1-U44$^{(-)}$ at 72 hours than in the vector transfected culture (Figure 29A and B). Such effects were not observed using vital dye staining.

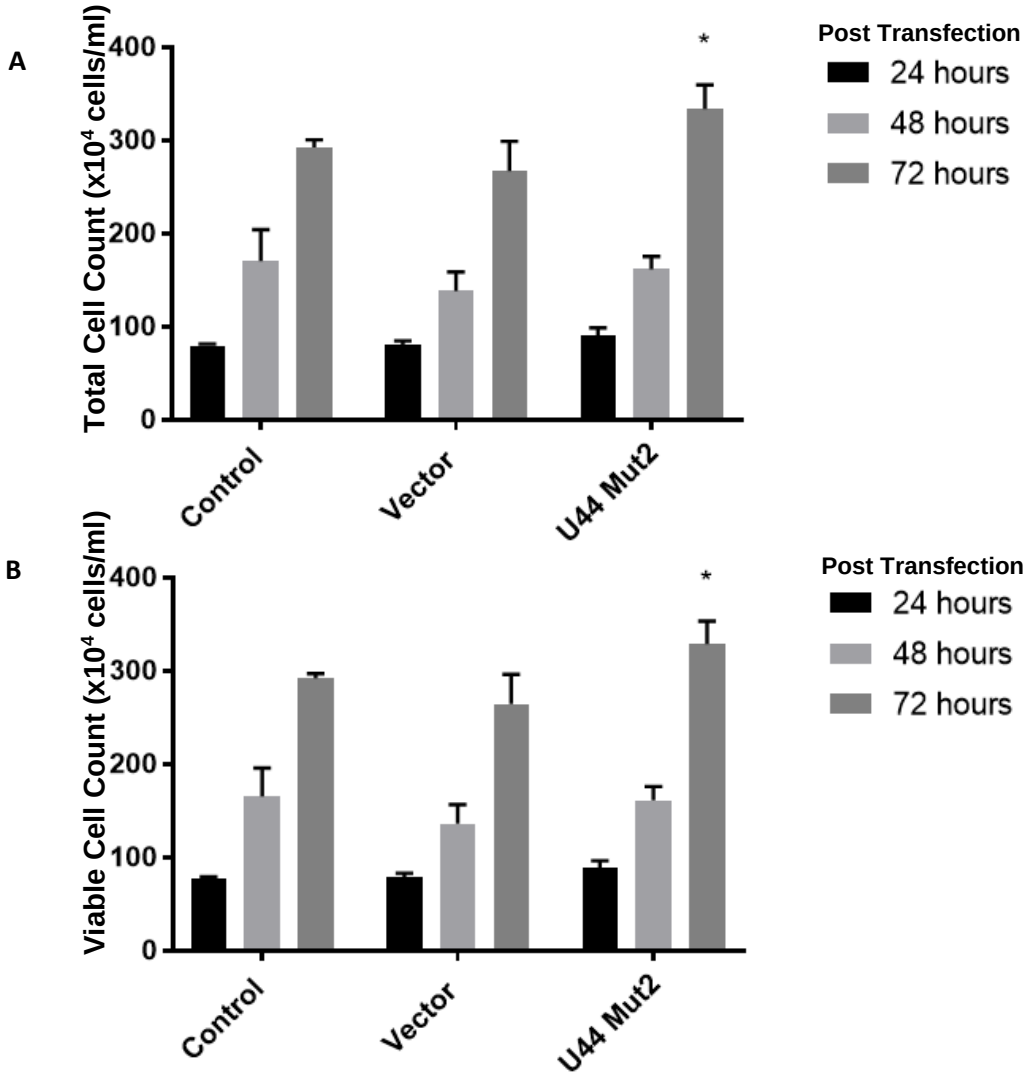

Figure 29: **Effect of overexpressing SNORD44$^{(-)}$ on the viable and total cell count in Jurkat cells.** 1x10^6 Jurkat cells were transfected with either pcDNA3.1 or pcDNA3.1-U44$^{(-)}$. Using flow cytometry, the cell count was analysed after 24, 48 and 72 hours. (A) Represents total cell number and (B) represent viable cell number. A one-way ANOVA with a tukey test was performed to analyse the statistical significance of the results. The asterisk above the bars symbolises a statistical significance between pcDNA3.1-U44$^{(-)}$ and the vector transfections. *P<0.001 comparing the vector and pcDNA3.1-U44$^{(-)}$ transfections at equal time points. U44 Mut2 = *SNORD44$^{(-)}$*

Acridine orange staining revealed that overexpression of the SNORD44$^{(-)}$ had no statistical significant effects on the basal apoptosis levels, implying that *SNORD44$^{(-)}$* does not affect basal apoptosis in these cells and the *SNORD44* has lost its pro-apoptotic activity (Figure 30).

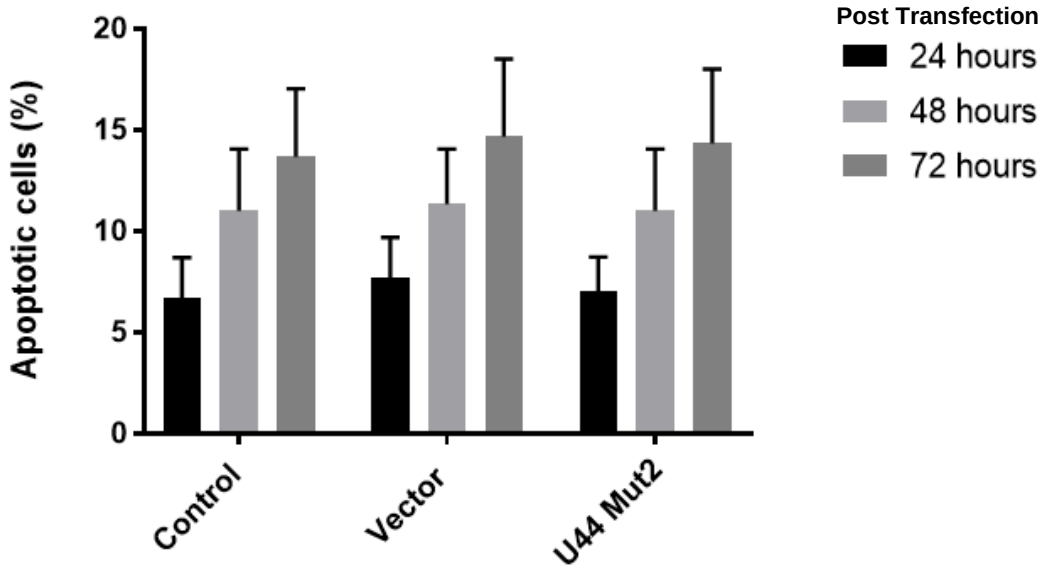

Figure 30: **Effect of overexpressing SNORD44$^{(-)}$ on basal apoptosis in Jurkat cells.** Graph to show the percentage of apoptotic cells of transfected Jurkat cells at 24, 48 and 72 hours post transfection(n=3). Apoptosis rate was assessed using acridine orange. A one-way ANOVA with a tukey test was performed to analyse the statistical significance of the results**.** U44 Mut2 = *SNORD44$^{(-)}$*

The effects of overexpressing SNORD44$^{(-)}$ was also assessed in CEM-C7 cells using electroporation. Transfection of pcDNA3.1-U44$^{(-)}$ results in a ~16-fold increase in SNORD44 expression levels (Figure 31).

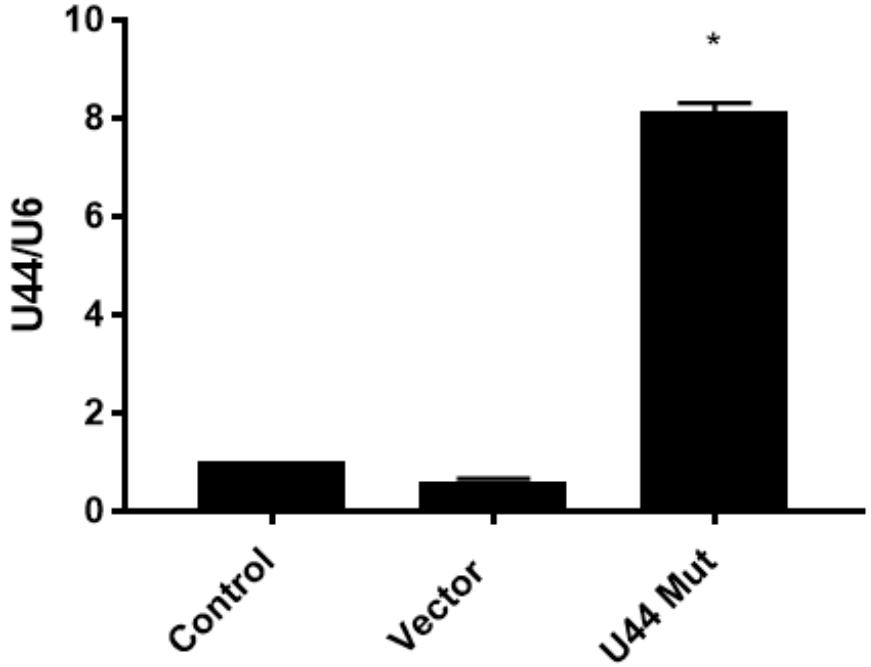

Figure 31: **qRT-PCR analysis to determine SNORD44 expression levels in the transfected CEM-C7 cells.** 1x10^7 CEM-C7 cells were transfected with either pcDNA3.1 or pcDNA3.1-U44$^{(-)}$ (n=3). A control was the mock transfected cells. RNA was isolated and collected from the transfected cells and used to synthesise cDNA. SYBR green RT-PCR experiments were run using the cDNA produced and analysed using the $2^{-\Delta\Delta Ct}$ method to calculate the U44:U6 ratio. An unpaired T-test was used to analyse the statistical significance of the results. *P<0.0001 for pcDNA3.1-U44$^{(-)}$ transfections compared to pcDNA3.1 transfections into CEM-C7 cells. U44 Mut2 = *SNORD44$^{(-)}$*

Similar to the results obtained with Jurkat T cells, transfection of CEM-C7 cells with pcDNA3.1-U44$^{(-)}$ did not have any significant difference on the total and viable cell number in these cells when compared to the control using vital dye staining (Figure 32 A and B) and flow cytometry (Figure 33 A and B). pcDNA3.1-U44$^{(-)}$ transfection did not affect basal apoptosis levels (Figure 34). Together, these results provide evidence that the mutation in *SNORD44* has abolished its growth inhibitory and pro-apoptotic effects.

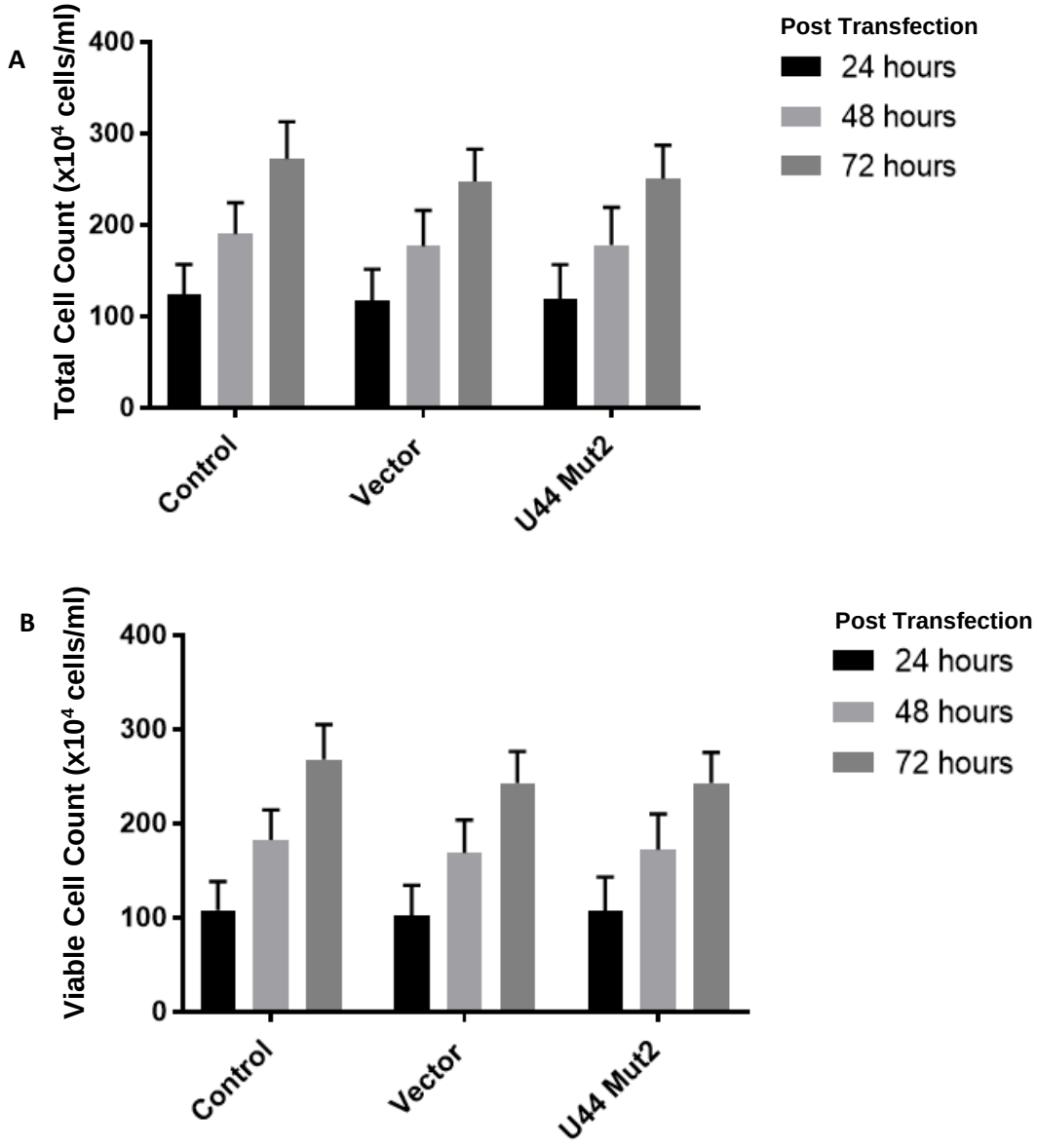

Figure 32: **Effect of overexpressing SNORD44$^{(-)}$ on total and viable cell count of CEM-C7 cells.** Graph of the total (A) and viable (B) cell count (cells/ml) of transfected CEM-C7 cells at 24, 48 and 72 hours post transfection using vital dye staining (n=3). A one-way ANOVA with a tukey test was performed to analyse the statistical significance of the results. U44 Mut2 = *SNORD44$^{(-)}$*

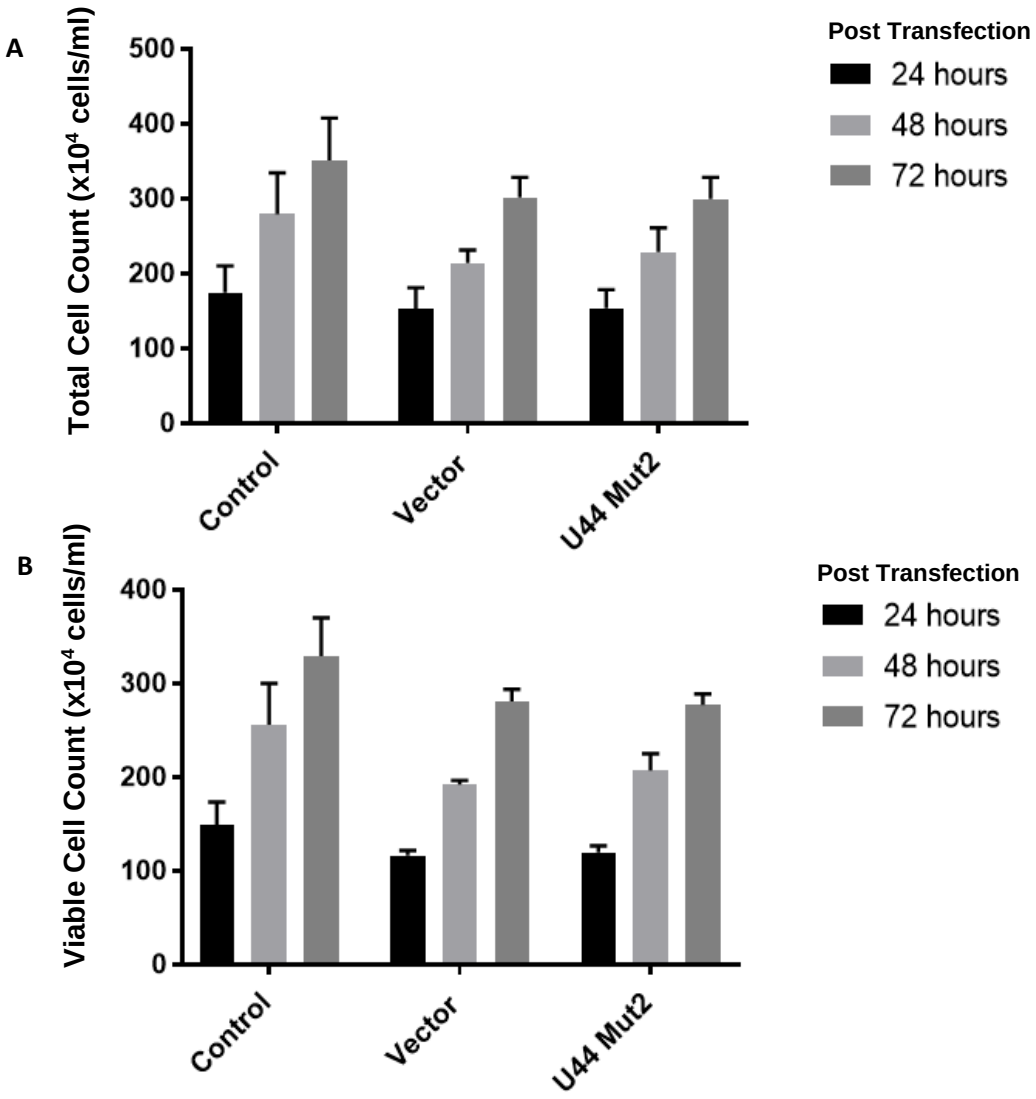

Figure 33: **Effect of SNORD44$^{(-)}$ overexpression on total and viable cell count of CEM-C7 cells.** Graph of the total (A) and viable (B) cell count (cells/ml) of transfected CEM-C7 cells at 24, 48 and 72 hours post transfection (n=3). CEM-C7 cells electroporated with pcDNA3.1 and pcDNA3.1- U44$^{(-)}$. Cell number was determined using flow cytometry. A one-way ANOVA and tukey test was performed to analyse the statistical significance of the results. U44 Mut2 = *SNORD44$^{(-)}$*

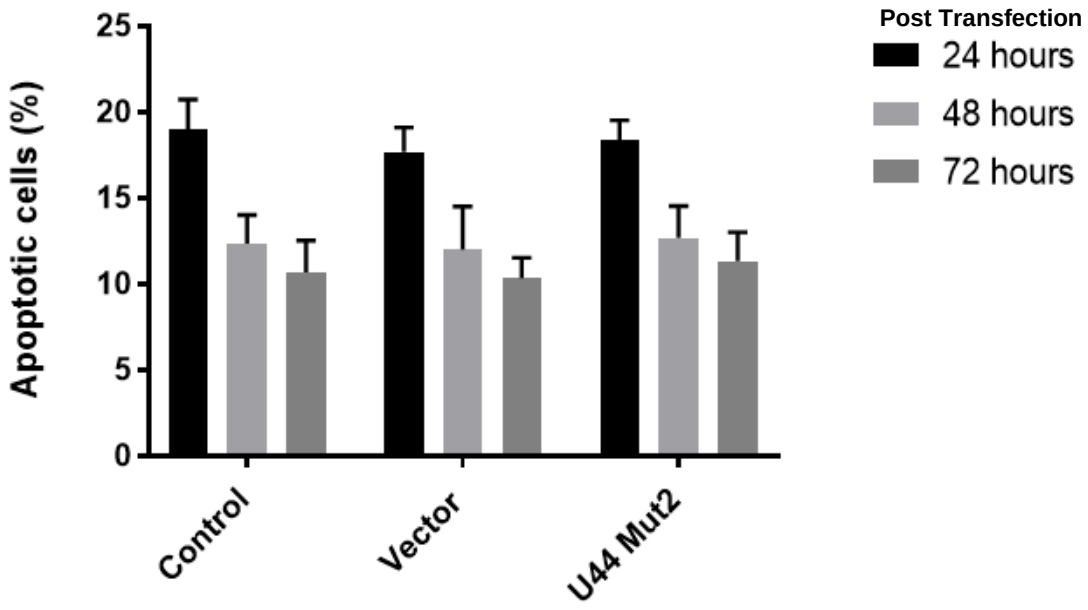

Figure 34: **Effect of overexpression of SNORD44$^{(-)}$ on basal apoptosis of transfected CEM-C7 cells.** Graph to show the percentage of apoptotic cells of transfected CEM-C7 cells at 24, 48 and 72 hours post transfection (n=3). Apoptosis was determined using acridine orange staining. A one-way ANOVA and tukey test was performed to analyse the statistical significance of the results**.** U44 Mut2 = *SNORD44$^{(-)}$*

3.5 Effects of pan-caspase Inhibitor Z-VAD-FMK on the pro-apoptotic effects of *SNORD44*

In the next series of experiments, pan-caspase Inhibitor Z-VAD-FMK was used to determine whether the growth inhibitory and apoptotic effects caused by *SNORD44* involves caspases. Z-VAD-FMK is a pan-caspase inhibitor which binds to the catalytic site of caspase proteases inhibiting their activity. This binding of Z-VAD-FMK with the proteases is irreversible. Cells were pre-incubated with the pan caspase inhibitor Z-VAD-FMK for 24 hours prior to transfection with pcDNA3.1-U44 and control cells received the vehicle (10% DMSO). 24h post incubation, cells were transfected with either pcDNA3.1 or pcDNA3.1-U44. The results show that cells transfected with pcDNA3.1-U44 without pre-incubation with Z-VAD-FMK treatment showed a significantly lower viability at 48 hours and 72 hours compared to the vector as assessed using MTS assay. There was a ~23% decrease in cell viability in pcDNA3.1-U44 transfected cultures compared to pcDNA3.1 transfections at 48 hours and 72 hours. Pre-incubation of Jurkat cells with Z-VAD-FMK abolished the growth inhibitory effects of *SNORD44*. The results show that SNORD44 overexpression in Jurkat cells treated with Z-VAD-FMK did not have any effect on the cell viability (Figure 35). The results suggest that the pro-apoptotic activity of *SNORD44* may require the activity of caspases.

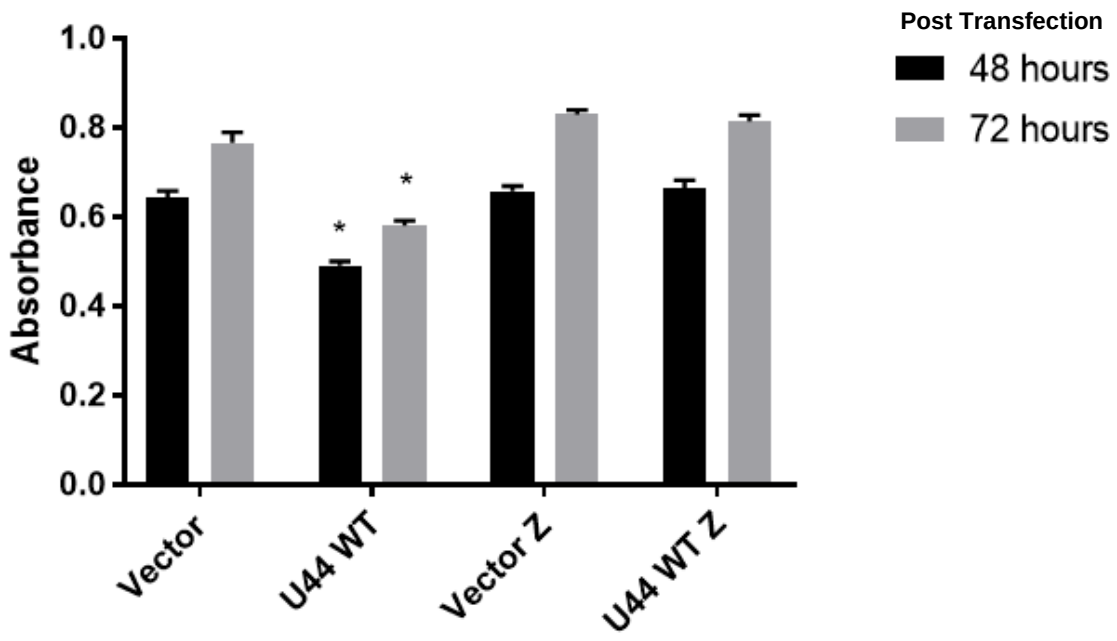

Figure 35: Effect of inhibiting caspases on the apoptotic function of *SNORD44* in transfected Jurkat cells. Jurkat cells were incubated in the absence or presence of Z-VAD-FMK. Cells were transfected with either pcDNA3.1-U44 or empty vector. Cell viability was assessed using MTS at 48 and 72 hours post transfection (n=3). The bars labelled with a 'z' along the x axis signifies the samples in which Z-VAD-FMK had been applied. A one-way ANOVA with a tukey test was performed on the results from this experiment. The significant results are indicated by placing an asterisk above the bar on the graph. *P<0.01 comparing all transfections to one another at equal time points. U44 WT = *SNORD44*

Flow cytometry was also used to confirm the results obtained with the MTS assay. The results showed that the total and viable cell count of cells transfected with pcDNA3.1-U44 and not treated with Z-VAD-FMK was significantly lower than cells transfected with pcDNA3.1 vector (29% and 38% respectively for total cell count and 40% and 43% respectively for the viable cell count). On the other hand, when Jurkat cells were treated with Z-VAD-FMK pre-transfection, the cells transfected with pcDNA3.1-U44 did not show a decrease in the number of total and viable cells as seen in the cells without Z-VAD-FMK (Figure 36 A and B). This result was concordant with Figure 35 as a lower metabolic activity seen in a sample suggests a lower number of total or viable cells.

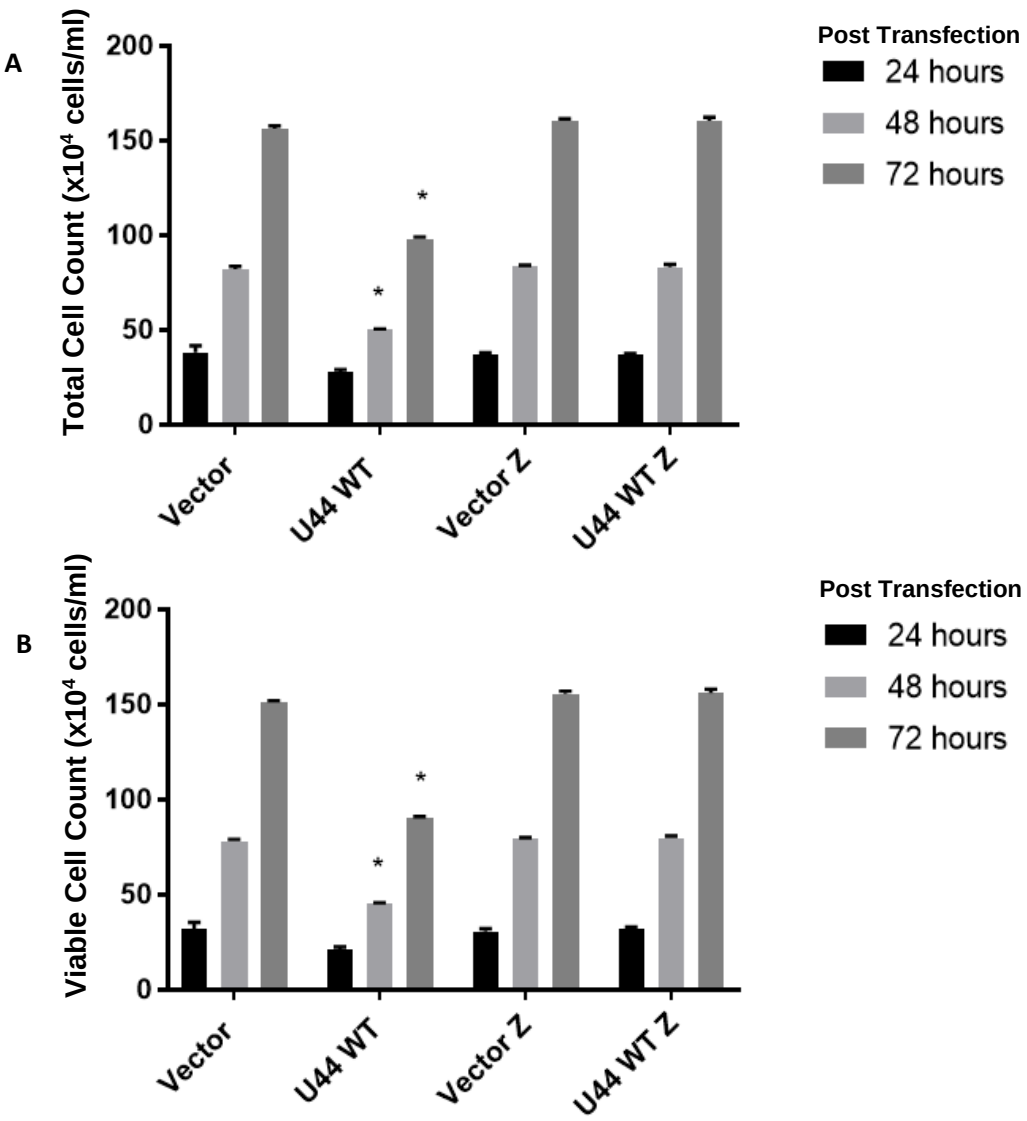

Figure 36: Effect of inhibiting caspases on the growth inhibitory effects of *SNORD44* in Jurkat cells. Graph to show the total (A) and viable (B) cell count (n=3) in transfected cells that have been pre-incubated with Z-VAD-FMK or vehicle. Cell count was determined using flow cytometry at 24, 48 and 72 hours post transfection. Bars labelled with a 'z' along the x axis signifies the samples in which Z-VAD-FMK had been applied. A one-way ANOVA with a tukey test was performed on the results from this experiment. The significant results are indicated by placing an asterisk above the bar on the graph. **P<0.01 comparing all transfections to one another at equal time points. U44 WT = *SNORD44*

CEM-C7 cells were also used to investigate the effects of Z-VAD-FMK pre-treatment on the growth inhibitory effects of *SNORD44*. Consistent with the observations obtained from Jurkat T cells, pre-incubation of CEM-C7 cells with Z-VAD-FMK abolished the growth inhibitory effects of *SNORD44*. pcDNA3.1-U44 transfection into CEM-C7 cells that were treated with Z-VAD-FMK and without Z-VAD-FMK for 24 hours did not have any effects on the cell viability and the number of total and viable cells as assessed with MTS assay and flow cytometry (Figure 37 and 38).

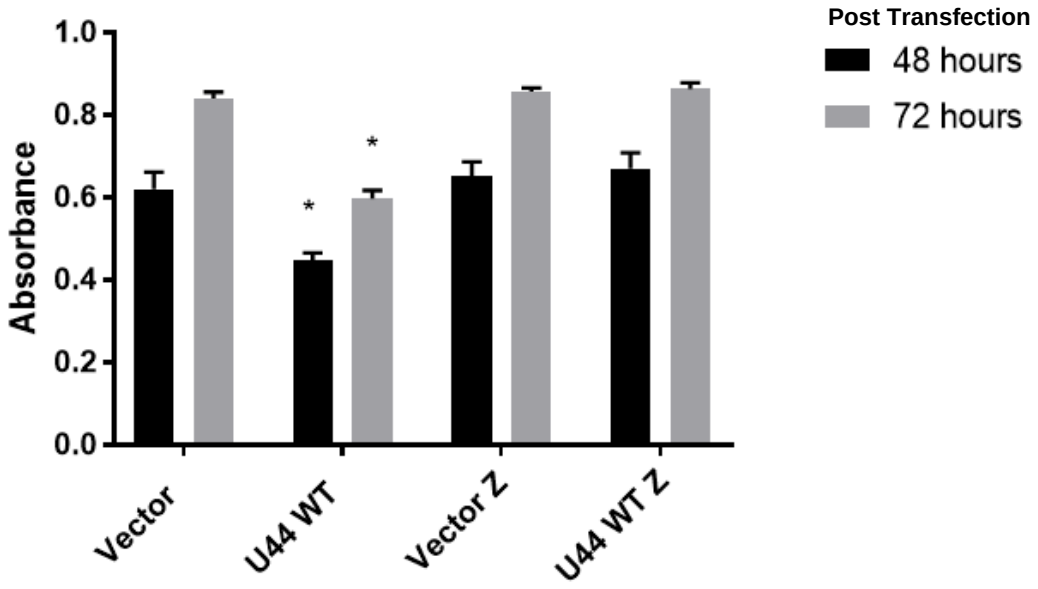

Figure 37: Effect of inhibiting caspases on the growth inhibitory effects of *SNORD44* in CEM-C7 cells. Graph to show the absorbance values of transfected CEM-C7 cells which were treated with the presence or absence of Z-VAD-FMK (n=3). Cell viability was assessed using an MTS assay. Bars labelled with a 'z' along the x axis signifies the samples in which Z-VAD-FMK had been applied. A one-way ANOVA with a tukey test was performed on the results from this experiment. The significant results are indicated by placing an asterisk above the bar on the graph. *P<0.01 comparing all transfections to one another at equal time points. U44 WT = *SNORD44*

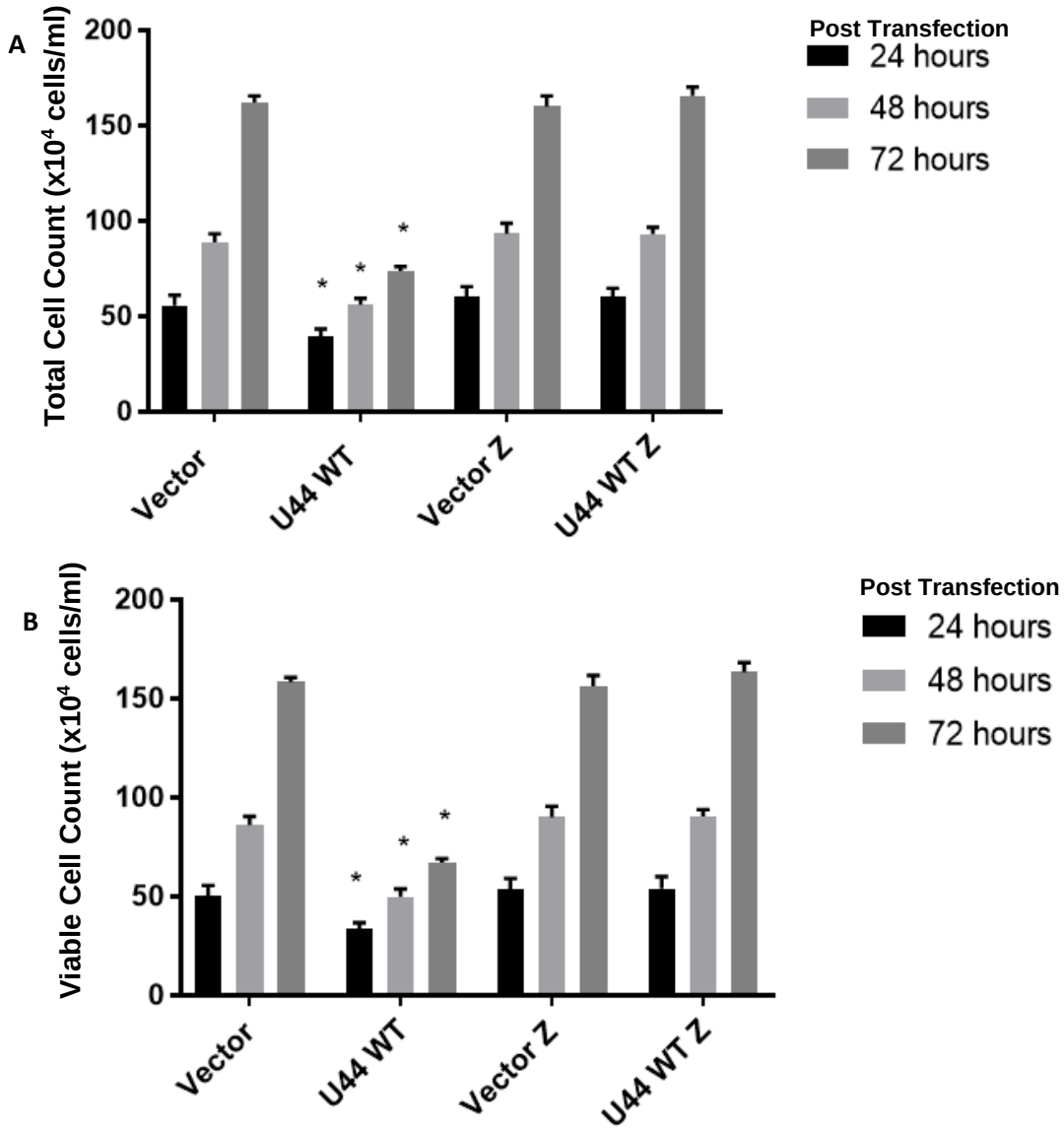

Figure 38: Effect of inhibiting caspases on the growth inhibitory effects of *SNORD44* in CEM-C7 cells. Graph to show the total (A) and viable (B) cell count (cells/ml) as assessed using flow cytometry. Bars labelled with a 'z' along the x axis signifies the samples in which Z-VAD-FMK had been applied. A one-way ANOVA with a tukey test was performed on the results from this experiment. The significant results are indicated by placing an asterisk above the bar on the graph. *P<0.01 comparing all transfections to one another at equal time points. U44 WT = *SNORD44*

4 Discussion

The long non-coding RNA growth arrest specific 5 (*GAS5*) transcript has been shown to have a role in regulating cell growth and apoptosis in human T-cells, prostate, breast cancer and colorectal cancer cells (Mourtada-Maarabouni et al., 2009; Pickard et al., 2013; Li et al., 2018). Strong lines of evidence implicated *GAS5* in the pathogenesis of various types of cancer and supported the fact that it acts as tumour suppressor gene. In addition of its 12 exons, human *GAS5* encodes within its introns ten box C/D snoRNAs U74, U75, U76, U77, U44, U78, U79, U80, U47 and U81 (Smith and Steitz, 1998). Previous studies have confirmed that the only conserved regions of the *GAS5* transcript between mouse and humans are the snoRNAs and its 5' end sequence, suggesting that these sequences are functionally important and therefore they show greater conservation (Smith and Steitz, 1998). Recent studies have reported a link between the dysregulation of *GAS5* snoRNAs and some types of human cancer, highlighting the need for further research to characterise the functions of *GAS5* snoRNAs.

The current study investigates the role of *SNORD44,* one of *GAS5* snoRNAs, in the regulation of leukemic cell fate. *SNORD44* is a C/D box snoRNA encoded by a *GAS5* intron located between exon 5 and 6. The housekeeping function of *SNORD44* is well established as it is known to serve as a guide to modify 18S rRNA. However, emerging evidence suggests a new role for *SNORD44* in cancer. Decreased expression levels of SNORD44 were reported to be directly related to poor prognosis in breast cancer (Gee et al., 2011). Low levels of *SNORD44* was also described to correlate strongly with poor survival of patients with head and neck squamous cell carcinoma (Gee et al., 2011). On the other hand, *SNORD44* is

upregulated in colorectal tumours compared to benign colon tissues (Krell et al., 2014). Interestingly, *SNORD44* was also upregulated in human cells infected with chikungunya virus, suggesting that it may be involved in the regulation of T-cell growth (Saxena et al., 2013). These results highlight the importance of further studies to characterise the function of *SNORD44*. The current study investigated the role of *SNORD44* in the regulation of leukemic cell survival. The results showed that overexpression of SNORD44 in two different leukemic T cells Jurkat and CEM-C7 leads to growth inhibition and an increase in basal apoptosis. Taken together, the results suggest that *SNORD44* regulates leukemic cell survival and has pro-apoptotic activity in these cells.

The role of *SNORD44* in the regulation of leukemic T-cell survival is unknown. The results from this current study have shown that *SNORD44* may have an important role in the regulation of leukemic cell fate decision and suggests that this snoRNA might function independently from its host gene *GAS5*. Overexpressing the SNORD44 in two different human T-cell lines, Jurkat and CEM-C7 cells, resulted in an increase in the overall percentage of apoptotic cells, implying that high expression levels of SNORD44 induces basal apoptosis in both leukemic T cells. Increased SNORD44 expression levels were associated with a decrease in both total and viable cell number in both cell lines. The decrease in the number of total and viable cells is not due to the transfection process since transfection of T-cells with the empty vector did not affect basal apoptosis and cell number. The results confirm that *SNORD44* regulates T cell survival and consistent with previous findings, it might act as a tumour suppressor gene. Other studies have reported that *GAS5* snoRNA, *SNORD76* (U76), also acts as tumour suppressor in glioblastoma (Chen et al, 2015). Overexpression of SNORD76 inhibited proliferation and growth

of glioma cells. On the other hand, decreased expression of SNORD76 was associated with increased survival and a more malignant phenotype (Chen et al., 2015). Additionally, *SNORD76*, not its host gene *GAS5*, was found to be downregulated in glioblastoma grade IV (Chen et al., 2015), providing evidence that these snoRNAs might be acting independently of their host gene. *GAS5 SNORD*47 (U47) was also found to act as tumour suppressor in glioblastoma. *SNORD47* was found to be downregulated in glioma tissues samples and its levels inversely correlated with poor prognosis. Increased *SNORD47* suppressed invasion and migration and sensitized the cells to the chemotherapy drug temozolomide (Xu et al., 2017). However, *SNORD76* was found to be upregulated in hepatocellular carcinoma compared to adjacent non-tumour cells and its increased expression level was related to a poor survival rate of patients with the disease (Wu et al., 2018). Silencing *SNORD76* in hepatocellular carcinoma cells inhibited cell proliferation by promoting G0/G1 cell cycle arrest and apoptosis. Knockdown of SNORD76 levels also resulted in decreased hepatocellular carcinoma cell growth in an animal model. In contrast, overexpression of SNORD76 promoted cell proliferation. Together, the present work and previous findings highlight the importance of investigating the roles of *GAS5* snoRNAs to determine their potential as diagnostic markers and therapeutic targets.

The growth inhibitory effects of *SNORD44* in leukemic T cells are consistent with the effects observed with *SNORD76* and *SNORD46* in other cell lines. However, the effects of *SNORD44* on cell cycle progression are not consistent with *SNORD47* and *SNORD76* effects on glioma cell cycle. Chen et al., (2015) have reported that overexpression of SNORD76, caused a cell cycle arrest in the S phase. However, the data from this study showed that SNORD44 expression had no apparent effect

on the cell cycle. Increased SNORD44 expression levels did not affect the cell cycle progression and percentage of cells in each of the cell cycle phases was comparable to control cells. These observations together with the enhanced basal apoptosis levels associated with SNORD44 over-expression suggests that *SNORD44* growth inhibitory effects are due to an increase in cell death but not to cell cycle arrest.

Known guided mutations have been used in many studies to determine important features of a molecules structure. Liang et al. (2010), studied snR10 snoRNA, a yeast specific snoRNA, to determine the important functional regions of the structure. To do this, guide domain mutations were carried out to determine whether the function of this snoRNA changed. In the present study, a mutant version of *SNORD44* was transfected into cells to determine whether the mutation in its sequence can interfere with *SNORD44* growth inhibitory effects. The mutations are located at nucleotide 16 and nucleotide 25 of the snoRNA sequence, changing G base to an A (Appendix A for the base sequence of *SNORD44* mutant). The results showed that overexpression of the mutant SNORD44 did not have any effect on cell number or apoptosis of Jurkat and CEM-C7 cells. The proapoptotic and growth inhibitory effects of *SNORD44* were lost in the mutant form of *SNORD44*. Dong et al. (2008) identified a mutant form of U50 after analysing the expression levels of U50 in prostate cancer cells. After mutation screening, it was determined that a homozygous mutation of a TT deletion (2 base pairs) was found in 2 of 30 prostate cancer cell lines. Normal prostate cell samples did not express the mutant U50 snoRNA. While overexpression of U50 led to inhibition of cell growth and decrease in short and long term cell survival of prostate cancer cells, the mutant U50 had no effect on these cells which suggests that the mutation has abolished the tumour

suppression function of U50. This study and the findings in the present study suggest that the mutations in U50 and *SNORD44* may result in the loss of functional sequences and consequently the loss of their growth inhibitory and pro-apoptotic effects.

The mutation at base 25 is in one of the D boxes. The mutation means that the first D' Box cannot be produced which effects the rest of the structure. The second mutation at base 16 is located within the 19nt and 25nt reads which means these smaller RNA molecules cannot be produced. It can be hypothesised that the structure of *SNORD44* is important in its apoptotic function. The predicted structure of *SNORD44* is depicted in figure 41 below.

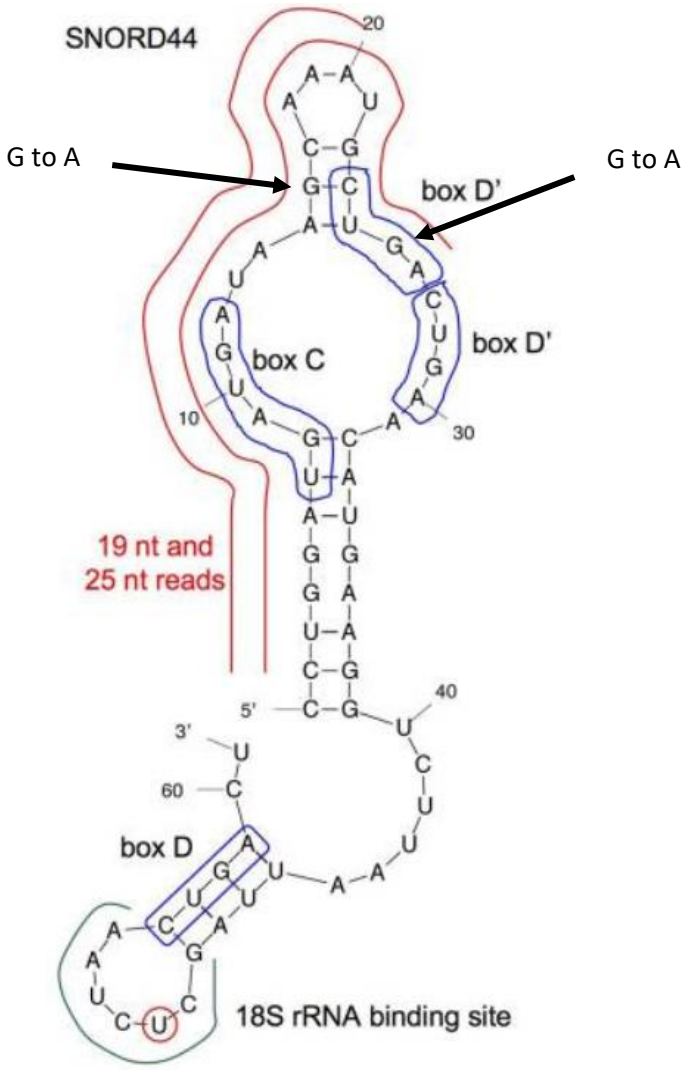

Figure 41: Predicted secondary structure of *SNORD44*. The locations of the 18s rRNA binding site and the C/D boxes are labelled in the diagram. The 19nt and 25nt sdRNA reads are shown using a red line from bases 2 to 26. The arrows show the location of the mutations within the structure (Bai et al., 2014).

In recent years, it has been well established that snoRNAs can be processed into miRNAs named small nucleolar RNA-derived RNAs (sdRNAs). These sdRNAs have been shown to have functions similar to miRNAs. A mature miRNA forms a RISC complex to silence target mRNA. Argonaute proteins are essential to the RISC complex and therefore have associations with miRNA. At least three of *GAS5* snoRNAs may be processed to yield miRNAs. These snoRNAs include *SNORD44* in addition to U74 and U78 (Brameier et al., 2011). If *SNORD44* is processed into miRNA, the miRNA product may stimulate RNA interference

pathways leading to inhibition of a protein or RNA involved in promoting cell survival and therefore leading to cell death. Ender et al. (2008) identified that snoRNA ACA45 is processed into smaller non-coding RNAs that associate with Ago proteins. It was observed that the snoRNA ACA45 product associated with Ago1 and Ago2 similarly to miRNA. Sequencing analysis on snoRNA ACA45 showed that the section producing the sdRNA is conserved in mammals and therefore must have an important processing function. Another snoRNA derived miRNA-like non-coding RNA named sno-miR-28, inhibits TAF9B (a p53 stabilising gene) which controls the stability of p53. P53 is important to perform apoptosis and therefore sno-miR-28 may indirectly control apoptosis induced by p53 (Yu et al., 2015). It is well known that miRNAs can regulate p53 which proves further that these smaller sdRNAs act in a similar fashion to miRNAs (Liu et al., 2017). Patterson et al. (2017) investigated the hypothesis that some sdRNAs may contribute to breast cancer malignancy and conducted RNA-seq-based comparison of the small nucleolar RNA-derived RNAs in MCF-7 and the metastatic MDA-MB-231 breast cancer cell lines. Results identified sdRNAs derived from 13 different snoRNAs, all of which are overexpressed in the metastatic MDA-MB-231 breast cancer cell line. sdRNA-93 was the most prevalent of all the sdRNAs identified and inhibiting sdRNA-93 resulted in a decrease in the ability of the breast cancer cells to invade. The opposite occurred when sdRNA-93 expression was increased in breast cancer cell lines. This suggests that sdRNA-93 plays an active role in the malignancy of breast cancer cell lines. Interestingly, *SNORD44* produces 71.4% of all the sdRNAs found in the nucleolus with sdRNA lengths of 20 nt and 25 nt (Bai et al., 2014).

piRNAs are another class of small non-coding RNA typically 26-31 nucleotides long. Initially these small non-coding RNAs were discovered to inhibit transposable

elements and maintain genomic stability. piRNAs associate themselves with PIWI proteins to form a complex which aid in the gene silencing of transposable elements. He et al. (2015) discovered that *GAS5* produces a piRNA named pi-sno75 which is downregulated in MCF7 cells and HEK293T breast cancer cells compared to adjacent healthy tissue. Interestingly, this study found that pi-sno75 upregulated the expression of tumour necrosis factor (TNF) related apoptosis. This means that pi-sno75 could also be a functional tumour suppressor in breast cancer cells originating from the *GAS5* transcript. piRNAs are involved in inducing chromatin modifications and affects gene expression. It is interesting to investigate if *SNORD44* can also be processed into piRNA and whether *SNORD44* derived piRNA is involved in mediating *SNORD44* effects.

The mechanism of action as to which *SNORD44* exerts its apoptotic effect is unknown. It has been reported that Jurkat cells do not produce p53. Cheng and Haas (1990) observed the presence of a heterozygous single-nucleotide substitution in codon 196 in Jurkat cells which results in a shorter version of p53 that does not hold an apoptotic effect seen normally. This factor may mean that *SNORD44* exerts its apoptotic effect independently of p53. The Bcl-2 gene *BAX* is also mutated in Jurkat and CEM-C7 cells. These two cell lines possess two heterozygous frameshift mutations in codon 41 affecting Bcl-2 expression (Meijerink et al., 1998). *BAX* usually functions in the intrinsic apoptosis pathway as an apoptosis activator by binding to Bcl-2 to form a heterodimer. This heterodimer releases cytochrome C to induce apoptosis of cells. Due to this mutation being present in both cell lines used in the present study, it can be concluded that *SNORD44* pro-apoptotic effects do not involve Bcl-2, *BAX* or P53. More analysis must be performed to further understand how *SNORD44* causes apoptosis.

Caspases were first discovered in 1993, when the ced-3 gene was observed to encode a cysteine protease. This cysteine protease was similar to another molecule found earlier named human interleukin-1β-converting enzyme (Caspase-1). Miura et al. (1993), identified that caspase-1 was enough to induce apoptosis in Rat-1 (rat fibroblast) cells. This study sparked many other studies to identify 11 human genes that encode different caspases. Caspases can be subdivided into two groups based on their functions. These two groups are pro-apoptotic and pro-inflammatory (Li and Yuan, 2008). The pro-apoptotic group of caspases can be divided again into two sub groups, the initiator caspases and the executioner caspases. The initiator caspases produce a chain reaction which activates the executioner caspases which perform the degradation of cellular components. An example of a caspase chain reaction is the intrinsic apoptotic pathway. This pathway begins when cytochrome c is released in response to cellular stress. Cytochrome c binds to apoptotic protease activating factor 1 (APAF-1) to recruit caspase-9. This leads to the formation of the apoptosome of caspase-9 and APAF-1 which activates the executioner caspases (Salvesen, 2002). To determine whether the apoptotic effects of *SNORD44* are caspase dependent, the pan-caspase inhibitor Z-VAD-FMK was used. Z-VAD-FMK is a synthetic permeable peptide that acts as a pan-caspase inhibitor by binding to the catalytic site of caspases to inhibit them. This reaction is irreversible (Costa Pereira et al., 2018). Z-VAD-FMK has been used by many studies to inhibit apoptosis including Gamen et al. (1997) who used Z-VAD-FMK to inhibit the toxicity of doxorubicin. This study also observed that Fas-mediated apoptosis was inhibited in Jurkat cells when Z-VAD-FMK was applied to the cells. In the present study, when Z-VAD-FMK was applied to Jurkat and CEM-C7 cells pre-transfection with *SNORD44*, the apoptotic activity and growth inhibitory

effects of *SNORD44* were diminished. This suggests that the proapoptotic function of *SNORD44* is caspases-dependent. More investigation is required to identify which caspases are involved.

In conclusion, this study provides important evidence that *SNORD44* might act as a tumour suppressor in leukemic T-cells by inducing apoptosis. It is not clear how *SNORD44* is performing this function although the absence of p53 and *BAX* in Jurkat and CEM-C7 cells indicates *SNORD44* mode of action does not involve these proteins. More studies are required to assess the diagnostic and therapeutic potentials of *SNORD44*. More research is also needed to fully understand the mechanisms of action of *SNORD44*.

Further work is essential to further characterise *SNORD44* mode of action. It would be beneficial to identify the proteins that *SNORD*44 interacts with to determine the way in which it exerts an apoptotic effect. To do this, a protein pulldown followed by mass spectrometry could be performed. Treiber et al. (2017) conducted a protein pulldown to identify RNA-binding proteins that bind miRNA precursors to regulate their expression. This protein pulldown was followed by mass spectrometry to identify the proteins that the miRNA hairpins interacted with. A similar approach could be used with *SNORD44* to identify the proteins that it interacts with in leukemic cells.

Determining the therapeutic potential of *SNORD44* would also be very valuable research to conduct. To do this, oligonucleotides mimicking *SNORD44* could be utilised. Oligonucleotide therapy is a novel method in which short strings of synthetic nucleotides resembles DNA. These oligonucleotides are designed to be able to alter the expression of targeted genes (Lundin et al., 2015). An oligonucleotide could be

designed to overexpress SNORD44 to allow it to exert its tumour suppressing effect. Pickard and Williams (2016), used a DNA oligonucleotide based on the *GAS5* hormone response element which also exerted an apoptotic effect seen from *GAS5*. This study analysed the long-term effect on breast cancer cell lines when treated with this oligonucleotide which resulted in a reduced colony formation. Breast cancer cell lines treated with the *GAS5* oligonucleotide had a poor cell survival. It is also important to investigate the role of *SNORD44* in the control of cell survival of other cancer cell lines and to determine its expression levels in other types of cancer. The role and significance of other *GAS5* snoRNAs should also be investigated.

Conclusion

The present work determined the role of *SNORD44* in the control of cell fate of leukemic cell lines. SNORD44 overexpression inhibited cell growth and survival in two leukemic cell lines. SNORD44 overexpression also enhanced basal apoptosis in these leukemic cells Mutations in *SNORD44* led to a loss of function. Pre-incubation with the pan-caspase inhibitor also abolished the effects produced by *SNORD44* suggesting that the proapoptotic effects of *SNORD44* are caspase dependent. More studies are required to determine the diagnostic and therapeutic potentials of *SNORD44* in leukaemia.

5 References

miRCURY LNA miRNA PCR System at a glance2018-last update [Homepage of Qiagen], [Online]. Available: https://www.qiagen.com/gb/shop//pcr/mircury-lna-sybr-green-pcr-kits/#productdetails [09/30, 2018].

AJI ALEX, M.R., NEHATE, C., VEERANARAYANAN, S., KUMAR, D.S., KULSHRESHTHA, R. and KOUL, V., 2017. *Self assembled dual responsive micelles stabilized with protein for co-delivery of drug and siRNA in cancer therapy.*

AZIMI, A., MAJIDINIA, M., SHAFIEI-IRANNEJAD, V., JAHANBAN-ESFAHLAN, R., AHMADI, Y., KARIMIAN, A., MIR, S.M., KARAMI, H. and YOUSEFI, B., 2017. Suppression of p53R2 gene expression with specific siRNA sensitizes HepG2 cells to doxorubicin. *Gene*

BAI, B., YEGNASUBRAMANIAN, S., WHEELAN, S.J. and LAIHO, M., 2014. RNA-Seq of the nucleolus reveals abundant *SNORD*44-derived small RNAs. *PloS one,* **9**(9), pp. e107519.

BALAKIN, A.G., SMITH, L. and FOURNIER, M.J., 1996. The RNA world of the nucleolus: two major families of small RNAs defined by different box elements with related functions. *Cell,* **86**(5), pp. 823-834.

BRAMEIER, M., HERWIG, A., REINHARDT, R., WALTER, L. and GRUBER, J., 2011. Human box C/D snoRNAs with miRNA like functions: expanding the range of regulatory RNAs. *Nucleic acids research,* **39**(2), pp. 675-686.

BRANNAN, C.I., DEES, E.C., INGRAM, R.S. and TILGHMAN, S.M., 1990. The product of the H19 gene may function as an RNA. *Molecular and cellular biology,* **10**(1), pp. 28-36.

BROWN, C.J., BALLABIO, A., RUPERT, J.L., LAFRENIERE, R.G., GROMPE, M., TONLORENZI, R. and WILLARD, H.F., 1991. A gene from the region of the human X inactivation centre is expressed exclusively from the inactive X chromosome. *Nature,* **349**(6304), pp. 38-44.

CALIN, G.A., SEVIGNANI, C., DUMITRU, C.D., HYSLOP, T., NOCH, E., YENDAMURI, S., SHIMIZU, M., RATTAN, S., BULLRICH, F., NEGRINI, M. and CROCE, C.M., 2004. Human microRNA genes are frequently located at fragile sites and genomic regions involved in cancers. *Proceedings of the National Academy of Sciences of the United States of America,* **101**(9), pp. 2999-3004.

CARNINCI, P., KASUKAWA, T., KATAYAMA, S., GOUGH, J., FRITH, M.C., MAEDA, N., OYAMA, R., RAVASI, T., LENHARD, B., WELLS, C., KODZIUS, R., SHIMOKAWA, K., BAJIC, V.B., BRENNER, S.E., BATALOV, S., FORREST, A.R., ZAVOLAN, M., DAVIS, M.J., WILMING, L.G., AIDINIS, V., ALLEN, J.E., AMBESI-IMPIOMBATO, A., APWEILER, R., et al., 2005. The transcriptional landscape of the mammalian genome. *Science (New York, N.Y.),* **309**(5740), pp. 1559-1563.

CHANG, L.S., LIN, S.Y., LIEU, A.S. and WU, T.L., 2002. Differential expression of human 5S snoRNA genes. *Biochemical and biophysical research communications,* **299**(2), pp. 196-200.

CHEN, L., HAN, L., WEI, J., ZHANG, K., SHI, Z., DUAN, R., LI, S., ZHOU, X., PU, P., ZHANG, J. and KANG, C., 2015. *SNORD*76, a box C/D snoRNA, acts as a tumor suppressor in glioblastoma. *Scientific reports,* **5**, pp. 8588.

CHEN, X., LU, P., WANG, D., YANG, S., WU, Y., SHEN, H., ZHONG, S., ZHAO, J. and TANG, J., 2016. *The role of miRNAs in drug resistance and prognosis of breast cancer formalin-fixed paraffin-embedded tissues.*

CHENG, J. and HAAS, M., 1990. Frequent mutations in the p53 tumor suppressor gene in human leukemia T-cell lines. *Molecular and cellular biology,* **10**(10), pp. 5502-5509.

CHING, T., PEPLOWSKA, K., HUANG, S., ZHU, X., SHEN, Y., MOLNAR, J., YU, H., TIIRIKAINEN, M., FOGELGREN, B., FAN, R. and GARMIRE, L.X., 2016. *Pan-Cancer Analyses Reveal Long Intergenic Non-Coding RNAs Relevant to Tumor Diagnosis, Subtyping and Prognosis.*

COSTA PEREIRA, L.M., THONGKITTIDILOK, C., LOPES, M.D. and SONGSASEN, N., 2018. *Effect of anti-apoptotic drug Z-VAD-FMK on in vitro viability of dog follicles.*

DONG, X.Y., RODRIGUEZ, C., GUO, P., SUN, X., TALBOT, J.T., ZHOU, W., PETROS, J., LI, Q., VESSELLA, R.L., KIBEL, A.S., STEVENS, V.L., CALLE, E.E. and DONG, J.T., 2008. SnoRNA U50 is a candidate tumor-suppressor gene at 6q14.3 with a mutation associated with clinically significant prostate cancer. *Human molecular genetics,* **17**(7), pp. 1031-1042.

DONG, X.Y., GUO, P., BOYD, J., SUN, X., LI, Q., ZHOU, W. and DONG, J.T., 2009. Implication of snoRNA U50 in human breast cancer. *Journal of genetics and genomics = Yi chuan xue bao,* **36**(8), pp. 447-454.

ENCODE PROJECT CONSORTIUM, BIRNEY, E., STAMATOYANNOPOULOS, J.A., DUTTA, A., GUIGO, R., GINGERAS, T.R., MARGULIES, E.H., WENG, Z., SNYDER, M., DERMITZAKIS, E.T., THURMAN, R.E., KUEHN, M.S., TAYLOR, C.M., NEPH, S., KOCH, C.M., ASTHANA, S., MALHOTRA, A., ADZHUBEI, I., GREENBAUM, J.A., ANDREWS, R.M., FLICEK, P., BOYLE, P.J., CAO, H., CARTER, N.P., CLELLAND, G.K., DAVIS, S., DAY, N., DHAMI, P., DILLON, S.C., DORSCHNER, M.O., FIEGLER, H., GIRESI, P.G., GOLDY, J., HAWRYLYCZ, M., HAYDOCK, A., et al., 2007. Identification and analysis of functional elements in 1% of the human genome by the ENCODE pilot project. *Nature,* **447**(7146), pp. 799-816.

ENDER, C., KREK, A., FRIEDLANDER, M.R., BEITZINGER, M., WEINMANN, L., CHEN, W., PFEFFER, S., RAJEWSKY, N. and MEISTER, G., 2008. A human snoRNA with microRNA-like functions. *Molecular cell,* **32**(4), pp. 519-528.

FAGHIHI, M.A., MODARRESI, F., KHALIL, A.M., WOOD, D.E., SAHAGAN, B.G., MORGAN, T.E., FINCH, C.E., ST LAURENT, G.,3RD, KENNY, P.J. and WAHLESTEDT, C., 2008. Expression of a noncoding RNA is elevated in Alzheimer's disease and drives rapid feed-forward regulation of beta-secretase. *Nature medicine,* **14**(7), pp. 723-730.

FAROOQI, A.A. and SIDDIK, Z.H., 2015. Platelet-derived growth factor (PDGF) signalling in cancer: rapidly emerging signalling landscape. *Cell biochemistry and function,* **33**(5), pp. 257-265.

FERRARA, N., 2010. Pathways mediating VEGF-independent tumor angiogenesis. *Cytokine & growth factor reviews,* **21**(1), pp. 21-26.

FREY, M.R., WU, W., DUNN, J.M. and MATERA, A.G., 1997. The U22 host gene (UHG): chromosomal localization of UHG and distribution of U22 small nucleolar RNA. *Histochemistry and cell biology,* **108**(4-5), pp. 365-370.

GAMEN, S., ANEL, A., LASIERRA, P., ALAVA, M.A., MARTINEZ-LORENZO, M.J., PIÑEIRO, A. and NAVAL, J., 1997. *Doxorubicin-induced apoptosis in human T-cell leukemia is mediated by caspase-3 activation in a Fas-independent way.*

GANOT, P., BORTOLIN, M.L. and KISS, T., 1997. Site-specific pseudouridine formation in preribosomal RNA is guided by small nucleolar RNAs. *Cell,* **89**(5), pp. 799-809.

GAO, L., MA, J., MANNOOR, K., GUARNERA, M.A., SHETTY, A., ZHAN, M., XING, L., STASS, S.A. and JIANG, F., 2015. Genome-wide small nucleolar RNA expression analysis of lung cancer by next-generation deep sequencing. *International journal of cancer,* **136**(6), pp. E623-9.

GEE, H.E., BUFFA, F.M., CAMPS, C., RAMACHANDRAN, A., LEEK, R., TAYLOR, M., PATIL, M., SHELDON, H., BETTS, G., HOMER, J., WEST, C., RAGOUSSIS, J. and HARRIS, A.L., 2011. The small-nucleolar RNAs commonly used for microRNA normalisation correlate with tumour pathology and prognosis. *British journal of cancer,* **104**(7), pp. 1168-1177.

GONG, J., LI, Y., LIU, C., XIANG, Y., LI, C., YE, Y., ZHANG, Z., HAWKE, D.H., PARK, P.K., DIAO, L., PUTKEY, J.A., YANG, L., GUO, A., LIN, C. and HAN, L., 2017. *A Pan-cancer Analysis of the Expression and Clinical Relevance of Small Nucleolar RNAs in Human Cancer.*

GRIVENNIKOV, S.I., GRETEN, F.R. and KARIN, M., 2010. Immunity, inflammation, and cancer. *Cell,* **140**(6), pp. 883-899.

GUFFANTI, A., IACONO, M., PELUCCHI, P., KIM, N., SOLDA, G., CROFT, L.J., TAFT, R.J., RIZZI, E., ASKARIAN-AMIRI, M., BONNAL, R.J., CALLARI, M., MIGNONE, F., PESOLE, G., BERTALOT, G., BERNARDI, L.R., ALBERTINI, A., LEE, C., MATTICK, J.S., ZUCCHI, I. and DE BELLIS, G., 2009. A transcriptional sketch of a primary human breast cancer by 454 deep sequencing. *BMC genomics,* **10**, pp. 163-2164-10-163.

GUTSCHNER, T. and DIEDERICHS, S., 2012. The hallmarks of cancer: a long non-coding RNA point of view. *RNA biology,* **9**(6), pp. 703-719.

HAMILTON, A.J. and BAULCOMBE, D.C., 1999. A Species of Small Antisense RNA in Posttranscriptional Gene Silencing in Plants. *Science,* **286**(5441), pp. 950-952.

HAN, Y., LIU, Y., GUI, Y. and CAI, Z., 2013. Inducing cell proliferation inhibition and apoptosis via silencing Dicer, Drosha, and Exportin 5 in urothelial carcinoma of the bladder. *Journal of surgical oncology,* **107**(2), pp. 201-205.

HAN, L., MA, P., LIU, S.M. and ZHOU, X., 2016. Circulating long noncoding RNA GAS5 as a potential biomarker in breast cancer for assessing the surgical effects. *Tumour biology : the journal of the International Society for Oncodevelopmental Biology and Medicine,* **37**(5), pp. 6847-6854.

HANAHAN, D. and WEINBERG, R.A., 2000. The hallmarks of cancer. *Cell,* **100**(1), pp. 57-70.

HANAHAN, D. and WEINBERG, R., 2011. Hallmarks of Cancer: The next generation. **144**(5), pp. 646.

HE, X., CHEN, X., ZHANG, X., DUAN, X., PAN, T., HU, Q., ZHANG, Y., ZHONG, F., LIU, J., ZHANG, H., LUO, J., WU, K., PENG, G., LUO, H., ZHANG, L., LI, X. and ZHANG, H., 2015. An Lnc RNA (*GAS5*)/SnoRNA-derived piRNA induces activation of TRAIL gene by site-specifically recruiting MLL/COMPASS-like complexes. *Nucleic acids research,* **43**(7), pp. 3712-3725.

HU, S., CHANG, J., LI, Y., WANG, W., GUO, M., ZOU, E.C., WANG, Y. and YANG, Y., 2017. Long non-coding RNA XIST as a potential prognostic biomarker in human cancers: a meta-analysis. *Oncotarget,* **9**(17), pp. 13911-13919.

JACOB, F. and MONOD, J., 1961. Genetic regulatory mechanisms in the synthesis of proteins. *Journal of Molecular Biology,* **3**, pp. 318-356.

JI, P., DIEDERICHS, S., WANG, W., BOING, S., METZGER, R., SCHNEIDER, P.M., TIDOW, N., BRANDT, B., BUERGER, H., BULK, E., THOMAS, M., BERDEL, W.E., SERVE, H. and MULLER-TIDOW, C., 2003. MALAT-1, a novel noncoding RNA, and thymosin beta4 predict metastasis and survival in early-stage non-small cell lung cancer. *Oncogene,* **22**(39), pp. 8031-8041.

KHALIL, A.M., GUTTMAN, M., HUARTE, M., GARBER, M., RAJ, A., RIVEA MORALES, D., THOMAS, K., PRESSER, A., BERNSTEIN, B.E., VAN OUDENAARDEN, A., REGEV, A., LANDER, E.S. and RINN, J.L., 2009. Many human large intergenic noncoding RNAs associate with

chromatin-modifying complexes and affect gene expression. *Proceedings of the National Academy of Sciences of the United States of America,* **106**(28), pp. 11667-11672.

KINO, T., HURT, D.E., ICHIJO, T., NADER, N. and CHROUSOS, G.P., 2010. Noncoding RNA *GAS5* is a growth arrest- and starvation-associated repressor of the glucocorticoid receptor. *Science signaling,* **3**(107), pp. ra8.

KISS-LASZLO, Z., HENRY, Y., BACHELLERIE, J.P., CAIZERGUES-FERRER, M. and KISS, T., 1996. Site-specific ribose methylation of preribosomal RNA: a novel function for small nucleolar RNAs. *Cell,* **85**(7), pp. 1077-1088.

KOVALCHUK, O., FILKOWSKI, J., MESERVY, J., ILNYTSKYY, Y., TRYNDYAK, V.P., CHEKHUN, V.F. and POGRIBNY, I.P., 2008. Involvement of microRNA-451 in resistance of the MCF-7 breast cancer cells to chemotherapeutic drug doxorubicin. *Molecular Cancer Therapeutics,* **7**(7), pp. 2152-2159.

KOZOMARA, A. and GRIFFITHS-JONES, S., 2014. miRBase: annotating high confidence microRNAs using deep sequencing data. *Nucleic acids research,* **42**(Database issue), pp. D68-73.

KRELL, J., FRAMPTON, A.E., MIRNEZAMI, R., HARDING, V., DE GIORGIO, A., ROCA ALONSO, L., COHEN, P., OTTAVIANI, S., COLOMBO, T., JACOB, J., PELLEGRINO, L., BUCHANAN, G., STEBBING, J. and CASTELLANO, L., 2014. Growth arrest-specific transcript 5 associated snoRNA levels are related to p53 expression and DNA damage in colorectal cancer. *PloS one,* **9**(6), pp. e98561.

LANDSKRON, G., DE LA FUENTE, M., THUWAJIT, P., THUWAJIT, C. and HERMOSO, M.A., 2014. Chronic inflammation and cytokines in the tumor microenvironment. *Journal of immunology research,* **2014**, pp. 149185.

LEE, R.C., FEINBAUM, R.L. and AMBROS, V., 1993. The C. elegans heterochronic gene lin-4 encodes small RNAs with antisense complementarity to lin-14. *Cell,* **75**(5), pp. 843-854.

LI, C., CUI, Y., LIU, L., REN, W., LI, Q., ZHOU, X., LI, Y., LI, Y., BAI, X. and ZU, X., 2017. *High Expression of Long Noncoding RNA MALAT-1 Indicates a Poor Prognosis and Promotes Clinical Progression and Metastasis in Bladder Cancer.*

LI, G., HE, Y., LIU, X., ZHENG, Z., ZHANG, M., QIN, F. and LAN, X., 2017. Small nucleolar RNA 47 promotes tumorigenesis by regulating EMT markers in hepatocellular carcinoma. *Minerva medica,* **108**(5), pp. 396-404.

LI, J., WANG, Y., ZHANG, C.G., XIAO, H.J., HOU, J.M. and HE, J.D., 2018. Effect of long non-coding RNA *GAS5* on proliferation, migration, invasion and apoptosis of colorectal cancer HT-29 cell line. *Cancer cell international,* **18**, pp. 4-017-0478-7. eCollection 2018.

LI, J. and YUAN, J., 2008. Caspases in apoptosis and beyond. *Oncogene,* **27**(48), pp. 6194-6206.

LI, T., XUE, Y., WANG, G., GU, T., LI, Y., ZHU, Y.Y. and CHEN, L., 2016. Multi-target siRNA: Therapeutic Strategy for Hepatocellular Carcinoma. *Journal of Cancer,* **7**(10), pp. 1317-1327.

LIANG, W., LV, T., SHI, X., LIU, H., ZHU, Q., ZENG, J., YANG, W., YIN, J. and SONG, Y., 2016. Circulating long noncoding RNA *GAS5* is a novel biomarker for the diagnosis of nonsmall cell lung cancer. *Medicine,* **95**(37), pp. e4608.

LIAO, J., YU, L., MEI, Y., GUARNERA, M., SHEN, J., LI, R., LIU, Z. and JIANG, F., 2010. Small nucleolar RNA signatures as biomarkers for non-small-cell lung cancer. *Molecular cancer,* **9**, pp. 198-4598-9-198.

LIU, G., MATTICK, J.S. and TAFT, R.J., 2013. A meta-analysis of the genomic and transcriptomic composition of complex life. *Cell cycle (Georgetown, Tex.),* **12**(13), pp. 2061-2072.

LIU, J., ZHANG, C., ZHAO, Y. and FENG, Z., 2017. MicroRNA Control of p53. *Journal of cellular biochemistry,* **118**(1), pp. 7-14.

LU, G., JIE, M., KAIISSAR, M., GUARNERA, M.A., AMOL, S., MIN, Z., LINGXIAO, X., STASS, S.A. and FENG, J., 2014. Genome-wide small nucleolar RNA expression analysis of lung cancer by next-generation deep sequencing. *International Journal of Cancer,* **136**(6), pp. E623-E629.

LUAN, W., LI, L., SHI, Y., BU, X., XIA, Y., WANG, J., DJANGMAH, H.S., LIU, X., YOU, Y. and XU, B., 2016. Long non-coding RNA MALAT-1 acts as a competing endogenous RNA to promote malignant melanoma growth and metastasis by sponging miR-22. *Oncotarget,* **7**(39), pp. 63901-63912.

LUNDIN, K.E., GISSBERG, O. and SMITH, C.I., 2015. Oligonucleotide Therapies: The Past and the Present. *Human Gene Therapy,* **26**(8), pp. 475-485.

MA, X.Y., WANG, J.H., WANG, J.L., MA, C.X., WANG, X.C. and LIU, F.S., 2015. Malat1 as an evolutionarily conserved lncRNA, plays a positive role in regulating proliferation and maintaining undifferentiated status of early-stage hematopoietic cells. *BMC genomics,* **16**, pp. 676-015-1881-x.

MATTICK, J.M., IGOR., 2006. Non-coding RNA. **15**(1), pp. 17-29.

MEI, Y.P., LIAO, J.P., SHEN, J., YU, L., LIU, B.L., LIU, L., LI, R.Y., JI, L., DORSEY, S.G., JIANG, Z.R., KATZ, R.L., WANG, J.Y. and JIANG, F., 2012. Small nucleolar RNA 42 acts as an oncogene in lung tumorigenesis. *Oncogene,* **31**(22), pp. 2794-2804.

MEIJERINK, J.P., MENSINK, E.J., WANG, K., SEDLAK, T.W., SLOETJES, A.W., DE WITTE, T., WAKSMAN, G. and KORSMEYER, S.J., 1998. Hematopoietic malignancies demonstrate loss-of-function mutations of BAX. *Blood,* **91**(8), pp. 2991-2997.

MISHRA, S., SRIVASTAVA, A.K., SUMAN, S., KUMAR, V. and SHUKLA, Y., 2015. *Circulating miRNAs revealed as surrogate molecular signatures for the early detection of breast cancer.*

MIURA, M., ZHU, H., ROTELLO, R., HARTWIEG, E.A. and YUAN, J., 1993. Induction of apoptosis in fibroblasts by IL-1 beta-converting enzyme, a mammalian homolog of the C. elegans cell death gene ced-3. *Cell,* **75**(4), pp. 653-660.

MOURTADA-MAARABOUNI, M., PICKARD, M.R., HEDGE, V.L., FARZANEH, F. and WILLIAMS, G.T., 2009. *GAS5*, a non-protein-coding RNA, controls apoptosis and is downregulated in breast cancer. *Oncogene,* **28**(2), pp. 195-208.

MOURTADA-MAARABOUNI, M., HEDGE, V.L., KIRKHAM, L., FARZANEH, F. and WILLIAMS, G.T., 2008. Growth arrest in human T-cells is controlled by the non-coding RNA growth-arrest-specific transcript 5 (*GAS5*). *Journal of cell science,* **121**(7), pp. 939-946.

MULLER, A.J., CHATTERJEE, S., TERESKY, A. and LEVINE, A.J., 1998. The gas5 gene is disrupted by a frameshift mutation within its longest open reading frame in several inbred mouse strains and maps to murine chromosome 1. *Mammalian genome : official journal of the International Mammalian Genome Society,* **9**(9), pp. 773-774.

OGATA-KAWATA, H., IZUMIYA, M., KURIOKA, D., HONMA, Y., YAMADA, Y., FURUTA, K., GUNJI, T., OHTA, H., OKAMOTO, H., SONODA, H., WATANABE, M., NAKAGAMA, H., YOKOTA, J., KOHNO, T. and TSUCHIYA, N., 2014. Circulating exosomal microRNAs as biomarkers of colon cancer. *PloS one,* **9**(4), pp. e92921.

PATTERSON, D.G., ROBERTS, J.T., KING, V.M., HOUSEROVA, D., BARNHILL, E.C., CRUCELLO, A., POLSKA, C.J., BRANTLEY, L.W., KAUFMAN, G.C., NGUYEN, M., SANTANA, M.W., SCHILLER, I.A., SPICCIANI, J.S., ZAPATA, A.K., MILLER, M.M., SHERMAN, T.D., MA, R., ZHAO, H., ARORA, R., COLEY, A.B., ZEIDAN, M.M., TAN, M., XI, Y. and BORCHERT, G.M., 2017. Human snoRNA-93 is processed into a microRNA-like RNA that promotes breast cancer cell invasion. *NPJ breast cancer,* **3**, pp. 25-017-0032-8. eCollection 2017.

PELLIZZONI, L., CROSIO, C., CAMPIONI, N., LORENI, F. and PIERANDREI-AMALDI, P., 1994. Different forms of U15 snoRNA are encoded in the introns of the ribosomal protein S1 gene of Xenopus laevis. *Nucleic acids research,* **22**(22), pp. 4607-4613.

PESCHANSKY, V.W., CLAES., 2014. Non-coding RNAs as direct and indirect modulators of epigenetic regulation. **9**(1), pp. 3.

PICKARD, M.R., MOURTADA-MAARABOUNI, M. and WILLIAMS, G.T., 2013. *Long non-coding RNA GAS5 regulates apoptosis in prostate cancer cell lines.*

PICKARD, M.R. and WILLIAMS, G.T., 2016. The hormone response element mimic sequence of *GAS5* lncRNA is sufficient to induce apoptosis in breast cancer cells. *Oncotarget,* **7**(9), pp. 10104-10116.

PICKARD, M.R. and WILLIAMS, G.T., 2014. Regulation of apoptosis by long non-coding RNA *GAS5* in breast cancer cells: implications for chemotherapy. *Breast cancer research and treatment,* **145**(2), pp. 359-370.

PRATT, A.J. and MACRAE, I.J., 2009. The RNA-induced silencing complex: a versatile gene-silencing machine. *The Journal of biological chemistry,* **284**(27), pp. 17897-17901.

QIAO, H.P., GAO, W.S., HUO, J.X. and YANG, Z.S., 2013. Long non-coding RNA *GAS5* functions as a tumor suppressor in renal cell carcinoma. *Asian Pacific journal of cancer prevention : APJCP,* **14**(2), pp. 1077-1082.

RAJENDRA,T.PRASANTH,K.LAKHOTIA,S., 2001. Male sterility associated with overexpression of the noncoding hsr gene in cyst cells of testis of Drosophila melanogaster. **80**(2), pp. 97.

RYVKIN, P., LEUNG, Y.Y., UNGAR, L.H., GREGORY, B.D. and WANG, L., 2014. *Using machine learning and high-throughput RNA sequencing to classify the precursors of small non-coding RNAs.*

SAAD, M., GARBUZENKO, O.B. and MINKO, T., 2008. Co-delivery of siRNA and an anticancer drug for treatment of multidrug-resistant cancer. *Nanomedicine (London, England),* **3**(6), pp. 761-776.

SALVESEN, G.S., 2002. Caspases and apoptosis. *Essays in biochemistry,* **38**, pp. 9-19.

SAXENA, T., TANDON, B., SHARMA, S., CHAMEETTACHAL, S., RAY, P., RAY, A.R. and KULSHRESHTHA, R., 2013. Combined miRNA and mRNA signature identifies key molecular players and pathways involved in chikungunya virus infection in human cells. *PloS one,* **8**(11), pp. e79886.

SCHNEIDER, C., KING, R.M. and PHILIPSON, L., 1988. Genes specifically expressed at growth arrest of mammalian cells. *Cell,* **54**(6), pp. 787-793.

SCOTT, M.S. and ONO, M., 2011. From snoRNA to miRNA: Dual function regulatory non-coding RNAs. *Biochimie,* **93**(11), pp. 1987-1992.

SHEN, Y., LIU, Y., SUN, T. and YANG, W., 2017. *LincRNA-p21 knockdown enhances radiosensitivity of hypoxic tumor cells by reducing autophagy through HIF-1/Akt/mTOR/P70S6K pathway.*

SHIMIZU, S., KHAN, M.Z., HIPPENSTEEL, R.L., PARKAR, A., RAGHUPATHI, R. and MEUCCI, O., 2007. Role of the transcription factor E2F1 in CXCR4-mediated neurotoxicity and HIV neuropathology. *Neurobiology of disease,* **25**(1), pp. 17-26.

SMITH, C.M. and STEITZ, J.A., 1998. Classification of *GAS5* as a multi-small-nucleolar-RNA (snoRNA) host gene and a member of the 5'-terminal oligopyrimidine gene family reveals common features of snoRNA host genes. *Molecular and cellular biology,* **18**(12), pp. 6897-6909.

SPANKUCH-SCHMITT, B., BEREITER-HAHN, J., KAUFMANN, M. and STREBHARDT, K., 2002. Effect of RNA silencing of polo-like kinase-1 (PLK1) on apoptosis and spindle formation in human cancer cells. *Journal of the National Cancer Institute,* **94**(24), pp. 1863-1877.

SUN, M., JIN, F.Y., XIA, R., KONG, R., LI, J.H., XU, T.P., LIU, Y.W., ZHANG, E.B., LIU, X.H. and DE, W., 2014. Decreased expression of long noncoding RNA *GAS5* indicates a poor prognosis and promotes cell proliferation in gastric cancer. *BMC cancer,* **14**, pp. 319-2407-14-319.

TALMADGE, J.E. and FIDLER, I.J., 2010. AACR centennial series: the biology of cancer metastasis: historical perspective. *Cancer research,* **70**(14), pp. 5649-5669.

TAMAS, K., 2002. **Small Nucleolar RNA: An Abundant Group of Noncoding RNAs with Diverse Cellular Functions**. *minireview,* **109**(2), pp. 145.

TODESCHINI, P., SALVIATO, E., PARACCHINI, L., FERRACIN, M., PETRILLO, M., ZANOTTI, L., TOGNON, G., GAMBINO, A., CALURA, E., CARATTI, G., MARTINI, P., BELTRAME, L., MARAGONI, L., GALLO, D., ODICINO, F.E., SARTORI, E., SCAMBIA, G., NEGRINI, M., RAVAGGI, A., D'INCALCI, M., MARCHINI, S., BIGNOTTI, E. and ROMUALDI, C., 2017. *Circulating miRNA landscape identifies miR-1246 as promising diagnostic biomarker in high-grade serous ovarian carcinoma: A validation across two independent cohorts.*

TREIBER, T., TREIBER, N., PLESSMANN, U., HARLANDER, S., DAISS, J.L., EICHNER, N., LEHMANN, G., SCHALL, K., URLAUB, H. and MEISTER, G., 2017. A Compendium of RNA-Binding Proteins that Regulate MicroRNA Biogenesis. *Molecular cell,* **66**(2), pp. 270-284.e13.

TYCOWSKI, K.T., SHU, M.D., KUKOYI, A. and STEITZ, J.A., 2009. A conserved WD40 protein binds the Cajal body localization signal of scaRNP particles. *Molecular cell,* **34**(1), pp. 47-57.

VINAY, D.S., RYAN, E.P., PAWELEC, G., TALIB, W.H., STAGG, J., ELKORD, E., LICHTOR, T., DECKER, W.K., WHELAN, R.L., KUMARA, H.M.C.S., SIGNORI, E., HONOKI, K., GEORGAKILAS, A.G., AMIN, A., HELFERICH, W.G., BOOSANI, C.S., GUHA, G., CIRIOLO, M.R., CHEN, S., MOHAMMED, S.I., AZMI, A.S., KEITH, W.N., BILSLAND, A., BHAKTA, D., HALICKA, D., FUJII, H., AQUILANO, K., ASHRAF, S.S., NOWSHEEN, S., YANG, X., CHOI, B.K. and KWON, B.S., 2015. *Immune evasion in cancer: Mechanistic basis and therapeutic strategies.*

WAHID, F., SHEHZAD, A., KHAN, T. and KIM, Y.Y., 2010. *MicroRNAs: Synthesis, mechanism, function, and recent clinical trials.*

WAN, Y., DAI, W., NEVAGI, R.J., TOTH, I. and MOYLE, P.M., 2017. *Multifunctional peptide-lipid nanocomplexes for efficient targeted delivery of DNA and siRNA into breast cancer cells.*

WANG, M., GUO, C., WANG, L., LUO, G., HUANG, C., LI, Y., LIU, D., ZENG, F., JIANG, G. and XIAO, X., 2018. Long noncoding RNA *GAS5* promotes bladder cancer cells apoptosis through inhibiting EZH2 transcription. *Cell death & disease,* **9**(2), pp. 238-018-0264-z.

WARBURG, O., WIND, F. and NEGLEIS, E., 1930. On the Metabolism of Tumors in the Body. In: Warburg. , pp. 254.

WARNER, W.A., SPENCER, D.H., TRISSAL, M., WHITE, B.S., HELTON, N., LEY, T.J. and LINK, D.C., 2018. Expression profiling of snoRNAs in normal hematopoiesis and AML. *Blood advances,* **2**(2), pp. 151-163.

WILUSZ, J.E., SUNWOO, H. and SPECTOR, D.L., 2009. Long noncoding RNAs: functional surprises from the RNA world. *Genes & development,* **23**(13), pp. 1494-1504.

WU, L., CHANG, L., WANG, H., MA, W., PENG, Q. and YUAN, Y., 2018. *Clinical significance of C/D box small nucleolar RNA U76 as an oncogene and a prognostic biomarker in hepatocellular carcinoma.*

XU, B., YE, M.H., LV, S.G., WANG, Q.X., WU, M.J., XIAO, B., KANG, C.S. and ZHU, X.G., 2017. *SNORD*47, a box C/D snoRNA, suppresses tumorigenesis in glioblastoma. *Oncotarget,* **8**(27), pp. 43953-43966.

Xue-hai Liang, Qing Liu, Quansheng Liu, Thomas H. King, Maurille J. Fournier; Strong dependence between functional domains in a dual-function snoRNA infers coupling of rRNA processing and modification events, *Nucleic Acids Research*, Volume 38, Issue 10, 1 June 2010, Pages 3376–3387,

YI, C., WAN, X., ZHANG, Y., FU, F., ZHAO, C., QIN, R., WU, H., LI, Y. and HUANG, Y., 2018. SNORA42 enhances prostate cancer cell viability, migration and EMT and is correlated with prostate cancer poor prognosis. *The international journal of biochemistry & cell biology,* **102**, pp. 138-150.

YILDIRIM, E., KIRBY, J.E., BROWN, D.E., MERCIER, F.E., SADREYEV, R.I., SCADDEN, D.T. and LEE, J.T., 2013. Xist RNA is a potent suppressor of hematologic cancer in mice. *Cell,* **152**(4), pp. 727-742.

YOSHIDA, K., TODEN, S., WENG, W., SHIGEYASU, K., MIYOSHI, J., TURNER, J., NAGASAKA, T., MA, Y., TAKAYAMA, T., FUJIWARA, T. and GOEL, A., 2017. *SNORA21 – An Oncogenic Small Nucleolar RNA, with a Prognostic Biomarker Potential in Human Colorectal Cancer.*

YU, F., BRACKEN, C.P., PILLMAN, K.A., LAWRENCE, D.M., GOODALL, G.J., CALLEN, D.F. and NEILSEN, P.M., 2015. p53 Represses the Oncogenic Sno-MiR-28 Derived from a SnoRNA. *PloS one,* **10**(6), pp. e0129190.

ZHOU, K., LIU, M. and CAO, Y., 2017. New Insight into microRNA Functions in Cancer: Oncogene-microRNA-Tumor Suppressor Gene Network. *Frontiers in molecular biosciences,* **4**, pp. 46.

ZUO, Y., LI, Y., ZHOU, Z., MA, M. and FU, K., 2017. *Long non-coding RNA MALAT-1 promotes proliferation and invasion via targeting miR-129-5p in triple-negative breast cancer.*

6 Appendices

Appendix A

Sequence results from MWG eurofins of SNORD44 mutant and SNORD44 wild type

Maxi prep of SNORD44 mutant version was performed and a sample of the collected elution was sent to MWG eurofins to be sequenced. The correct sequence was received back and therefore the correct construct was produced. The first sequence is for SNORD44 mutant type. The highlighted section is the bases that encode the snoRNA.

>U44 M_T7

CTGTAGCTTGGTACCGAGCTCGGATCCACTAGTCCAGTGTGGTGGAATTGCC

CTTTGGGCAAACTTCCTACGGCACAAATGGCTTTTTAGTTACCTCCTAGTGCT

GAATGCATTAAATAAATGGCGGATTCTTGTCTTGTTATGATTAATAAGAAAGTT

TGTAAATGCAGCCTGGATGATGATAAGCAAATGCTAACTGAACATGAAGGTCT

TAATTAGCTCTAACTGACTAAAGGCATTTGTTAGCTTTGGCAGGGGGTGAACA

CTAAGGGCAATTCTGCAGATAT

Figure A-1: Sequence results from a sample of SNORD44 mutant. The highlighted section is the base sequence that encodes SNORD44 mutant. The red highlighted bases show the location of the mutations within the sequence. The sequencing was performed by MWG eurofins.

The second sequence is for SNORD44 wild type, this is the correct sequence as proved on NCBI blast. The highlighted section shows the bases that encode the snoRNA.

AGAGCTCTCTGGCTACTAGAGAACCCACTGCTTACTGGCTTATCGAAATTAAT

ACGACTCACTATAGGGAGACCCAAGCTGGCTAGTTAAGCTTGGTACCGAGCT

CGGATCCACTAGTCCAGTGTGGTGGAATTGCCCTTTGGGCAAACTTCCTACG

GCACAAATGGCTTTTTAGTTACCTCCTAGTGCTGAATGCATTAAATAAATGGC

GGATTCTTGTCTTGTTATGATTAATAAGAAAGTTTGTAAATGCAGCCTGGATGA

TGATAAGCAAATGCTGACTGAACATGAAGGTCTTAATTAGCTCTAACTGACTA

AAGGCATTTGTTAGCTTTGGCAGGGGGTGAACACTAAGGGCAATTCTGCAGA

TATCCAGCACAGTGGCGGCCGCTCGAGTCTAGAGGGCCCGCGGTTCGAAGG

TAAGCCTATCCCTAACCCTCTCCTCGGTCTCGATTCTACGCGTACCGGTCATC

Figure A-2: Sequence results from a sample of SNORD44 wild type. The highlighted section is the base sequence that encodes SNORD44. The sequencing was performed by MWG eurofins.

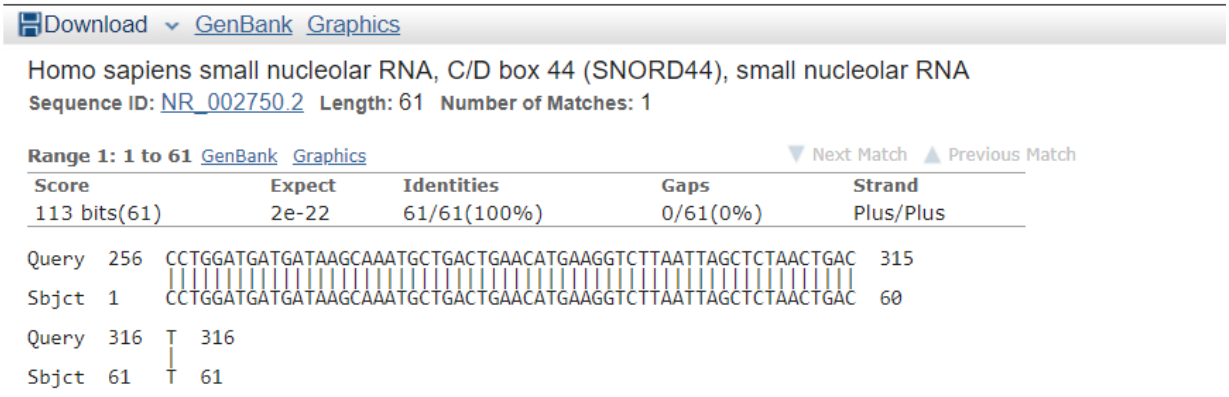

Figure A-3: Results of using NCBI Blast to analyse sequencing data of SNORD44 wild type. Using NCBI blast showed that the sequence received back from a sample of SNORD44 wild type isolated using maxi prep was the correct snoRNA.

Appendix B

Melting curves produced when performing sybr green RT-PCR on cells transfected with SNORD44 mutant and wild type to determine if overexpression has been successful.

A successful RT-PCR reaction would have one peak present on the melting curve. More than one peak suggests contamination in the samples. The first graph is from the transfection of SNORD44 wild type into Jurkat cells. 3 samples from the control, vector and SNORD44 wild type transfections were taken and run. Only one peak is present in these samples which suggests no contamination.

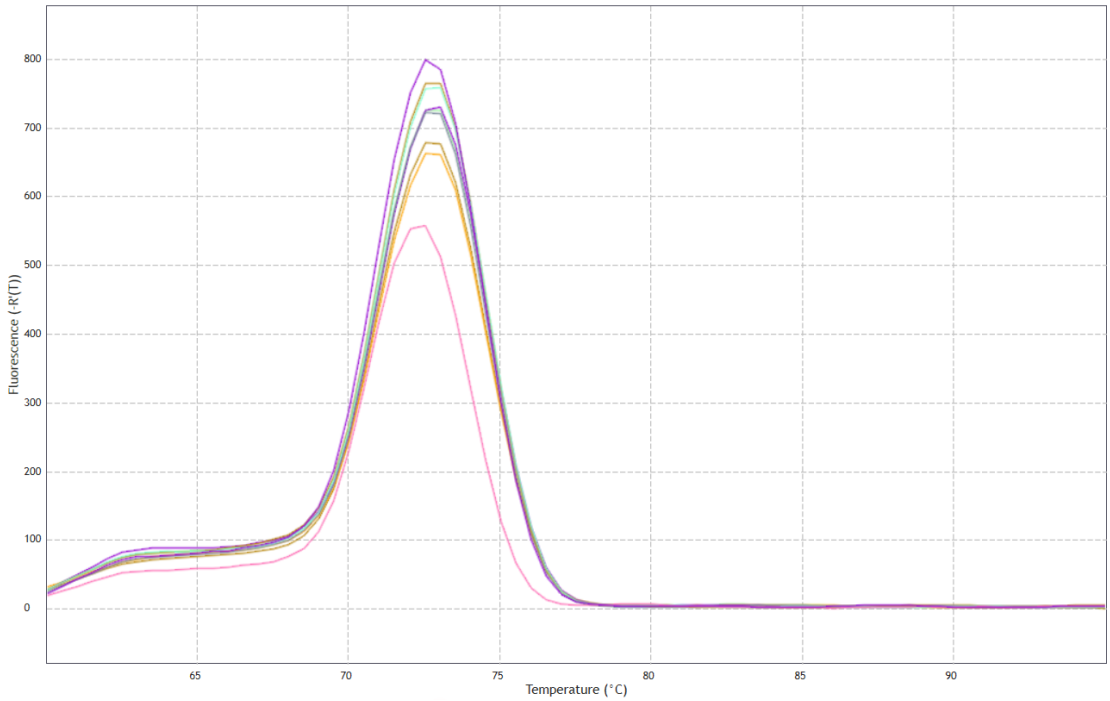

Figure B-1: Melting curve from Sybr green RT-PCR of overexpressed SNORD44 in Jurkat cells. $1x10^6$ Jurkat cells were used during this nucleofection. pcDNA3.1 and snoRNA U44 wild type were transfected into Jurkat cells. A control was also used in which no RNA was transfected into Jurkat cells. RNA was collected from the transfected cells which was used to produce cDNA. 3 separate SYBR green RT-PCR experiments were run. The melting curve shows one peak which suggest only one product is present and there is no contamination.

The second graph is from the transfection of SNORD44 wild type into CEM-C7 cells. 3 samples from the control, vector and SNORD44 wild type transfections were taken

and run. Only one peak is present in these samples which suggests no contamination.

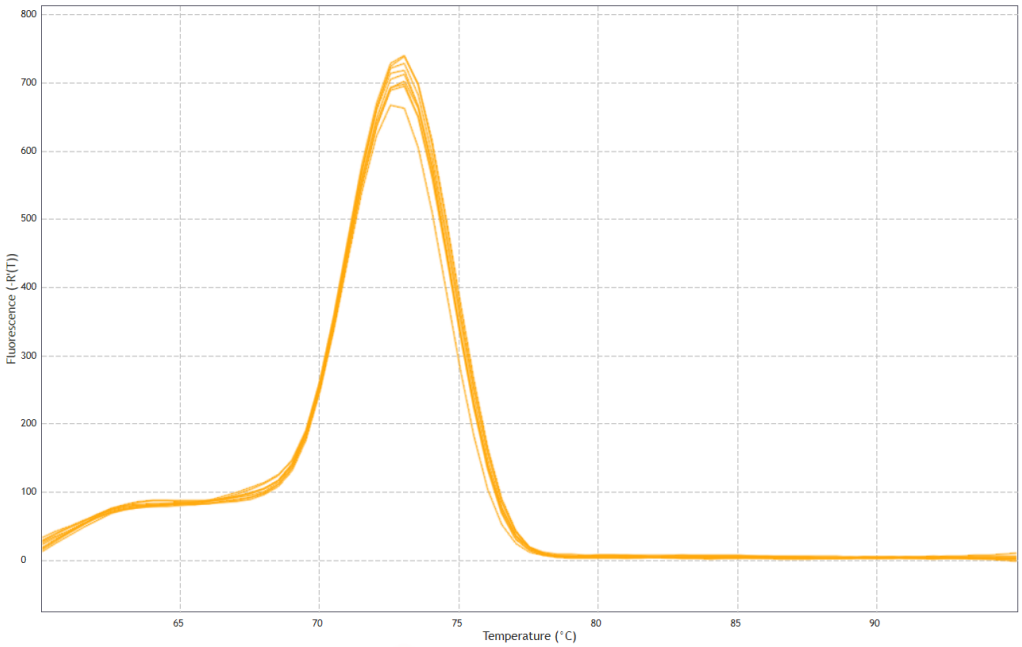

Figure B-2: Melting curve from Sybr green RT-PCR of overexpressed SNORD44 in CEM-C7 cells. 1x10^7 CEM-C7 cells were used during this nucleofection. pcDNA3.1 and snoRNA U44 wild type were transfected into CEM-C7 cells. A control was also used in which no RNA was transfected into the cells. RNA was collected from the transfected cells which was used to produce cDNA. 3 separate SYBR green RT-PCR experiments were run. The melting curve shows one peak which suggest only one product is present and there is no contamination.

The third graph is from the transfection of SNORD44 mutant into Jurkat cells. 3 samples from the control, vector and SNORD44 wild type transfections were taken and run. Only one peak is present in these samples which suggests no contamination.

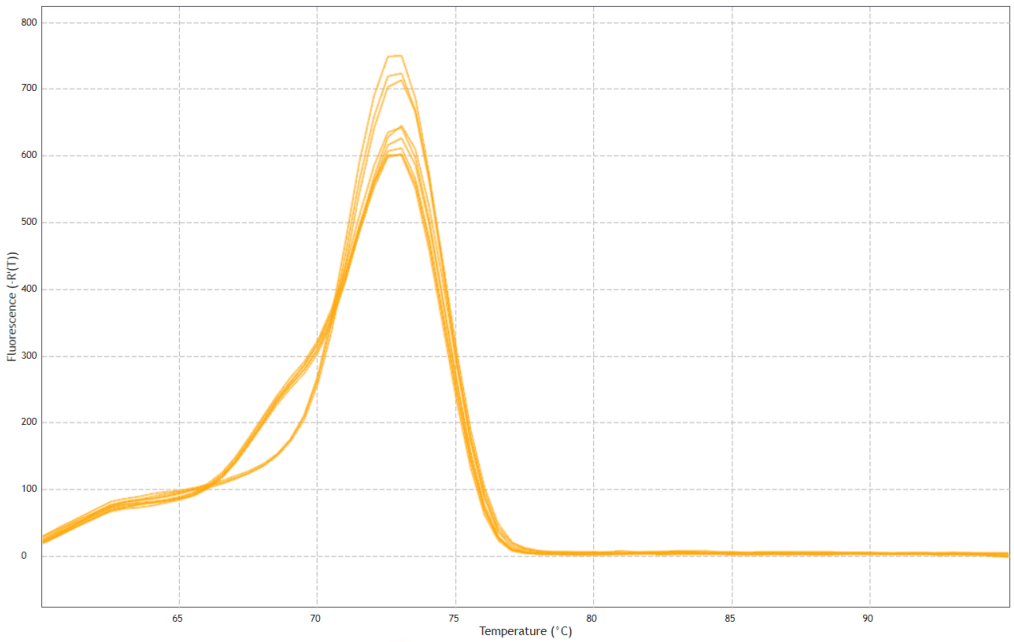

Figure B-3: Melting curve from Sybr green RT-PCR of overexpressed SNORD44 mutant in Jurkat cells. $1x10^6$ Jurkat cells were used during this nucleofection. pcDNA3.1 and snoRNA U44 mutant were transfected into Jurkat cells. A control was also used in which no RNA was transfected into Jurkat cells. RNA was collected from the transfected cells which was used to produce cDNA. 3 separate SYBR green RT-PCR experiments were run. The melting curve shows one peak which suggest only one product is present and there is no contamination.

The fourth graph is from the transfection of SNORD44 mutant into CEM-C7 cells. 3 samples from the control, vector and SNORD44 wild type transfections were taken and run. Only one peak is present in these samples which suggests no contamination.

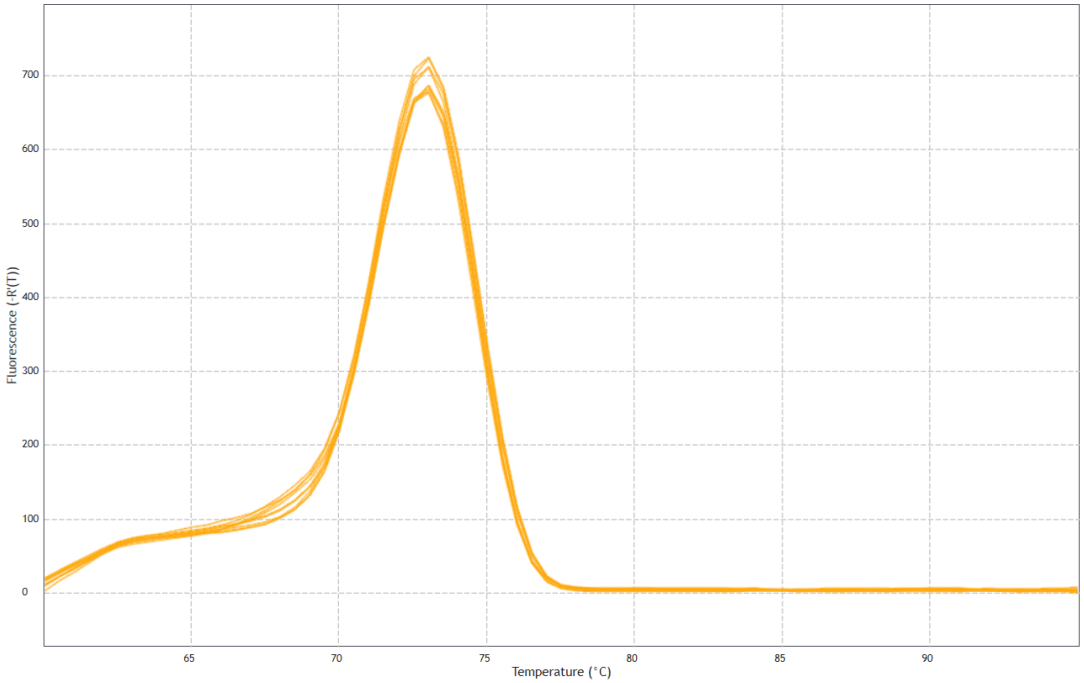

Figure B-4: Melting curve from Sybr green RT-PCR of overexpressed SNORD44 mutant in CEM-C7 cells. 1x10^7 CEM-C7 cells were used during this nucleofection. pcDNA3.1 and snoRNA U44 mutant were transfected into the cells. A control was also used in which no RNA was transfected into cells. RNA was collected from the transfected cells which was used to produce cDNA. 3 separate SYBR green RT-PCR experiments were run. The melting curve shows one peak which suggest only one product is present and there is no contamination.

Appendix C

A diagram of the pmaxGFP plasmid used during transfections

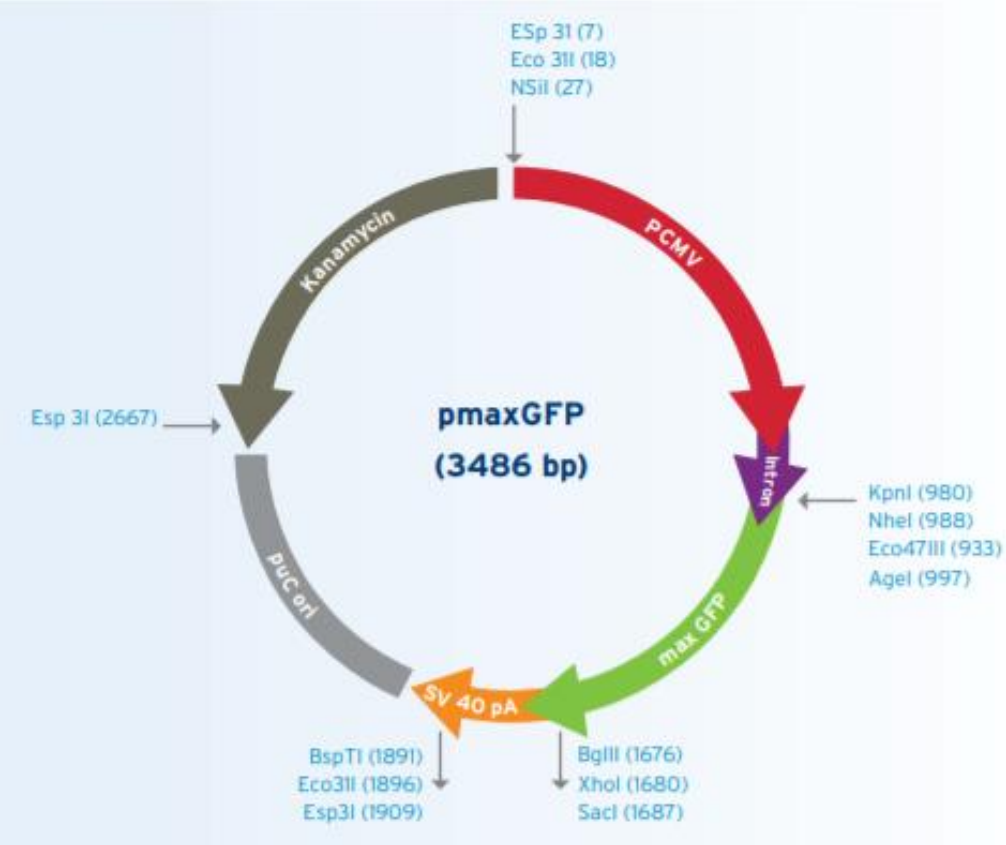

Figure C-1: Plasmid map of pmaxGFP used in transfections. The plasmid map shows the location of GFP using the green arrow. (Shimizu et al., 2007).